NTNU

Norwegian University of
Science and Technology

Improved Casing Collapse Prediction with a Case Study of Asset Life Extension

Even Mikael Kornberg

Petroleum Geoscience and Engineering
Submission date: June 2017
Supervisor: Bjørn Astor Brechan, IGP

Norwegian University of Science and Technology
Department of Geoscience and Petroleum

Abstract

The current industry accepted standards of predicting collapse strength of casings are pessimistic and inaccurate. With wells being drilled ever deeper, high strength pipes are required in order to comply with rules and regulations. A new ultimate limit strength (ULS) model is highly desirable.

A workgroup from ISO tasked with modernising current standards have identified the model introduced by Klever & Tamano in 2006 as the most accurate predictor of collapse strength. A simplified version of this model with calibrated parameters was suggested by ISO to replace the empirical API equations for casing collapse strength estimations.

This report reviews the predictive accuracy of the proposed model by comparison with a dataset, DEA-130, of 113 actual collapse tests. An adjustment was made to the model parameter, c, to best fit actual collapse pressures. For seamless, quenched & tempered, and hot rotary straightened casings the actual/predicted collapse strength ratio featured a Gaussian distribution with average of 0.999 and standard deviation of 0.0648.

Since actual collapse tests are limited an indirect method was used to estimate design collapse strength of a typical 9 5/8 in 53.5 ppf P-110 casing. This method requires only input parameter probability density functions (PDF). The PDFs for each input parameter were obtained by measurements of the 113 samples. The workgroup from ISO obtained similar PDFs from an ensemble of 20 datasets. Random value generators in a mathematical spreadsheet allowed for Monte Carlo simulations to output 100 000 collapse strength predictions for the 9 5/8 in casing in question. With confidence level of 97.5%, the basic strength was 9900 psi using DEA-130 PDFs. Using ensemble PDFs, the basic strength was 9500 psi – considerably more than API's standard rating of 7950 psi.

Collapse resistance can be significantly altered by secondary effects. Experimental and numerical results of the effects of axial loading, internal pressure, imposed ovality, casing wear, and cement support were obtained by literature review and compared with the ULS model. Linear derating factors to account for imposed ovality and casing wear were implemented to the model. The increased collapse strength of compressed pipes were

conservatively approximated by polynomial curve fitting of an alternative formulation of yield collapse strength and included in the model.

The new ULS model was used to evaluate the feasibility of asset life extension, i.e. prolonged production, of an existing well. Two loads were modelled: low pressure production and full evacuation of casing. With current industry standards the minimum bottom hole flowing pressure (BHFP) is 2500 psi, significantly more than the suggested design life extension pressure of 870 psi.

Using the new ULS model, the candidate well still cannot with confidence withstand the external pressure with full evacuation of the production casing. If BHFP is limited to 870 psi, up to 2.5% wear is allowed for non-ovalised casing. If the design factor of 1.1 is ignored, up to 10% wear is allowed. Moderate strength increase due to support from cement allows for safe operation even when including design factor. The critical point is then at top of cement where casing wear is likely and ovality may have been imposed. A casing collapse strength matrix as a function of wear and ovality was proposed for easy identification of minimum allowable internal pressure.

With some support of internal pressure and/or cement, maintaining well integrity at low pressure production is plausible but cannot be guaranteed

Sammendrag

Gjeldende industristandarder for beregning av kollapsstyrke til foringsrør er pessimistisk og unøyaktig. Brønner blir boret stadig dypere og sterkere rør kreves for å overholde regler og forskrifter. En ny modell basert på grensetilstand (ULS) er ønskelig.

En arbeidsgruppe fra ISO, som har til oppgave å modernisere dagens industristandarder, har identifisert modellen presentert av Klever & Tamano i 2006 som den mest presise estimatoren for kollapsstyrke. En forenklet versjon av denne modellen med kalibrerte parametere ble anbefalt av ISO til å erstatte de empiriske API-ligningene for foringsrørkollaps.

Denne rapporten evaluerer prediktiv presisjon til den foreslåtte modellen gjennom sammenligning med et datasett, DEA-130, bestående av 113 faktiske kollapstester. En justering av modellparameteren, c, ble utført for å best replikere faktisk kollapsstyrke. For sømløs, bråkjølt og temperert, varmt roterende-rettet foringsrør var faktisk/antatt kollapsstyrkeforhold normalfordelt med gjennomsnitt på 0,999 med standardavvik på 0,0648.

Siden faktiske kollapstester er begrenset ble en indirekte metode brukt til å estimere design kollapsstyrke for et typisk 9 5/8" 53.5 ppf P-110 forsingsrør. Denne metoden krever bare kjennskap til sannsynlighetstettheten (PDF) til input parameterne. Sannsynlighetstettheten til alle parametere ble identifisert ved målinger av de 113 prøvene fra DEA-130. Arbeidsgruppen fra ISO fikk lignende sannsynlighetstettheter fra sin samling av 20 datasett. Tilfeldige tall-generatorer i et matematisk regneark muliggjorde utførelsen av 100 000 kollapsstyrkeestimat gjennom Monte Carlo-simuleringer for foringsrøret. Med konfidensnivå på 97,5% var grunnstyrken beregnet til 9900 psi ved bruk av DEA-130 PDF. Ved bruk av PDF fra samlingen av 20 datasett var grunnstyrken 9500 psi – betydelig mer enn APIs standardverdi på 7950 psi.

Kollapsstyrke kan endres vesentlig av sekundære effekter. Eksperimentelle og numeriske resultater av effektene til aksielle laster, internt trykk, påført ovalitet, foringsrørslitasje, og sementstøtte ble hentet fra litteratursøk og sammenlignet med ULS modellen. Lineære reduksjonsfaktorer som vurderer effekten av påført ovalitet og foringsrørslitasje ble implementert i modellen. Den økte kollapsstyrken til komprimerte rør ble konservativt estimert ved polynomisk kurvetilpasning av en alternativ formulering for flytkollaps og inkludert i modellen.

Den nye ULS modellen ble brukt til å evaluere muligheten for forlengelse av levetiden til en eksisterende brønn. To scenarier ble modellert: produksjon ved lavt trykk og full evakuering av foringsrør. Med dagens industristandarder er kravet til minste bunnhullstrømningstrykket (BHFP) 2500 psi, betydelig mer enn det ønskede designtrykket på 870 psi.

Ved bruk av den nye ULS modellen vil ikke kandidatbrønnen kunne motstå kollapstrykket ved full evakuering av produksjonsforingsrøret. Hvis BHFP er begrenset til 870 psi vil opptil 2,5% slitasje være tillatt for et ikke-ovalisert foringsrør. Hvis designfaktoren på 1,1 er ignorert vil opptil 10% slitasje være tillatt. Moderat styrkeøkning grunnet støtte fra sement tillater sikker operasjon av brønnen selv når designfaktor er inkludert. Det kritiske punktet er da ved toppen av sement hvor slitasje er sannsynlig og foringsrøret kan ha blitt oval. En matrise for kollapsstyrke som funksjon av slitasje og ovalitet ble presentert slik at minimum internt trykk kan estimeres.

Med noe støtte fra internt trykk og/eller sement vil det være en viss mulighet til å ivareta brønnintegritet ved produksjon med lavt trykk, men det kan ikke garanteres.

Acknowledgment

This thesis is the final product of a Master of Science degree at the Norwegian University of Science and Technology (NTNU). The thesis is carried out at the Department of Geoscience and Petroleum during the spring of 2017.

I would like to express my deepest gratitude to supervisor, Assistant Professor Bjørn A. Brechan, for continuous support throughout the entirety of the process. This thesis would not have been successful without his suggestion of topic, expertise, and guidance. His availability any time of the day is much appreciated.

Special thanks go to Professor Sigbjørn Sangesland for helpful advice.

Table of contents

List of Figures

List of Tables

Nomenclature

Abbreviations

API	American Petroleum Institute
Avg	Average
BHFP	Bottom Flowing Pressure
CBL	Cement Bond Log
Cmt	Cement
COV	Coefficient of Variance
CRS	Cold Rotary Straightened
DEA	Drilling Engineering Association
DF	Design Factor
FEA	Finite Element Analysis
HC	High Collapse
HRS	Hot Rotary Straightened
ILS	Industry Leading Software
ISO	International Standardisation Organisation
K&T	Klever and Tamano
LPP	Low Pressure Production
MD	Measured Depth
N/A	Not Applicable
OBM	Oil Based Mud
OCTG	Oil Country Tubular Goods
OD	Outer Diameter
PDF	Probability Density Function
Std	Standard Deviation
SPE	Society of Petroleum Engineers
TR	Technical Report
TVD	True Vertical Depth
ULS	Ultimate Limit State
USIT	UltraSonic Imager Tool
Q&T	Quenched and Tempered
WBM	Water Based Mud
ppf	Pounds per Foot
psi	Pounds per Square Inch

Variables

All equations in this report use consistent field units, unless otherwise stated where the equation is given. The two sections below list all greek variables and all latin variables used in this report.

Greek

α	Dog leg severity
Δp	Pressure Differential, p_o-p_i
Δp_{actual}	Actual Collapse Pressure
Δp_{ec}	Elastic Collapse Pressure Differential
$\Delta p_{predicted}$	Predicted Collapse Pressure
Δp_{tc}	Transition Collapse Pressure Differential
$\Delta p_{tc,o}$	Transition Collapse Pressure Differential of Neutral Axial Loading
Δp_{yc}	Yield Collapse Pressure Differential
Δp_{yM}	von Mises Yield Collapse Pressure Differential
Δp_{yT}	Tresca Yield Collapse Pressure Differential
$\Delta p_{yTamano}$	Tamano Yield Collapse
λ	Collapse Mode Characteristic $\Delta p_{yc}/\Delta p_{ec}$
σ	Standard Deviation
σ_a	Axial Load
σ_c	Collapse Stress, Δp_{tc} D/2t
σ_e	Equivalent Yield Strength
σ_{eff}	Effective Axial Load
σ_y	Yield Strength
σ_y'	Derated Yield Strength, $\sigma_y k_y$ (1-H_y)
ξ	$1/(D_{av}/t_{av}-1)$

Latin

A	Area
D	Outer Diameter
E	Young's Modulus
E'	Derated Young's Modulus
F_a	Axial Force
F_{eff}	Effective Axial Force
H_e	Decrement Function for Elastic Collapse
H_t	Decrement Function for Transition Collapse
H_y	Decrement Function for Yield Collapse
L	Length
R	Radius
S_i	$(\sigma_a + p_i)/ \sigma_y$'

c	Model Parameter
ec	Eccentricity
fac	Factor Used in Tamano Equation
$f_{compression}$	Compression Factor
$f_{ovality}$	Ovality Factor
f_{wear}	Wear Factor
h_n	Stress-Strain Curve Characteristic Correction Factor
k_e	Model Bias Factor for Elastic Collapse
k_y	Model Bias Factor for Yield Collapse
n	Number of Samples
ov	Ovality
p_e	External Pressure
p_i	Internal Pressure
p_o	External Pressure
rs	Residual Stress
t	Wall Thickness
v	Poisson's Ratio
w	Wear Percent

1 Introduction

Casing design is a set of steel pipes that are able to withstand all imposed loads throughout the lifetime of the well. Numerical and analytical models may be used in order to evaluate pipe performance and choose appropriate casing features. The objective is to establish barrier envelopes ensuring safe drilling, service and production operations.

The *American Petroleum Institute*, API, have introduced industry accepted standards by providing several quality test methods and standardisation of measurements. Burst, collapse, and tensile ratings at standard temperature will be given for any API casing, albeit based on a uniaxial stress state. For collapse strength, empirical equations are recommended by API and are currently used for casing design considerations. Several shortcomings have been identified, most notably the assumption of perfect pipes, and limit the use of these collapse strength equations as accurate predictors of strength. By the use of minimum performance properties, the collapse strength is underestimated. With wells being drilled ever deeper, high strength pipes are required in order to comply with rules and regulations. A new *ultimate limit strength* (ULS) model is highly desirable.

Different models exist in literature with various degrees of accuracy. Dr. Tamano of Nippon Steel and Dr. Klever of Shell have developed the most accurate predictor of collapse strength for API tubulars according ISO/TR 10400:2007. The model includes a decrement function to account for pipe imperfections. A workgroup tasked with modernising current standards proposed a simplified version of the Klever & Tamano model in 2007, denoted as "*the ISO model*". It was debated whether or not the model was ready for use in engineering applications. Ultimately, it was deemed necessary for the model to mature within the industry.

A direct method of determining collapse strengths for any API casing requires actual collapse test data for every type of API casing from every batch for a representative range of mills. An unprecedented amount of collapse tests would be required, in reality rendering the direct method inapplicable.

An indirect method requires only production quality statistics and a predictive equation for collapse strength. Using random value generators for each input parameter based on relevant

probability distributions in a mathematical spreadsheet, Monte Carlo simulations may be performed. Actual collapse tests are only required to verify the model.

The ISO model will form the basis for further development of a new model as to include the effects of imposed ovality, casing wear and cement support. It will be referred to as "*the ULS model*". Current industry practice handles casing wear separately in a pessimistic manner, while ovality and cement support are ignored all together.

Drilling Engineering Association provides full measurements of relevant parameters of 113 casings, most of which are quenched and tempered. All casings have been subjected to external pressure to investigate actual collapse strength. A publicly available collapse database of this size is unique as OCTG manufacturers are reluctant to share actual performance details. The tests are essential for development of the ULS model.

Once the model is developed and verified it will be used to evaluate the feasibility of asset life extension of an existing well. As internal pressure declines theoretical studies indicate the second well barrier is dependent upon the integrity of the first well barrier. A single barrier element failure may lead to loss of well integrity. Since conservative criteria were used for well design prior to drilling, a hidden safety factor may allow for safe operation after all. Using an accurate casing collapse strength predictor (ULS model) the integrity of the well after design life will be evaluated.

2 Theory

2.1 Well Integrity of Low Pressure Production Wells

In well design, all loads throughout the lifetime of the well should be modelled. The above/below packer criterion used for well design is typically the governing collapse load. The internal pressure is modelled as full hydrostatic completion fluid pressure above the production backer, and reservoir pressure below. The worst case scenario is full depletion of the reservoir, in which the internal pressure can be approximated as vacuum. The highest collapse pressure is experienced over the production casing below the discontinuity.

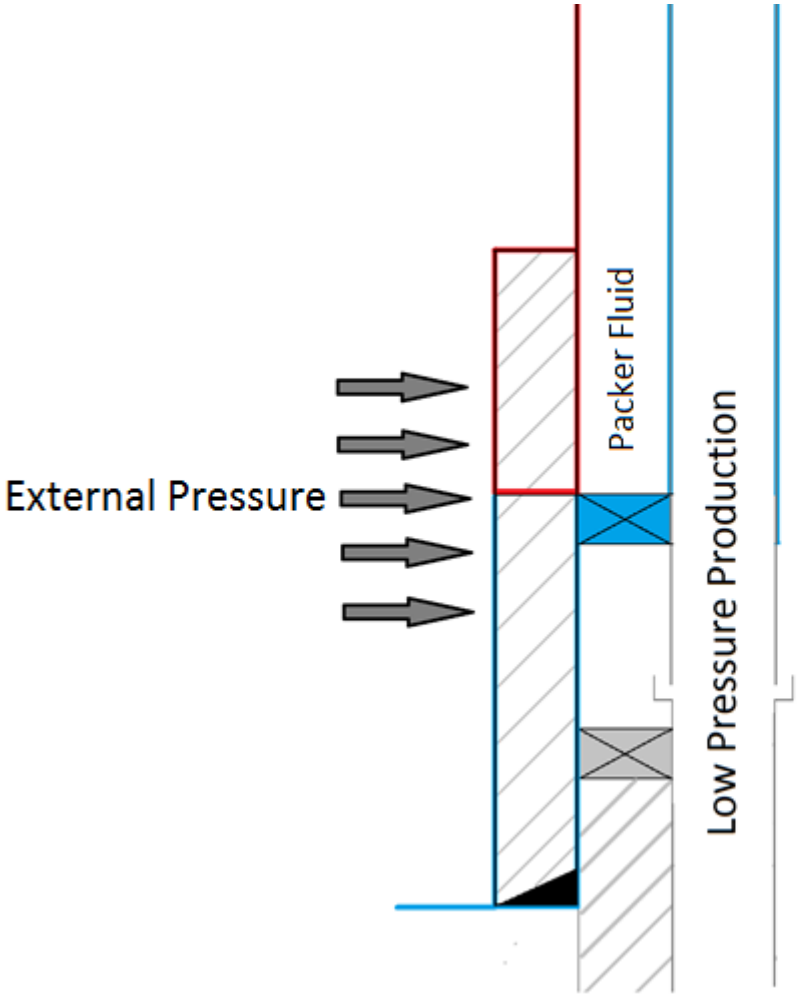

Figure 1: Overview of Above/Below packer criterion

Upon initial casing design conservative methods are currently used to select appropriate well material and equipment. The above/below packer criterion can be dismissed if it can be argued that vacuum below the packer is unlikely, if not impossible. Typical minimum well head pressure for a subsea well would be, say, 70 bar, meaning the reservoir pressure is even higher. The production casing is selected as to withstand the external collapse pressure with support from internal pressure equal to the well pressure at end of design life. New production technologies allow for lowering of the design pressure in a well. By utilising actual strength of casings rather than minimum performance ratings, new wells can feature casings previously exceeding design limits, and existing wells can capitalise on a hidden safety factor thus lowering the minimum internal pressure requirement.

2.2 Klever & Tamano

The following section is extracted in its entirety from Appendix D of Kornberg and Stavland (2016) - a specialisation project by the author forming the basis for this report. The following extract is aimed to provide background theory.

Many numerical and analytical approaches to collapse prediction of pipes have been published. Some well-known models include Timoshenko (1936), Tamano (1983), and the historical API approach explained in Appendix A. The classical Timoshenko model does not consider the effect of combined loads. Moreover, it is derived for thin-walled pipe whereas most oilfield pipes are thick-walled. The Tamano model includes the effect of internal pressure, but disregards axial loading. The API approach is a relatively poor predictor of pipe collapse, and does not assess the full pressure differential in its collapse strength determination (Klever and Tamano, 2006). It will predict collapse of an open end pipe in deep waters even though the pressure differential is zero.

Work performed by Klever and Tamano (2006) have resulted in a new equation for collapse under combined loads in which this section will be based upon.

The new OCTG collapse equation by Klever & Tamano features:

- An equation for elastic collapse of a perfect pipe
- An equation for through-wall yield collapse of a perfect pipe

- An equation for collapse in the transition between elastic and yield collapse
- A collapse characteristic criterion which determines the mode of collapse
- Factors which reduce collapse pressure resistance to account for pipe imperfections

2.2.1 Elastic collapse of an ideal pipe

The elastic collapse pressure differential, Δp_{ec}, of an ideal pipe subjected to combined loads is given by:

$$\Delta p_{ec} = \frac{2E}{1-\nu^2}\xi^3(1 + c\,\xi) \tag{1}$$

$$\xi = \frac{1}{D_{av}/\mathrm{t_{av}} - 1}$$

where c is a *model parameter*, v is *Poisson's ratio*, and E is *Young's modulus*.

The axial load is irrelevant for elastic collapse according to classical collapse theory (Klever and Tamano, 2006). In addition, Equation (1) is originally derived for thin-walled pipe, but the thickness correction factor, $c\xi$, makes it applicable for thick-walled pipes. Equation (1) is reduced to the original equation for ideal thin-walled pipes when c = 0.

To account for pipe imperfections, Young's modulus is modified by Equation (2) and replaces E in Equation (1).

$$\mathrm{E}' = k_e(1 - H_e)E \tag{2}$$

k_e is the model bias factor and H_e is the decrement function for elastic collapse - discussed in section 3.1.5. Imperfections effectively reduce the collapse strength rating as the original Young's Modulus is greater than the primed Young's Modulus.

2.2.2 Yield Collapse of an Ideal Pipe

Thick pipes will yield before collapse occurs. For materials with no or limited work hardening, there will be little difference in the yield pressure and actual collapse pressure, hence the historical term "*yield collapse*" (Klever and Tamano, 2006).

The traditional API approach evaluates initial yield collapse at the inside of the pipe. Equation (3) evaluates through-wall yield collapse pressure differential for ideal thick walled pipes:

$$\Delta p_{yc} = \min\left[\frac{1}{2}\left(\Delta p_{yM} + \Delta p_{yT}\right), \Delta p_{yM}\right] \tag{3}$$

where

$$\Delta p_{yM} = 2\xi\sigma_y \frac{2}{\sqrt{3}}\sqrt{1 - \left(\frac{F_{eff}}{2\pi R t \sigma_y}\right)^2} \tag{4}$$

$$\Delta p_{yT} = \frac{2\sigma_y t}{D} \tag{5}$$

Equation (3) is the through-wall yield pressure according to the von Mises yield criterion for positive values of Δp. Equation (4) is the through-wall yield pressure according to the Tresca yield criterion.

To account for pipe imperfections yield strength is replaced by Equation (6).

$$\sigma_y{}' = k_y\left(1 - H_y\right)\sigma_y \tag{6}$$

k_y is the model bias parameter and H_y is the decrement function for yield collapse. Again, the original values are greater than the primed values effectively reducing the yield strength and thus also the yield collapse strength.

2.2.3 Transition Collapse

Transition collapse denotes the collapse mode in between elastic collapse for very thin pipe and yield collapse for very thick pipe. The transition collapse pressure differential is given by Equation (7).

$$(1 - \mathrm{H_t})\Delta p_{tc}^2 - (\Delta p_{yc} + \Delta p_{ec})\Delta p_{tc} + \Delta p_{yc}\,\Delta p_{ec} = 0 \tag{7}$$

H_t is the decrement function for transition collapse. Equation (7) is quadratic in form and can be solved by Equation (8).

$$\Delta p_{tc} = \frac{2\Delta p_{yc}\Delta p_{ec}}{\Delta p_{yc} + \Delta p_{ec} + \sqrt{(\Delta p_{yc} - \Delta p_{ec})^2 - 4H_t\Delta p_{yc}\Delta p_{ec}}} \tag{8}$$

For thin-walled pipe, Δp_{tc} equals Δp_{ec}. Likewise, for thick-walled pipe, Δp_{tc} equals Δp_{tc}. The ratio $\lambda = \Delta p_{yc}/\Delta p_{ec}$, which is the ratio of yield collapse strength to elastic collapse strength, determines if the pipe is collapsing in the yield range, transition range, or elastic range according to Table 1.

Table 1: Collapse mode characteristics

Collapse Mode	Characteristic
Yield	$\log(\lambda_c) < -0.3$
Transition	$-0.3 < \log(\lambda_c) < 0.3$
Elastic	$\log(\lambda_c) > 0.3$

Ignoring the decrement function the solution of Equation (7) is then given by Equation (9) valid for perfect or ideal pipes.

$$\Delta p_{tc} = \frac{\Delta p_{yc} + \Delta p_{ec} - \sqrt{(\Delta p_{yc} + \Delta p_{ec})^2 - 4\Delta p_{yc}\Delta p_{ec}}}{2} \tag{9}$$

2.3 Project DEA-130

The DEA-130 project was initiated by the Drilling Engineering Association to modernise tubular collapse performance properties. Several industry partners joined forces in a project aimed to investigate the true nature of tubular collapse

A total of 151 pipes of sizes from 2.875 in to 16 in were donated from various batches for collapse testing. Full measurements of parameters such as yield strength, ovality, eccentricity, residual stress, outer diameter and wall thickness were performed to a satisfactory degree of accuracy. All parameters featured in the Klever & Tamano equation are present in the DEA-130 report.

The tubular goods are a mixture of different manufacturing methods and finishing processes. Availability of full performance details allows for easy analyses of different groups of casings, e.g. hot rotary straightened samples.

The actual collapse pressure is revealed and can be used for verification of analytical models. A publicly available collapse database of this size is unique as OCTG manufacturers are reluctant to share actual performance details.

3 Methodology

3.1 Development of Collapse Model

The current API approach for casing collapse estimation is explained in Appendix A. The empirical API collapse strength Equations (31) to (34) from ISO/TR 10400 (equivalent to API TR 5C3 which replaced API Bull 5C3) are as of 2007 recommended for use in casing and tubing design. These equations were developed in the 1960s and have been adjusted only to a minor extent, meaning they are essentially the same as in the original publication (ISO/TR 10400, 2007). Collapse test databases form the basis for the empirical coefficient used to calibrate these equations. Several shortcomings limit the use of the collapse strength equations as accurate predictors of strength.

Accurate prediction of collapse strength is highly desirable. Obtaining the exact performance ratings of tubular goods will help assess the feasibility of asset life extension of existing wells. The design limits plot may be expanded thus increasing design possibilities for potential cost savings. A work group was tasked with modernising current equations and calculations which resulted in a simplified ultimate limit state model for collapse strength based on Klever & Tamano. Further adjustments have been made in this report by the author and will be introduced and implemented gradually in what will be denoted as “the ULS model”. The ULS model is fully summarised in section 5.3.1.

3.1.1 Limitations of the historical API approach

- Some of the collapse tests have been conducted on short specimens which tend to overestimate collapse strength. For 9 5/8 in and smaller casings the length to diameter should be more than 8. For larger casings the L/D ratio should be at least 7 (ISO/TR 10400, 2007)
- Since the margin between the ultimate and design collapse strengths over the D/t range varies, the predicted failure probability will also follow suit with high variance (ISO/TR 10400, 2007).
- Equations (31) through (34) define the minimum collapse strength. Efforts have been made in order to predict the actual strength by the means of ‘average strength equations’, resulting in relatively poor predictions of strength.

- The same set of equations is used for Q&T (quenched and tempered) and non-Q&T pipes even though the two categories exhibit different collapse behaviour (ISO/TR 10400, 2007).
- The collapse tests were performed on both seamless and welded pipes from several manufacturers using different production methods. Collapse strength depends on many factors such as straightening and heat treatment and its effect should be included explicitly in any modern collapse strength formulation (ISO/TR 10400, 2007).
- Equation (32) is implicitly based on the assumption of proportionality of plastic collapse strength and the specified minimum yield strength rather than actual yield strength. This assumption is acceptable if the ratio of actual yield strength to specified minimum yield strength is constant for all grades. The latter ratio varies with grade resulting in the requirement of a new formulation for plastic collapse (ISO/TR 10400, 2007)
- Non-API grades, such as high collapse (HC), are not accommodated.

3.1.2 Predictive Accuracy of Current Analytical Models

Several collapse test datasets have been made available to the workgroup tasked with modernising ISO 10400 and API Bulletin 5C3. The datasets originate both from tests conducted by API and directly from leading manufacturers such as Nippon Steel, Mannesmann and Vallourec, in addition to some unnamed manufacturers who have donated test data in confidence. A total of 3171 tests are available, of which 2986 tests are conducted on Q&T-pipes manufactured from 1977 to 2000, including 1138 for API grades and 1848 for high collapse grades (ISO/TR 10400, 2007).

The lengths of all specimens are at least seven times greater than the pipe outer diameter. All relevant parameters have been successfully measured prior to applying external pressure. Values are reported as averages of each dataset and average of the total ensemble. Flawed specimens have been rejected as per quality assurance standards (ISO/TR 10400, 2007). Relevant parameters are yield strength (σ_y), average outer diameter (OD), average wall thickness (t), eccentricity (ec), ovality (ov), and residual stress (rs).

Several predictive collapse models exist in literature. The workgroup have reviewed the predictive accuracy of 11 models, where only the eight best performers are summarised in Table 2 for API grades.

It should be noted that only Klever & Tamano used all datasets to calibrate empirical coefficients. Where relevant, other models use fewer datasets in the calibration process.

Coefficient of variance is a dimensionless measure of the spread of a random variable, given by standard deviation/mean (ISO/TR 10400, 2007). The distribution of actual collapse strength divided by predicted collapse strength is assumed to be Gaussian.

For API grade pipes (and high collapse pipes reviewed separately), Klever & Tamano features the best predictive accuracy indicated by the near unity mean value and the lowest coefficient of variance.

API Product	Axial Force	Position(s) for geometry measurements	Tests	Abbassian and Parfitt 1995-9a		API Bull. 5C3 (average)		API Bull. 5C3/Clinedinst 1985		Haagsma and Schaap 1981		Jianzeng and Taihe 2001		Klever-Tamano		Tamano et al. 1983		Tamano modified 4	
				Mean	COV	Mean	COV	Mean	COV	Mean	COV	Mean	COV	Mean	COV	Mean	COV	Mean	COV
Mannesmann 1983	No	Multiple	89	**0,983**	0,069			1,035	0,049	0,955	0,067	0,930	0,069	0,956	0,055	0,968	0,064	0,964	0,064
API 1985	No	Unknown	106	1,023	0,046	0,978	0,083	1,016	0,048	0,925	0,082	0,973	0,060	0,989	0,044	1,004	0,051	**0,996**	0,042
Nippon 1977-87	No	Pipe centre	433	0,996	0,072	1,088	0,136	1,054	0,080	0,944	0,100	0,978	0,077	0,992	**0,057**	**1,003**	0,069	0,981	0,060
Nippon 1988-2000	No	Pipe centre	95	1,020	0,104	1,026	0,107	1,060	0,097	0,947	0,115	0,994	0,110	**1,004**	**0,093**	1,019	0,104	0,996	0,095
Manufacturer DF00	No	Pipe end	129	1,019	**0,077**	1,019	0,085	1,055	0,093	0,956	0,107	0,988	0,095	**1,000**	0,078	1,017	0,087	0,997	0,077
DEA-130	No	Pipe centre	52	1,019	0,066	1,017	0,097	1,065	0,071	0,966	0,083	0,974	0,082	0,993	**0,063**	**1,006**	0,073	0,987	0,066
API 1981	Yes	Collapse point	96	1,040	0,108	1,037	0,136	1,062	0,099	0,965	0,106	**1,004**	**0,080**	1,030	0,102	1,035	0,085	1,019	0,098
Mannesmann 1983	Yes	Multiple	63	1,030	0,098	1,114	0,168	1,052	**0,082**	1,009	0,084	0,976	0,087	1,003	0,084	1,021	0,085	1,016	0,090
Dataset average				1,016	0,080	1,040	0,116	1,050	0,077	0,958	0,093	0,977	0,083	**0,996**	**0,072**	1,009	0,077	0,994	0,074
Ensemble average			1138	1,012	0,080			1,049	0,081	0,952	0,097	0,981	0,083	**0,997**	**0,071**	1,010	0,077	0,992	0,072

Table 2: Predictive accuracy of eight ULS models for several datasets. Extracted from Table F.2 of ISO/TR 10400

3.1.3 Model Uncertainty

The Klever & Tamano equations feature several input parameters, all of which contribute to the model uncertainty. The model uncertainty is the statistical variation due to errors and/or limitations in the ultimate limit state model. A proposed methodology is to obtain the probability density function of each input parameter in order filter out the effect of variation of these parameters. Once removed, the remaining variability is then the model uncertainty, which is equal to the variation of actual/predicted strength (ISO/TR 10400, 2007).

In general the input variables have a slight negative cross-correlation when using measurements from the larger datasets available. The predicted failure probabilities are lower for correlated variables compared to independent variables. Treating all variables as independent will therefore be conservative and in line with general industry practice (ISO/TR 10400, 2007).

3.1.4 ISO Model

The workgroup of ISO simplifies the ULS equation from Klever & Tamano reproduced in section 2.2. It will be denoted as “the ISO model”. Most notably is the exclusion of the characteristic parameter, λ, used for determining mode of collapse. Elastic and plastic collapse are ignored and collapse is assumed to only occur in the transition region, which is the case for most thick-walled oilfield pipes. Nonetheless, both elastic and plastic collapse pressures are needed to calculate the ultimate collapse pressure. Originally, a decrement function was included for all modes of collapse. However, with simplifications only the transition collapse decrement function remains.

The ultimate collapse pressure is predicted by Equation (10). The effect of combined loads is attainable through the definition of Δp equal to the difference between external and internal pressure, and the axial force accounted for in Equation (14). Note elastic collapse pressure is not affected by axial loading, even for thick walled pipes (Klever and Tamano, 2006). The calibration of the model parameter c, model bias factors k_e and k_y, along with the decrement function H_t are explained in section 3.1.5.

$$\Delta p_{tc} = \frac{\Delta p_{yc} + \Delta p_{ec} - \sqrt{\left(\Delta p_{ec} - \Delta p_{yc}\right)^2 + 4\Delta p_{yc}\Delta p_{ec}}}{2(1 - H_t)} \tag{10}$$

$$\mathrm{H_t} = 0.127ov + 0.0039ec - 0.440(rs/\sigma_y) + h_n \tag{11}$$

The elastic collapse pressure differential, Δp_{ec}, is given by Equation. (12).

$$\Delta p_{ec} = \frac{2k_e E}{1 - v^2}\xi^3(1 + c\,\xi) \tag{12}$$

Yield collapse pressure differential should be calculated according to Equation (13).

$$\Delta p_{yc} = \min\left[\frac{1}{2}\left(\Delta p_{yM} + \Delta p_{yT}\right), \Delta p_{yM}\right] \tag{13}$$

$$\Delta p_{yM} = 2k_y\xi\sigma_y\frac{2}{\sqrt{3}}\sqrt{1 - \left(\frac{F_{eff}}{2\pi k_y Rt\sigma_y}\right)^2} \tag{14}$$

$$\Delta p_{yT} = \frac{2k_y\sigma_y t}{D} \tag{15}$$

3.1.5 Calibration of Parameters

The workgroup have calibrated parameters of the ISO model. The original K&T publication does not propose concrete values of relevant parameters.

3.1.5.1 Model Parameter c

Elastic collapse is associated with thin-walled pipes having a D/t ratio greater than, say, 40 (Klever and Tamano, 2006). The model parameter, c, features in the original K&T equation for elastic collapse in order to account for thickness effect. If c is set equal to zero, the original thin-walled elastic collapse pressure equation is recovered. The ISO workgroup

suggests the use of Equation (16) which is identical to the original K&T proposal in Equation (12) with c set to -1+t/D.

$$\Delta p_{ec} = \frac{2k_e E}{(1-v^2)(D/t)(D/t-1)^2} \tag{16}$$

Most oilfield pipes reviewed in this report are thick-walled with D/t ratio between 15 and 35. By default, the value for the model parameter would be lower than -0.90, effectively reducing the elastic collapse pressure for thick-walled pipes compared to thin-walled theory. This proposal contradicts the arguments of Klever & Tamano in their original publication which indicates thick-walled pipes should be expected to have greater elastic collapse pressure than predicted by thin-wall theory. By the historical API approach, the elastic collapse pressure for all oilfield pipes are lower than predicted by thin-wall theory, as seen by Figure 2.

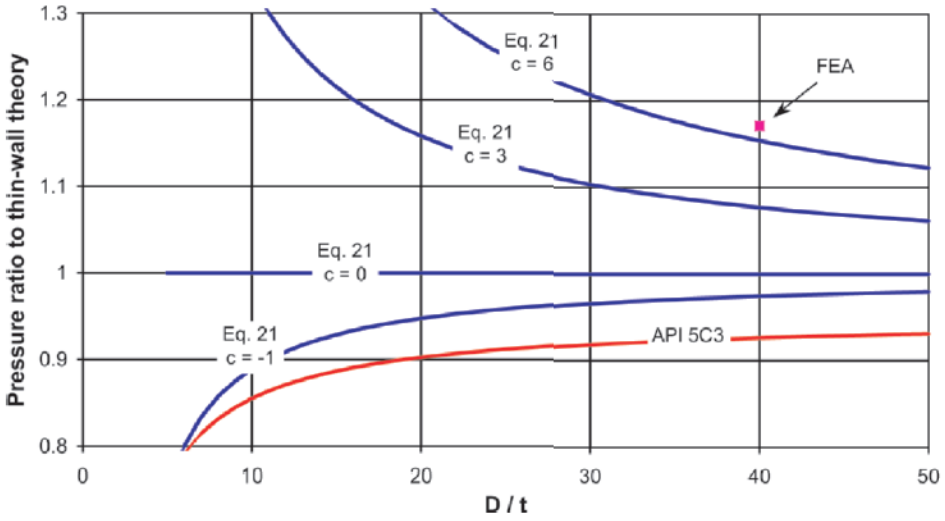

Figure 2: Deviation from thin-wall theory for D/t ratios. Extracted from Figure 2 of Klever and Tamano (2006).

If thick-walled pipes can resist higher elastic collapse pressures than predicted by thin-wall theory, the model parameter should be positive. In the K&T equation, the model parameter behaves such that positive values will increase the elastic collapse pressure and in turn the ultimate collapse pressure as defined by equation (10). Negative values will reduce the relevant collapse pressures.

Finite Element Analysis, FEA, indicate that for a pipe with D/t of 40, a model parameter of 6 will be of best fit (Klever and Tamano, 2006). When using this value for collapse tests from the DEA-130 dataset, near unity and near zero values are obtained for mean and variance respectively. Using the suggested value by the workgroup of -1+t/D results in very inaccurate collapse pressure predictions. The author therefore recommends the use of c = 6 in equation (12) rather than a negative value as suggested in ISO/TR 10400:2007.

3.1.5.2 Model bias factors

The model bias factors, k_e and k_y, were obtained empirically by the ISO work group. The factors were calibrated by iteration to give the flattest actual/predicted collapse strength response in each of the input variables for the 2986 tests performed on Q&T-casings.

Table 3 shows the resulting bias factors for both cold and hot rotary straightened casings of different grades where relevant. k_y varies from 0.840 to 0.910, while k_e has, for simplicity, been adopted as 0.825 for all grades

Table 3: Model bias factors for different grades. Extracted from Table F.8 in ISO/TR 10400 (2007)

	Cold rotary straightened		**Hot rotary straightened**	
Grade	K_e	K_y	K_e	K_y
H-40	0,830	0,910	N/A	N/A
J-55	0,830	0,890	N/A	N/A
K-55	0,830	0,890	N/A	N/A
L-80	0,825	0,855	0,825	0,865
N-80	0,825	0,870	0,825	0,870
P-110	0,825	0,855	0,825	0,855
Q-125	N/A	N/A	0,825	0,850

3.1.5.3 Decrement Function

The decrement function given by ISO in equation (11) was obtained from the means of ovality, eccentricity and residual stress, to give uniform scaling between the ultimate limit strengths and design (minimum performance) strengths (ISO/TR 10400, 2007). It is almost independent of the model bias factors and can therefore be set as a governing case of the relevant production variables, which will apply to all grades, sizes and weight (ISO/TR 10400, 2007). Ensemble averages rather than governing cases may also be used to obtain

values for the decrement function. The latter option will in most cases underpredict collapse strength, representing a pessimistic methodology.

$$\mathrm{H_t} = 0.127ov + 0.0039ec - 0.440(rs/\sigma_y) + h_n \qquad (17)$$

The last term, h_n, is a correction representing the shape of the stress/strain curve which is a material property. Round-knee stress/strain curves will feature a calibrated value of 0.017 for h_n, effectively increasing the value of the decrement function, and reducing the collapse strength. However, most Q&T-pipes feature a sharp-knee curve and need no additional correction, setting h_n to zero (ISO/TR 10400, 2007).

3.2 Verification of Model

Of all the datasets reviewed by the ISO task force, only DEA-130 containing actual collapse values have been made available to the public. Production quality data are available from the 2986 tests on Q&T-pipes in the form of probability density functions, means and deviations, but the actual collapse strengths are not listed. Instead the average actual/predicted collapse strength ratio is given for each dataset. However, this ratio cannot be used for verification purposes since the actual collapse strength is not known. Only 113 collapse tests in the DEA-130 dataset are reported with full details of all relevant parameters. Constant values have been used for Young's modulus and Poisson's ratio. Production statistics and actual collapse strengths from the DEA-130 dataset will be used to verify the predictability of the ULS model.

Casings are differentiated by manufacturing and finishing process according to the categories in Table 4. Only quenched and tempered casings are reviewed in this report. Category A features all Q&T casings from the dataset. Category B excludes the welded casings. Category C reviews only seamless hot rotary straightened casings, while category D reviews seamless, cold rotary straightened specimens.

Table 4: Categorisation of casings from DEA-130. Tests are conducted on 17 different API grade casings along with some non-API grade casings. Shell donated pipes are missing measurements and not included.

	Finish	Rotary straightening type	Forming process	DEA-130 Specimens	DEA-130 Non-API specimens
Category A	Q&T	Hot or cold	Seamless or Welded	80	18
Category B	Q&T	Hot or cold	Seamless	61	11
Category C	Q&T	Hot	Seamless	43	11
Category D	Q&T	Cold	Seamless	18	0

3.2.1 Using Production Quality Data from DEA-130

The predictive accuracy of the ULS model, as described in section 3.1.2, is determined by comparing predicted collapse pressure and actual collapse pressure. The probability distribution of actual/predicted collapse is assumed to be Gaussian and is confirmed by plotting relevant values, as seen in Figure 3.

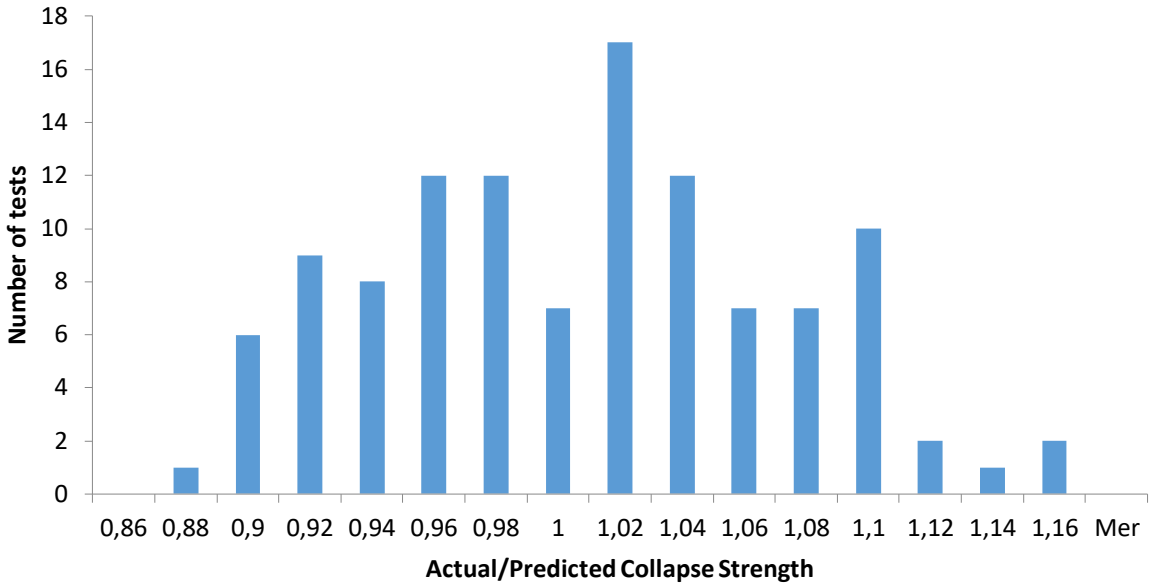

Figure 3: Predictive accuracy of the ULS model on Q&T pipes from DEA-130 with bin range of 0.02.

Table 5: Predictive accuracy of the ULS model on Q&T pipes from DEA-130 by category given in actual/predicted collapse strength.

Category	**A**	**B**	**C**	**D**
Specimens	80	61	43	18
min	0,8729	0,8873	0,8873	0,9472
max	1,1440	1,1440	1,1410	1,1440
Avg	0,9937	1,0124	**0,9990**	1,0445
Std	0,0661	0,0626	0,0648	0,0437
COV	0,0665	0,0618	0,0648	**0,0418**
1σ	0,9276	0,9499	0,9342	1,0008
2σ	0,8615	0,8873	0,8695	0,9571
3σ	0,7954	0,8247	0,8047	0,9134

The ULS model accuracy is summarised in Table 5. Bold entries mark best performance. On average the ULS model is a good predictor of collapse strength with the averages of each category near unity (1.0). The model performs best for the seamless, hot rotary straightened casings in category C. Although the model may be a good predictor of strength, it still holds uncertainty as seen by the standard deviations. The lowest standard deviation and coefficient of variance is obtained by category D casings. The worst predictions from the dataset may deviate as much as 13-14% compared to the actual collapse strength. All reported collapse strengths from the dataset are within 2 standard deviations of the category average value.

For quenched and tempered, hot rotary straightened and seamless casings, the model parameter, c, greatly impacts the accuracy of collapse pressure prediction as seen in Figure 4.

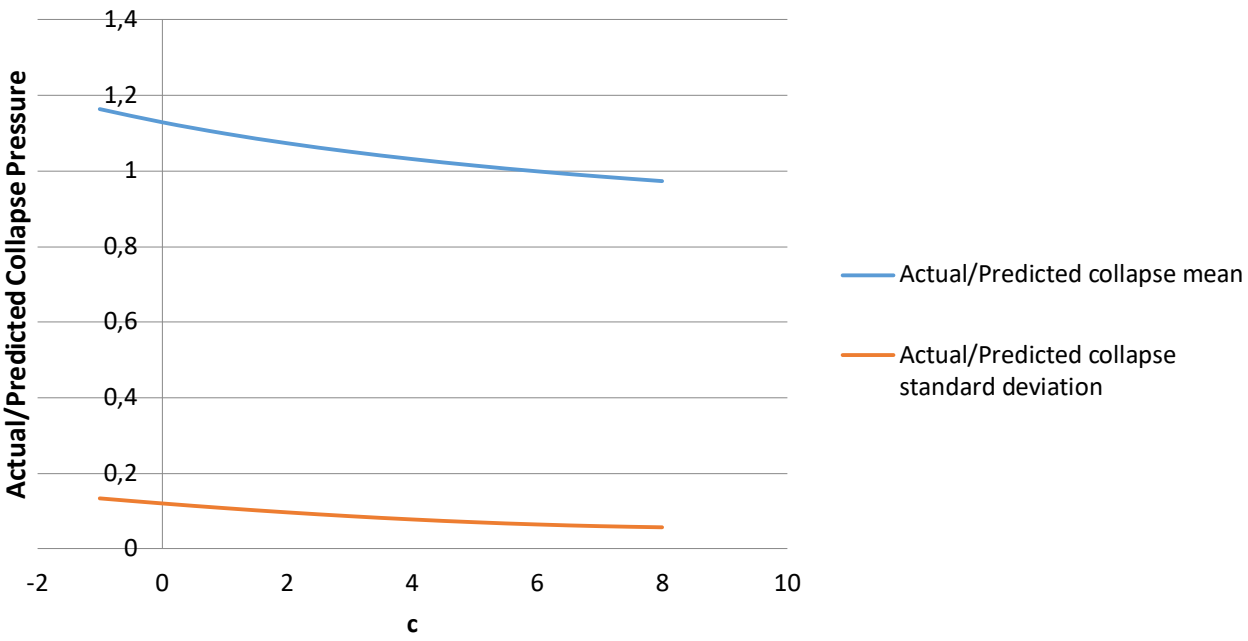

Figure 4: Accuracy sensitivity of model parameter

3.2.2 Using Governing Cases

In line with general industry practice, potential governing cases can be applied. The excellent work from the ISO task force has reviewed all input parameters available in the ensemble of 20 datasets and identified potential governing cases. Instead of using the linear decrement function as described in section 3.1.5.3, it is replaced by a constant value of 0.20 for hot rotary straightened casings, and 0.22 for cold rotary straightened casings. The exact values have been obtained by using the linear decrement function with governing cases, i.e. extreme values, of ovality, eccentricity and residual stress. As opposed to hot rotary straightened casings, the cold rotary straightened casings are assumed to have round-knee stress-strain curve, resulting in slightly higher value for the decrement function.

Table 6: Predictive accuracy using governing cases given in actual/predicted strength

Category	A	B	C	D
n	80	61	43	18
min	0,8822	0,9711	0,9711	1,0162
max	1,2807	1,2807	1,2807	1,2352
Avg	**1,0726**	1,0969	1,0890	1,1158
Std	0,0841	0,0734	0,0801	0,0513
COV	0,0784	0,0669	0,0736	**0,0460**

For seamless pipes, collapse strengths are underpredicted for very few samples. The lowest actual/predicted collapse strength ratio is 0.971 when using governing cases as opposed to 0.887 from *Table 5*. Using actual values in the decrement function gives, on average, a better prediction of collapse strength. However, from an engineering point of view, any ratio below unity can be catastrophic. For seamless, Q&T and cold rotary straightened casings, collapse strength was not underestimated. Nonetheless, the sample size of only 18 specimens is not sufficient from a statistical point of view.

3.3 Choice of Method

Collapse strength may be determined either directly by performing collapse tests, or indirectly with a predictive equation using production quality statistics and probabilistic analysis.

Casings are produced in batches at different mills of different quality by several worldwide manufacturers. The direct method requires actual collapse test data for every type of API casing from every batch for a representative range of mills. If such data were available, several thousand tests would be required, in reality rendering the direct method inapplicable. Production quality data are readily available and in large quantity, hence the indirect method has been chosen for this application. Collapse test data are only required to select ULS equation and calibrate parameters as in section 3.1.5, in addition to estimate model uncertainty (ISO/TR 10400, 2007).

The indirect method predicts collapse strength by using the ULS model as described in section 3.1. Once verified, the model can be used in conjunction with the production quality

data from the ensemble. The probability density function for each input parameter may be obtained. Using random value generators for each input parameter based on relevant probability distributions in a mathematical spreadsheet, a Monte Carlo simulation will be performed, resulting in 100 000 collapse strength predictions per type of casing.

The measured and reported parameters are yield strength, ovality, eccentricity, residual stress, outer diameter, wall thickness and collapse pressure. Where multiple values are reported, e.g. both minimum and average yield strength, the most detrimental value has been chosen as per industry standards. Constant values have been used for Young's modulus and Poisson's ratio of 30 000 000 psi and 0.28 respectively.

Yield strength, outer diameter and wall thickness have been normalised by nominal values. Residual stress is normalised by actual yield strength. Ovality is defined as $(OD_{max}-OD_{min})/OD_{av}$ and eccentricity is defined as $(t_{max}-t_{min})/t_{av}$, both given in %.

3.3.1 Input Parameter Probability Distribution

The six input parameters of the ULS model are all measured accurately and will vary for every specimen. Measuring parameters from a sufficient amount of samples will result in values over a specific spread. Plotting all data points will clearly reveal its probability distribution curve. Further statistical analyses will provide the properties of the probability density function, e.g. mean and deviation for a Gaussian distribution, for all input parameters.

The probability distribution of each parameter is obtained by reviewing data from DEA-130 with extreme outliers removed. The probability distributions are dependent upon specific factors. Each parameter should be represented by the factors listed in Table 7. For example, data from welded casings should not be used to obtain the wall thickness distribution for seamless casings. The four categories from Table 4 ensure reliable data representation.

Table 7: Probability distribution and data representativeness for each input parameter

Parameter	Data representativeness	Distribution
Yield strength	Grade, heat treatment, and rotary straightening type	Gaussian
Ovality	Forming process	Two-parameter Weibull
Eccentricity	Forming process	Two-parameter Weibull
Residual stress	Rotary straightening type	Gaussian
OD	Forming process	Gaussian
Wall thickness	Forming process	Gaussian
Collapse pressure	Product	Gaussian

Obtaining the value for both Weibull parameters are more difficult than obtaining the properties of a Gaussian distribution. For simplicity, the same PDF for ovality and the same PDF for eccentricity are adopted for all categories of casings. Since its shape is similar for all categories of casings this approximation is deemed acceptable.

Residual stresses are originally reported with the unit of psi. All residual stress measurements have been normalised by actual yield strength/stress.

Collapse pressure is the result of each test and should only be used to determine the model uncertainty as explained in section 3.1.3. The collapse ratings should be representative of the product itself.

3.3.1.1 DEA-130 Dataset

Yield strength should be represented by a specific grade, heat treatment, and rotary straightening type. In addition, yield strength bias varies with grade (ISO/TR 10400, 2007). Of the 113 collapse tests, only a handful are performed on a specific grade, i.e. only 15 samples of P-110 casings are tested. The number of applicable samples is even fewer when sorting by heat treatment and rotary straightening type. Plotting actual yield strengths from the DEA-130 dataset will result in an insignificant conclusion as the sample size is too small. However, work performed by the ISO task force confirms a Gaussian distribution of yield strength for all API grades with similar means and standard deviations.

For HRS and CRS seamless pipes the average normalised yield strength was found to be 1.1322 with a standard deviation of 0.0618.

*Table 8: Properties of Gaussian distribution function for σ_y of several grades obtained from DEA-130 dataset. *HRS and CRS. **Excludes J/K-55*

Grade	J/K-55*	L-80*	N-80*	P-110*	Q-125*	API Seamless* **
Samples	27	15	26	15	9	50
Avg	1,2120	1,0687	1,1808	1,1432	1,1010	1,1322
Std	0,0520	0,0378	0,0642	0,0306	0,0625	0.0618

Table 9: Probability distribution properties by category

	Category	A	B	C	D
rs	Avg	-0,1413	-0,1238	-0,1093	-0,1583
	Std	0,0869	0,0779	0,0774	0,0659
	COV	-0,6155	-0,6295	-0,7082	-0,4165
OD	Avg	1,0068	1,0062	1,0063	1,0061
	Std	0,0020	0,0017	0,0019	0,0011
	COV	0,0020	0,0017	0,0019	0,0011
t	Avg	1,0061	1,0101	1,0121	1,0054
	Std	0,0184	0,0178	0,0182	0,0163
	COV	0,0183	0,0176	0,0180	0,0162
ov	Scale	0,26	0,26	0,26	0,26
	Shape	1,50	1,50	1,50	1,50
	Shift	0,09	0,09	0,09	0,09
ec	Scale	1,60	1,60	1,60	1,60
	Shape	1,30	1,30	1,30	1,30
	Shift	0,33	0,33	0,33	0,33

3.3.1.2 Ensemble

For comparison, the ISO workgroup have collected production quality statistics from an ensemble of 20 datasets. Measurements of outer diameter, wall thickness, ovality and eccentricity are cheap and performed on approximately 6000 samples. Residual stress measurements are more expensive and only reported for 470 HRS samples and 943 CRS samples. Tensile tests are also less common with 1374 yield strength measurements of P-110 grade casings. Properties of probability density function are summarised in Table 12. The workgroup only present these results for seamless pipes, where residual stress is the only parameter to be differentiated by rotary straightening type. The workgroup reviews welded pipes for some specific datasets, but such pipes are not included in the ensemble as a whole.

Table 10: Properties of Gaussian distribution function for σ_y of several grades obtained from HRS ensemble data

HRS	Grade	**J/K-55**	**L-80**	**N-80**	**P-110**	**Q-125**
	Avg	-	1,10	1,21	1,10	1,10
	Std	-	0,04642	0,049005	0,0396	0,03619

Table 11: Properties of Gaussian distribution function for σ_y of several grades obtained from CRS ensemble data

CRS	Grade	**J/K-55**	**L-80**	**N-80**	**P-110**	**Q-125**
	Avg	1,23	1,10	1,21	1,10	1,10
	Std	0,08844	0,05819	0,06183	0,05104	0,04752

Table 12: Probability distribution properties from ensemble sorted by rotary straightening type

	Category	**Ensemble HRS**	**Ensemble CRS**
rs	Avg	-0,138	-0,237
	Std	0,06997	0,07868
	COV	-0,507	-0,332
OD	Avg	1,0059	1,0059
	Std	0,00182	0,00182
	COV	0,00181	0,00181
t	Avg	1,0069	1,0069
	Std	0,02608	0,02608
	COV	0,0259	0,0259
ov	Scale	0,236	0,236
	Shape	1,53	1,53
	Shift	0	0
ec	Scale	4,42	4,42
	Shape	1,60	1,60
	Shift	0	0

4 Analysis

4.1 Collapse Strength Prediction

The objective of this chapter is to predict the collapse strength of Q&T and seamless casings, both hot and cold rotary straightened. Using actual PDFs from the DEA-130 dataset (category C for HRS and category D for CRS) in Monte Carlo simulations, 100 000 values will be obtained with the aim to predict actual strength of a 9 5/8 in 53.5 ppf P-110 casing. Using governing case values for parameters featured in the decrement function, e.g. H_t equal to 0.20 or 0.22, the aim is not to accurately predict strength, but to provide minimum guaranteed collapse strength or design collapse strength.

To increase the robustness of such analyses, and for comparison purposes, actual PDFs from the ensemble provided by the ISO workgroup will be used for another set of simulations in section 4.1.2.

Assuming Gaussian distribution, 95% and 99.7% of all predictions should be within two and three standard deviations respectively from the mean.

4.1.1 DEA-130 PDFs

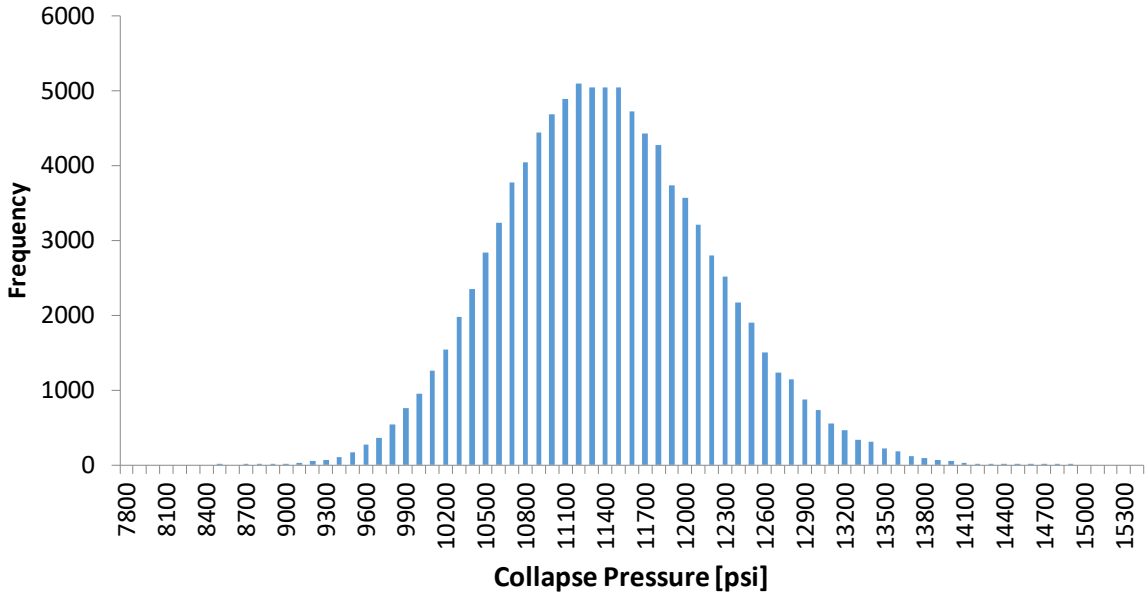

Figure 5: Collapse strength of HRS casing using DEA-130 production quality statistics

*Table 13: Results of Monte Carlo analysis using DEA-130 production quality statistics and governing cases. *Dimensionless*

	HRS	HRS 0.20	CRS	CRS 0.20
	[psi]	[psi]	[psi]	[psi]
Min	8481,5	8138,8	8601,5	8140,7
Max	14832,6	12492,1	13770,3	11343,4
Avg	11362,3	10269,4	10960,8	10001,7
Std	787,8	527,6	583,5	345,3
COV*	0,06933	0,05137	0,05324	0,0345
1σ	10574,5	9741,8	10377,3	9656,4
2σ	9786,8	9214,3	9793,7	9311,1
3σ	8999,0	8686,7	9210,2	8965,9
2.5% Exceedance	9900	9200	9900	9300
0.5% Exceedance	9500	8800	9500	8950
0.15% Exceedance	9250	8700	9350	8900

The probability density function properties are summarised in Table 13. Graphical representation of simulation results can be found in Figure 5 and Appendix D.1 Out of 400 000 predictions, the lowest collapse strength was found to be 8139 psi – only marginally better than the API value of 7950 psi. However, that extreme value exceeds the lower boundary of 2 standard deviations. In fact, it exceeds 4 standard deviations from the mean value of 10269 psi. Furthermore, using governing cases the exceedance values indicate that 99.85% of all casings can withstand more than 8700 psi. Similarly, 99.5% and 97.5% of the casings can withstand more than 8800 and 9200 psi respectively.

4.1.2 Ensemble PDFs

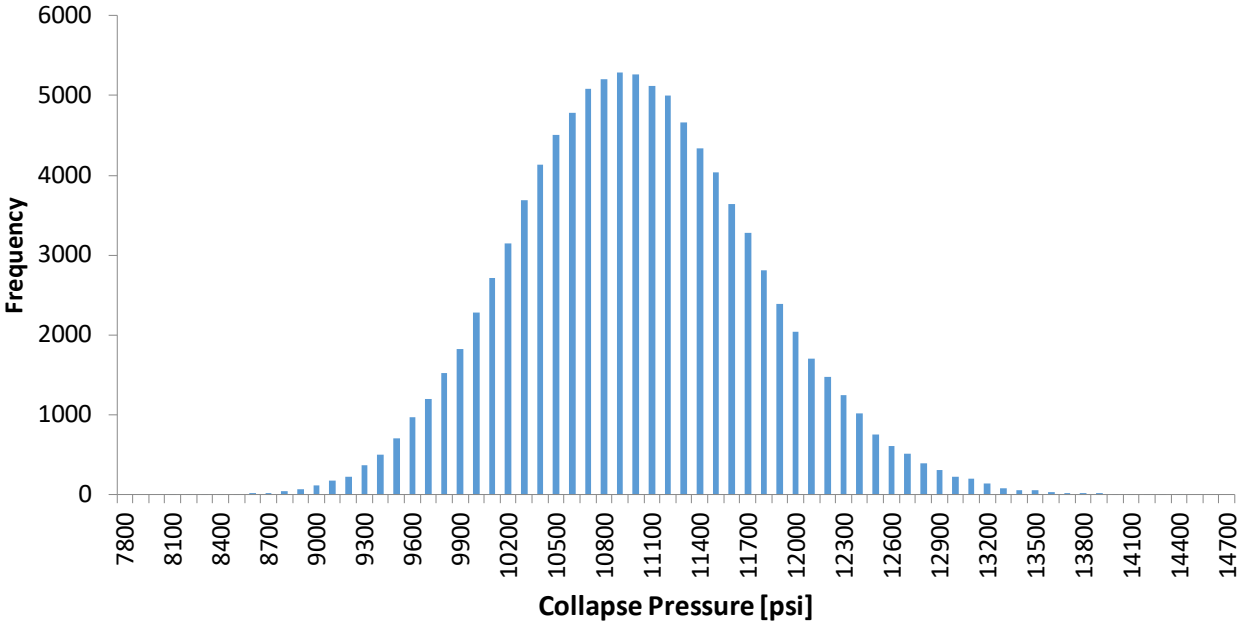

Figure 6: Collapse strength of HRS casing using ensemble production quality statistics

Using ensemble PDFs, the results are summarised in Table 14. Graphical representation of simulation results can be found in Figure 6 and Appendix D.2. Out of 400 000 predictions, the lowest indicated a strength of only 7422 psi – significantly lower than the conservative API collapse rating. It is more than 7 standard deviations from the mean, indicating it to be an outlier. The 0.15% (or 3 standard deviations) tolerance limit is exceeded at 8300 psi. The 0.5% and 2.5% limits are exceeded at 8500 and 8900 psi respectively - lower than that of the DEA-130 dataset PDFs.

*Table 14: Results of Monte Carlo analysis using ensemble production quality statistics and governing cases. *Dimensionless*

	HRS	HRS 0.20	CRS	CRS 0.20
	[psi]	[psi]	[psi]	[psi]
Min	8032,62	7535,28	7422,37	7584,28
Max	14350,2	12692,9	13899,8	12641,1
Avg	10953	9979,3	10467,9	9830,3
Std	414,97	321,19	399,23	330,14
COV*	0,03789	0,03219	0,03814	0,03358
1σ	10538	9658,1	10068,7	9500,1
2σ	10123	9336,9	9669,5	9170
3σ	9708,1	9015,7	9270,2	8839,9
2.5% Exceedance	9500	8900	9100	8700
0.5% Exceedance	9100	8500	8700	8400
0.15% Exceedance	8900	8300	8500	8100

4.2 Effect of Axial Loading and Internal Pressure

The standard API collapse values are reported with only external pressure acting on the casing. Axial forces and internal pressure are not accounted for. As wells are drilled ever deeper such representation of casing strength could be catastrophic with regards to well integrity. The upper most casing joint, just below the hanger, will be exposed to the full tension force exerted by the buoyed weight of the entire string. The historical API approach to calculate collapse ratings have been updated through revisions in order to account for axial loading. The latest revision suggests the use of an equivalent yield strength which incorporates both the effect of both axial loading and internal pressure, as seen in Equation (21). This approach is based on the von Mises yield criterion, and the ellipse of plasticity in Figure 37 represents the theoretical strength of a casing.

$$\Delta p_{yc} = \min\left[\frac{1}{2}\left(\Delta p_{yM} + \Delta p_{yT}\right), \Delta p_{yM}\right] \tag{18}$$

$$\Delta p_{yM} = 2\xi\sigma_y \frac{2}{\sqrt{3}}\sqrt{1 - \left(\frac{F_{eff}}{2\pi R t \sigma_y}\right)^2} \tag{19}$$

$$\Delta p_{yT} = \frac{2\sigma_y t}{D} \tag{20}$$

All collapse strength equations of Klever & Tamano are formulated as differential pressure over the casing wall. The three different mode of collapse are defined as yield collapse for thick-walled pipes, elastic collapse for thin-walled pipes and transition collapse as a weighted average of yield and elastic collapse. Elastic collapse is independent of axial loading, meaning that axial forces are only considered through the yield collapse formulation in Equation (19). In Klever & Tamano, yield collapse utilises the minimum value of the von Mises criterion alone, or the average of von Mises and Tresca as in Equation (18) . Only von Mises considers axial forces through the term $F_{eff}/2\pi Rt\sigma_y$, equivalent to σ_{eff}/σ_y.With tension and compression as positive and negative values respectively, the squared term provides the same numerical result. The collapse rating for pipes in tension would be exactly the same as pipes in compression if the magnitudes of axial forces are equal. This theoretical result contradicts the traditional formulation (Figure 37) where tension is detrimental for collapse strength, whereas

compression is beneficial. This contradiction seems strange as both formulations are based on the von Mises yield criterion. Unfortunately limited collapse test data for pipes in compression are readily available to validate either formulation. However, general industry practice do not utilise the extra strength provided by casings in compression according to the von Mises Ellipse. In industry leading software, casings in compression exhibit the same strength as casings without any axial loads.

4.2.1 Axial Tension

Some datasets reviewed by the ISO workgroup include axial loading during collapse testing. Unfortunately these datasets are not publicly available, and it is not stated if pipes are tested in tension or compression. The scientific paper, SPE-11238-PA, by Kyogoku et al. (1982) reveal the performance of pipes under axial tension loading by experimental data.

Kyogoku et al. (1982) from the former Sumitomo Metal Industries Ltd. perform physical experiments in a new collapse testing machine capable of applying axial loads. A total of 88 tests on 13 different types of casings are reported. Test results are normalised by calculating the collapse stress to yield stress ratio. *Collapse stress* is defined as half of the actual collapse pressure multiplied by the D/t ratio. The axial load is increased incrementally up to 80% of the yield strength. All results are presented in graphs showing the characteristic decline curve of collapse strength as axial load increases.

Direct comparison of the predicted collapse strengths from the ULS model and the experimental results from Kyogoku et al. (1982) are impossible. Unfortunately the only reported parameter that features in the ULS model is actual yield strength. Nominal values are used for OD and wall thickness. The decrement function, based on ovality, eccentricity, residual stress and a correction for the stress-strain curve, cannot be determined accurately since such information are not reported. However, most pipes reviewed by Kyogoku et al. (1982) feature a sharp-kneed stress-strain curve – an indication of hot rotary straightened casings.

From collapse test databases the decrement function is known to vary for every single specimen. The uncertainty in collapse strength is documented in section 3.1.3. For seamless,

hot rotary straightened Q&T casings, the strength could be overpredicted by 11.2% or underpredicted by 14.1%.

For two 9 5/8 in P-110 casings (58.4 ppf and 47 ppf) with yield strength of 124 600 psi and 117 700 psi respectively, the predicted collapse pressure is greatly affected by pipe imperfections through the decrement function. H_t set to zero represents a perfect pipe. Inserting average values in the decrement function provides a value of 0.1036. Similarly, the ensemble governing case for HRS samples is represented by a value of 0.20. Table 15 summarises the analysis.

Table 15: Pipe performance under axial loads predicted by ULS model.

Grade	σ_y	Weight	OD	t	H_t	σ_a/σ_y	σ_c/σ_y
[-]	[psi]	[ppf]	["]	["]	[-]	[-]	[-]
P-110	124600	58.4	9 5/8	0,595	0	0,6	0,75
P-110	124600	58.4	9 5/8	0,595	0,1036	0,6	0,61
P-110	124600	58.4	9 5/8	0,595	0,2	0,6	0,51
P-110	117700	47.0	9 5/8	0,472	0	0,6	0,74
P-110	117700	47.0	9 5/8	0,472	0,1036	0,6	0,53
P-110	117700	47.0	9 5/8	0,472	0,2	0,6	0,43

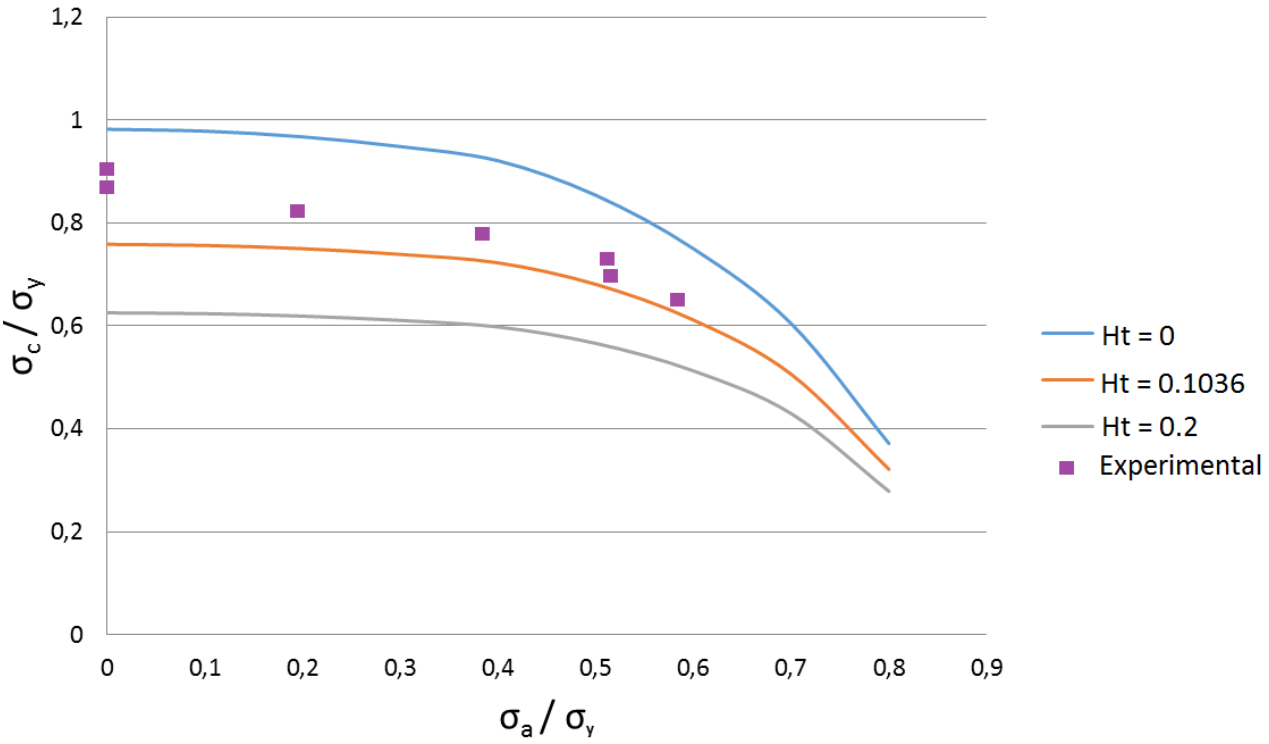

Figure 7: Analytical (ULS model) and experimental 9 5/8 in 58.4 ppf P-110 pipe performance under axial loads

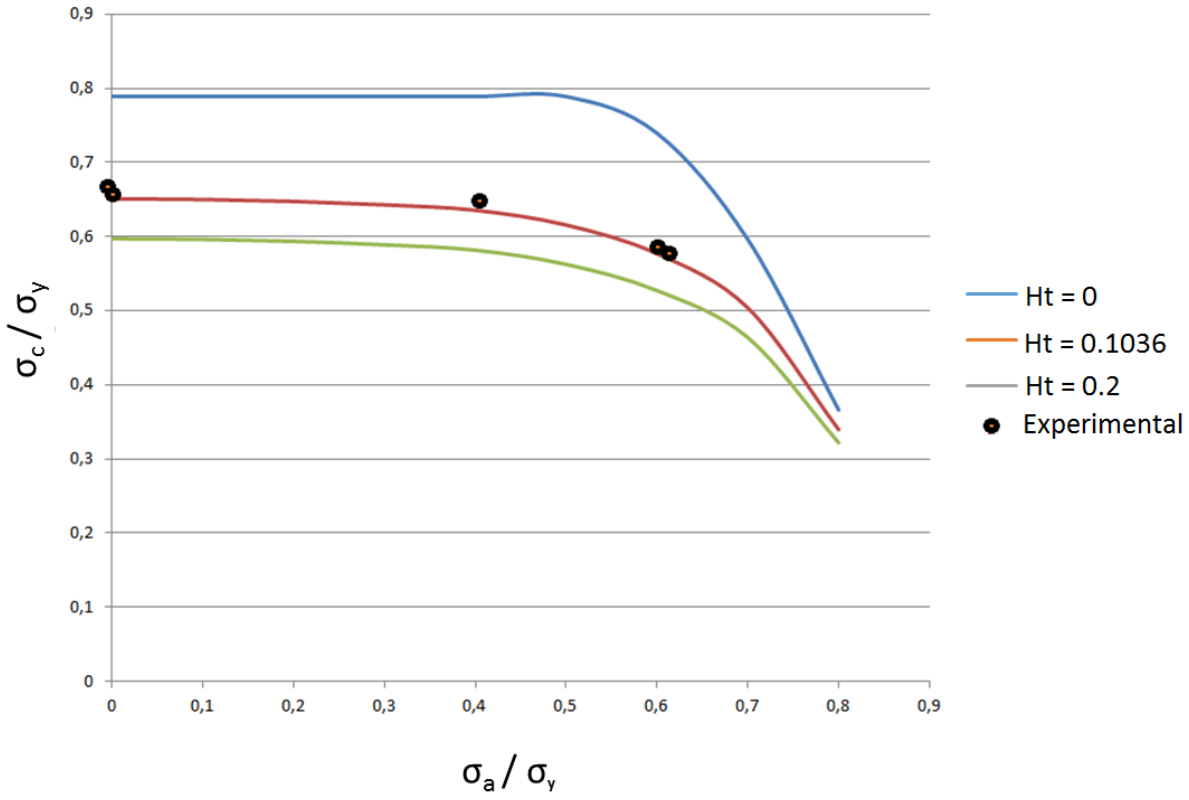

Figure 8: Analytical (ULS model) and experimental 9 5/8 in 47.0 ppf P-110 pipe performance under axial loads

The space between the upper and lower curves of Figure 7 and Figure 8 represents the plausible range of collapse strengths for a casing subjected to simultaneous loading. The uppermost curve represents a perfect casing, while the lowermost curve represents minimum performance values. Kyogoku et al. (1982) provide results with a similar presentation. All collapse pressures from experimental tests plot in the plausible region, representing casings that are better performers than average. Unfortunately the lack of property measurements leaves no hope of calculating the exact H_t value to verify the ULS model with regards to predictability for casings subjected to axial loading. However, the general curved shape in Figure 7 and Figure 8 is reproduced both for the analytical ULS model and experimental data.

4.2.2 Internal Pressure

The effect of internal pressure is investigated in IADC/SPE-178806-MS by Greenip (2016). API 7 in 26.00 ppf L-80 casings are used as test specimens. A pressure test chamber allows for up to 15 000 psi external pressure to be applied, while simultaneously maintaining fixed internal pressure. One test specimen from each of five batches is used for each setup. A total of 15 experimental tests are performed in three setups of 0, 5000, and 7500 psi internal pressure.

Actual yield strength is the only parameter measured for the samples. Assuming average decrement function value along with nominal values for OD and thickness, the predicted collapse pressures are listed in Table 16. Standard values for Young's modulus and Poisson's ratio have been used. The actual collapse pressures measured by Greenip (2016) are also listed.

*Table 16: Experimental test data with internal pressure from Greenip (2016). *Includes internal pressure, p_i*

	σ_y	H_t	σ_a	p_i	p_o	Δp_{actual}	$\Delta p_{Predicted}$*	$p_o/\Delta p_{Predicted}$
	[psi]	[-]	[psi]	[psi]	[psi]	[psi]	[psi]	[-]
Sample 1	87700	0,1036	0	0	7339	7339	7428	0,9881
Sample 2	86500	0,1036	0	0	7419	7419	7356	1,0085
Sample 3	87800	0,1036	0	0	7023	7023	7433	0,9448
Sample 4	87300	0,1036	0	0	7218	7218	7404	0,9749
Sample 5	88500	0,1036	0	0	7631	7631	7474	1,0210
Sample 1	87700	0,1036	0	4990	12342	7352	12418	0,9939
Sample 2	86500	0,1036	0	4900	12488	7588	12256	1,0189
Sample 3	87800	0,1036	0	5007	12185	7178	12440	0,9795
Sample 4	87300	0,1036	0	5010	12232	7222	12414	0,9853
Sample 5	88500	0,1036	0	4958	12319	7361	12432	0,9909
Sample 1	87700	0,1036	0	7509	14881	7372	14937	0,9963
Sample 2	86500	0,1036	0	7013	14636	7623	14369	1,0186
Sample 3	87800	0,1036	0	7519	14523	7004	14952	0,9713
Sample 4	87300	0,1036	0	7515	14645	7130	14919	0,9816
Sample 5	88500	0,1036	0	7517	14935	7418	14991	0,9962

The ULS model is a good predictor of strength also when incorporating internal pressure as indicated by the near unity ratios for the 15 casings. Klever and Tamano (2006) formulate collapse strength as pressure differential, meaning any incremental increase of internal pressure will consequently increase collapse strength by the same amount. Applying an average internal pressure of 4973 psi for the five samples will increase collapse strength, on average, by 4987 psi. Similarly, increasing the average internal pressure to 7414 psi will increase average strength of 7398 psi.

4.2.3 Axial Compression

4.2.3.1 Experimental Tests

Greenip (2016) also conducts two capped-end test scenarios for each of the five samples. Axial force is applied by internal pressure which acts on the inner cross sectional area of the

caps, and compression is applied by external pressure acting on the outer cross sectional area of the caps. The external pressure and area are greater in magnitude than internal pressure and area resulting in a net compressive force. The simplified K&T model presented by ISO does not consider pipes under compressional load, leaving the actual experimental test data without equivalent analytical counterpart for comparison. Qualitatively, from experimental data, it is seen that compression increases collapse strength compared to the vanilla case of no axial load. This result agrees with the historical API approach of calculating collapse pressure and contradicts the ISO model which predicts a reduction of collapse strength with introduction of axial compression. The experimental and predicted collapse strengths are listed in Table 17. The ratio of actual/predicted collapse strength all shift significantly to a value greater than 1.0, indicating underprediction of strength and confirms the limitation of ISO's simplified K&T model.

*Table 17: Experimental test data of compressed pipes from Greenip (2016) compared with ISO model. *Includes p_i*

	σ_y	F_a	σ_a	p_i	p_o	Δp_{actual}	$\Delta p_{Predicted}$*	$p_o / \Delta p_{Predicted}$
	[psi]	[lbf]	[-]	[psi]	[psi]	[psi]	[psi]	[-]
Sample 1	87700	-282000	-0,426	0	7221	7221	7045	1,025
Sample 2	86500	-288000	-0,441	0	7388	7388	6914	1,069
Sample 3	87800	-284000	-0,428	0	7286	7286	7043	1,034
Sample 4	87300	-297000	-0,451	0	7608	7608	6920	1,099
Sample 5	88500	-298000	-0,446	0	7641	7641	7011	1,090
Sample 1	87700	-306000	-0,462	2279	10071	7792	9670	1,041
Sample 2	86500	-328000	-0,502	4978	12423	7445	11597	1,071
Sample 3	87800	-337000	-0,508	4971	12651	7680	11633	1,088
Sample 4	87300	-327000	-0,496	5006	12404	7398	11705	1,060
Sample 5	88500	-329000	-0,492	5014	12474	7460	11803	1,057

4.2.3.2 Compression in Analytical Models

The latest recommended API approach to casing collapse strength predictions feature an equivalent yield strength formulation. The nominal yield strength is multiplied by a factor accounting for internal pressure and axial loads. As with the ISO model, a squared axial/yield stress ratio is used. However, the last term of Equation (21) differentiates tension and

compression. With compression characterised by negative values, the equivalent yield strength increases in compression. Likewise, tension reduces equivalent yield strength and thus also collapse strength.

$$\sigma_e = \sigma_y \left[\sqrt{1 - \frac{3}{4}\left(\frac{\sigma_a + p_i}{\sigma_y}\right)^2} - \frac{1}{2}\frac{(\sigma_a + p_i)}{\sigma_y} \right] \tag{21}$$

The original model from Tamano et al. (1983) uses the same factor, albeit without internal pressure which was only recently introduced to the API formulation. Equation (22) is reproduced from Tamano et al. (1983). Again, compression increases collapse strength.

$$\Delta p_{yTamano} = 2\sigma_y \frac{D/t - 1}{(D/t)^2}\left(1 + \frac{fac}{D/t - 1}\right)\left[\sqrt{1 - \frac{3}{4}\left(\frac{\sigma_a}{\sigma_y}\right)^2} - \frac{1}{2}\frac{\sigma_a}{\sigma_y} \right] \tag{22}$$

It is noteworthy that axial loading is exclusively denoted as tension only in the ISO model as described in section 3.1. No mention of compression loads is made. Klever and Tamano (2006) suggests a different formulation of yield collapse based on von Mises' criterion as seen in Equation (23) which accounts for performance in compression. However, it is not directly applicable with ISO's modified version due to the absence of a separate yield collapse decrement function, H_y. Replacing Equation (14) by Equation (23) in the ISO model will give the characteristic elliptic shape of strength (von Mises ellipse) with increase of collapse strength when axial compression is applied. However, the collapse strength is significantly lower compared to the use of equation (14) which has proven to be accurate according to section 3.2.

$$\Delta p_{yM} = \xi \sigma_y{}' \frac{4(1 + 2\xi)}{3 + (1 + 2\xi)^2}\left[-S_i \pm \sqrt{1 + 3\frac{1 - S_i^2}{(1 + 2\xi)^2}} \right] \tag{23}$$

$$S_i = \frac{\sigma_a + p_i}{\sigma_y{}'}$$

$$\sigma_y' = \sigma_y k_y (1 - H_y)$$

In Klever & Tamano yield collapse based on both Tresca and von Mises criteria must be calculated. The minimum value of the von Mises formulation and the average of von Mises and Tresca are used as yield collapse for further calculations. If only the average value of Tresca and von Mises is used as yield collapse, Equation (23) can be used to represent collapse strength of casings in compression with H_e and H_y set equal to zero.

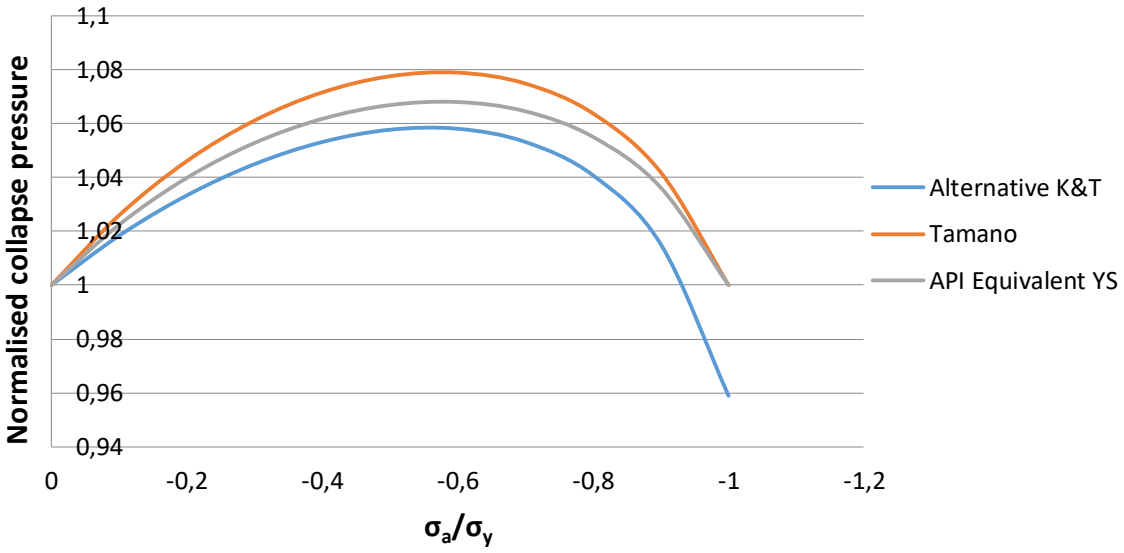

Figure 9: Collapse pressure for casings in compression normalised by performance of casings of neutral axial loading

Figure 9 shows the performance of pipes in compression when using the modified alternative K&T formulation, API equivalent yield strength and Tamano. The collapse values have been normalised by the collapse rating of an identical pipe without axial load. The three models show similar trend, with the alternative K&T formulation being the most conservative predictor of increased collapse strength. The original Tamano model have proven to be accurate by ISO/TR 10400 for the datasets which include axial loads, however, it is not clear if pipes are tested in tension or compression (ISO/TR 10400, 2007). The Tamano model shows a maximum of 8% collapse strength increase. The traditional API approach indicates a maximum of 6.8% increase.

The benefit of increased collapse strength of casings under axial compression is not utilised by engineers. As far as the author is aware, only Greenip (2016) have provided publicly

available experimental test data for collapse of pipes exposed to axial compression. For the 7 in pipes subjected to axial compression load equivalent to 40-50% of yield strength, pipe performance change from -1.6% to 5.4% with an average increase in strength of 1.5% (one outlier removed). These results are more conservative than the analytical models from Figure 9. A slight decrease of collapse strength occurred for 3 out of 9 samples contradicting theory. Still, no pipes are alike meaning a direct comparison of only a few samples without exact value for the decrement function is not sufficient to firmly draw any conclusion.

The ULS model is proven to be accurate for casings without axial load in section 3.2. The use of the alternative K&T formulation is only recommended for casings subjected to axial compression as a qualitative indication rather than accurate predictor. In any case it is believed to be more plausible than the suggested model by ISO which mirrors performance under tensional loads. More experimental tests of casing performance in compression are needed for model verification.

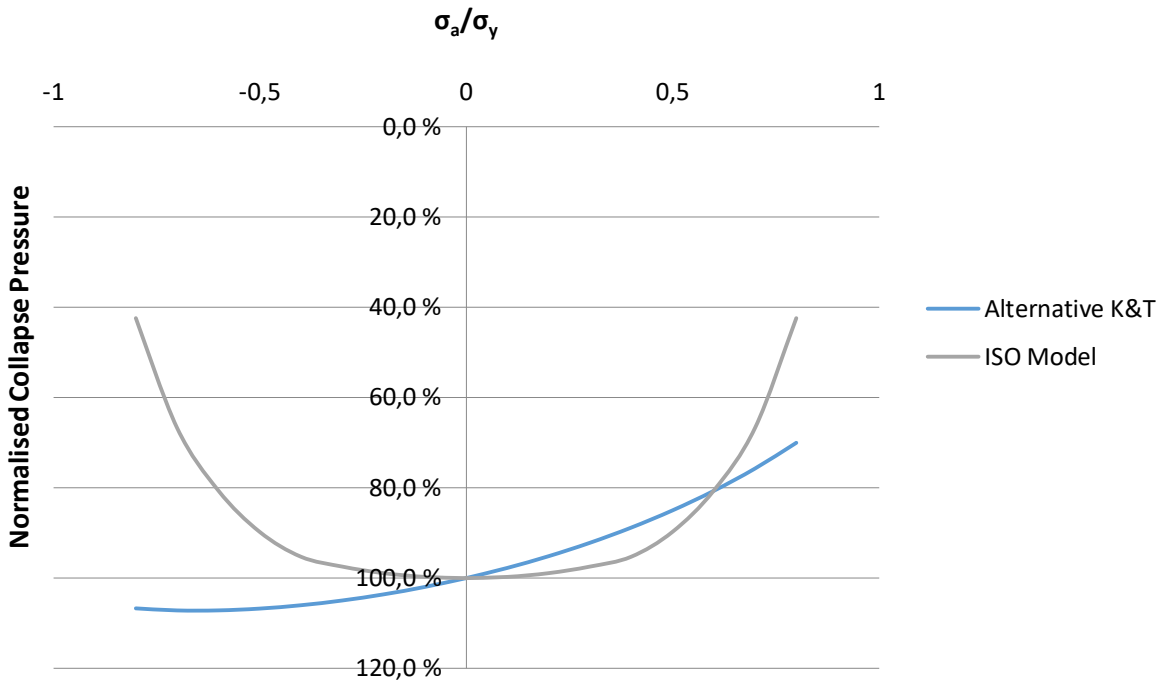

Figure 10: 9 5/8 in 53.5 ppf P-110 performance according to the ISO model and alternative K&T formulation

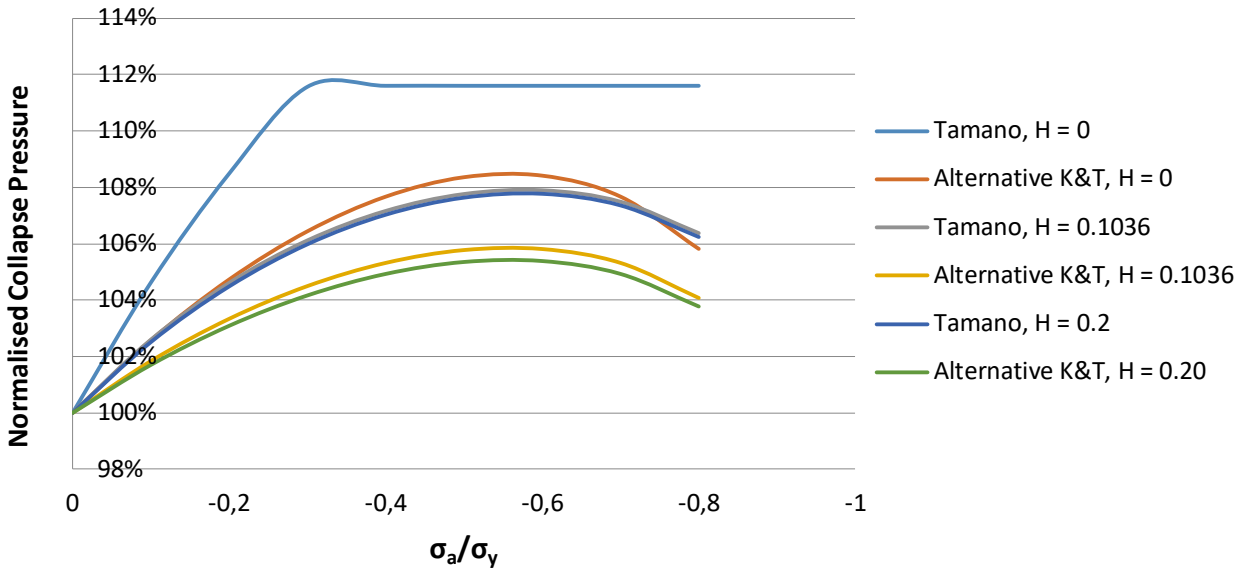

Figure 11: Casing performance dependence on decrement function according to Tamano and alternative K&T formulation normalised by neutral collapse rating

The increased strength predicted by the Tamano model and the alternative K&T formulation for casings subjected to axial compression is dependent upon geometric properties featured in the decrement function. Figure 11 summarises the results where increased strength varies according to the value of the decrement function. For both models the shape of the curve is similar. The perfect pipe modelled by Tamano seems to converge to its limit of 12%.

4.2.3.3 Suggested Compression Factor

It should be noted that the estimated collapse pressures obtained by the different models do not provide the exact same absolute value. Depending on geometric properties, the alternative K&T formulation may overestimate or underestimate strength of a casing of neutral axial loading compared to the ULS model. The latter model has been proven to be accurate for such applications.

It is clear that the alternative K&T formulation cannot be used for accurate prediction of strength unless verified or parameters are calibrated. No such effort has been made in this report. It is suggested that the results from this section will be used as qualitative indication of increased strength. In doing so, the effect of geometric properties, e.g. decrement function, on

the alternative K&T formulation must be investigated. Figure 12 shows the strength dependence of the decrement function in compression. The maximum increased strength is 8.3% for a perfect pipe. For the worst performing pipe the maximum increased strength is about 5%. It was proven to be less than predicted by Tamano and API. Using polynomial approximation of the most detrimental curve of Figure 12, a factor may be introduced to increase the strength predicted by the ULS model of a casing of neutral axial loading with a certain percentage. The trend line or *compression factor* is given in Equation (24).

$$f_{compression} = -2.4608\left(\frac{\sigma_z}{\sigma_y}\right)^6 - 6.3693\left(\frac{\sigma_z}{\sigma_y}\right)^5 - 6.0504\left(\frac{\sigma_z}{\sigma_y}\right)^4 - 2.6474\left(\frac{\sigma_z}{\sigma_y}\right)^3 - 0.673\left(\frac{\sigma_z}{\sigma_y}\right)^2 - 0.2204\left(\frac{\sigma_z}{\sigma_y}\right) + 1 \quad (24)$$

Although this method needs verification by physical experiments it will be used qualitatively for discussion. Since the workgroup of ISO proposed a simplified version of K&T original publication in 2006 ignoring compression, their calibrated parameters may not directly be used in the alternative K&T formulation for compression without further analyses.

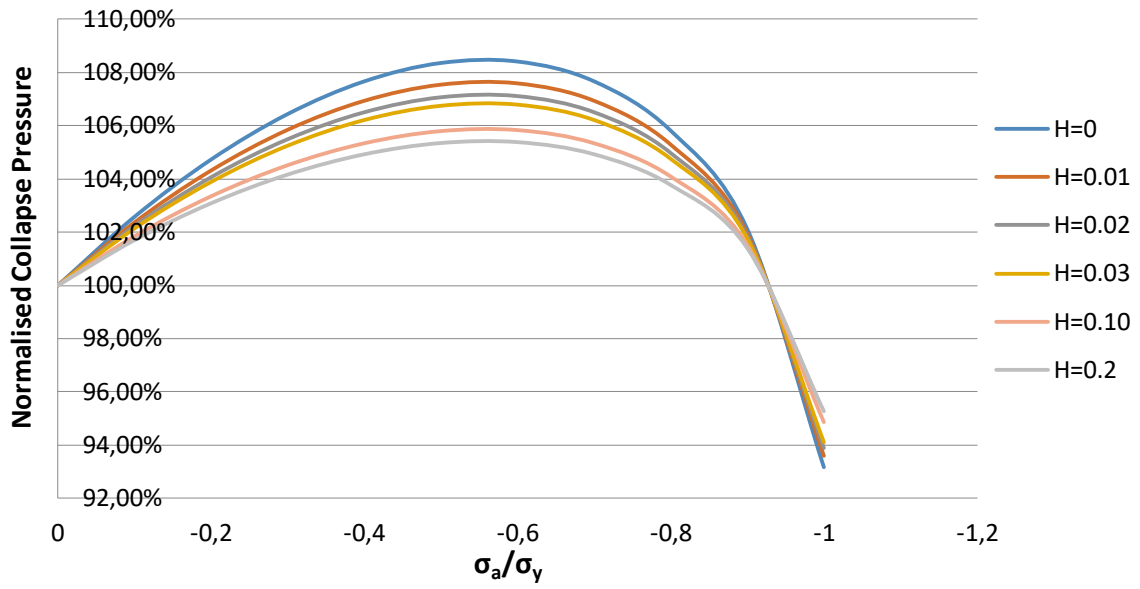

Figure 12: Collapse strength dependence on pipe imperfections according to the alternative K&T formulation

4.3 Effect of Imposed Ovality

The effect of ovality is featured in the decrement function introduced in both Tamano et al. (1983) and Klever and Tamano (2006). However, the decrement function is designed for small deformations. In the Tamano model only ovality from the manufacturing process is considered. Imposed ovality is not considered but may occur in the field and significantly reduce collapse resistance.

Average ovality from the ensemble was found to be 0.217% for seamless casings. The governing case features a mean value of 0.795% with a coefficient of variance of 0.1. The probability distribution plots from ISO clearly show that ovality rarely exceeds 1%. The target reliability level is exceeded at 1% ovalisation (ISO/TR 10400, 2007). However, a casing may be ovalised to a far greater extent than, for example by geotectonic loading, field handling or fluid pressure.

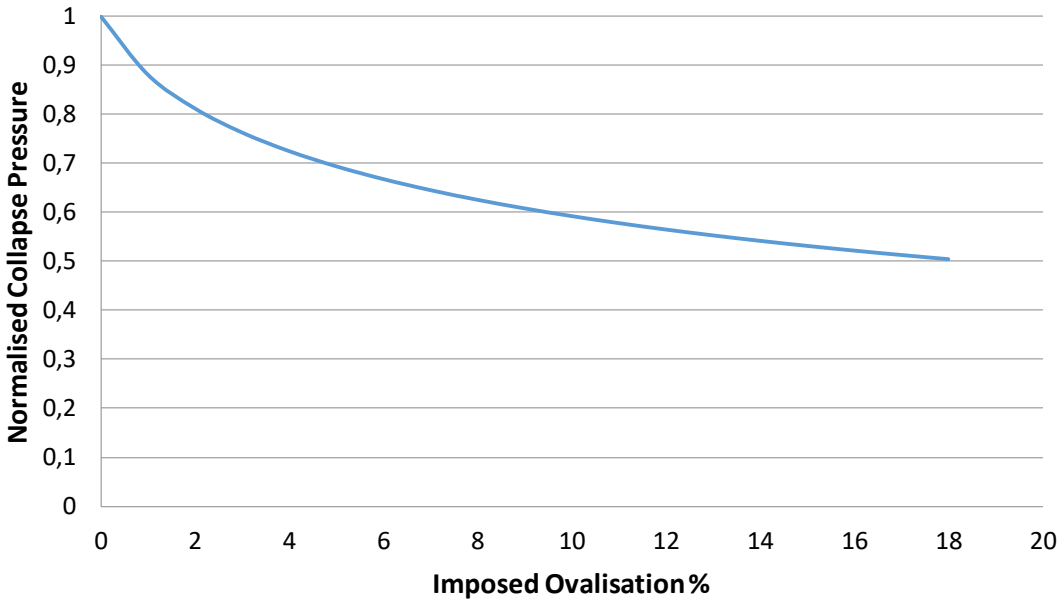

Figure 13: Effect of ovality in decrement function for the ULS model

As indicated by Figure 13 the collapse resistance predicted by the ULS model is greatly affected by ovalisation. Experimental data are needed for verification.

Pattillo et al. (2003) have performed physical tests on welded 4 ½ in 13.3 ppf P-110 casing samples by imposing non-uniform loading. An array of plates are placed on opposite sides of a casing and tightened or clamped on, exerting a force on the casing. The end result is an ovalised casing which was submerged into a pressure vessel and loaded by fluid pressure until collapse. If the ovalisation due to the plates is less than the ovalisation in the casing when it normally collapses due to external fluid pressure only, the plate ovalisation has no effect on the collapse pressure. In such a scenario, the casing will lose direct contact with the plates and collapse as if there were no plates present (Pattillo et al., 2003). This can be seen by the relative flat response in collapse resistance reduction for low ovality in the experimental data (Figure 14). The reduction in collapse resistance is not as severe as predicted, thus rendering the use of conventional collapse equations for non-uniform loading as inapplicable.

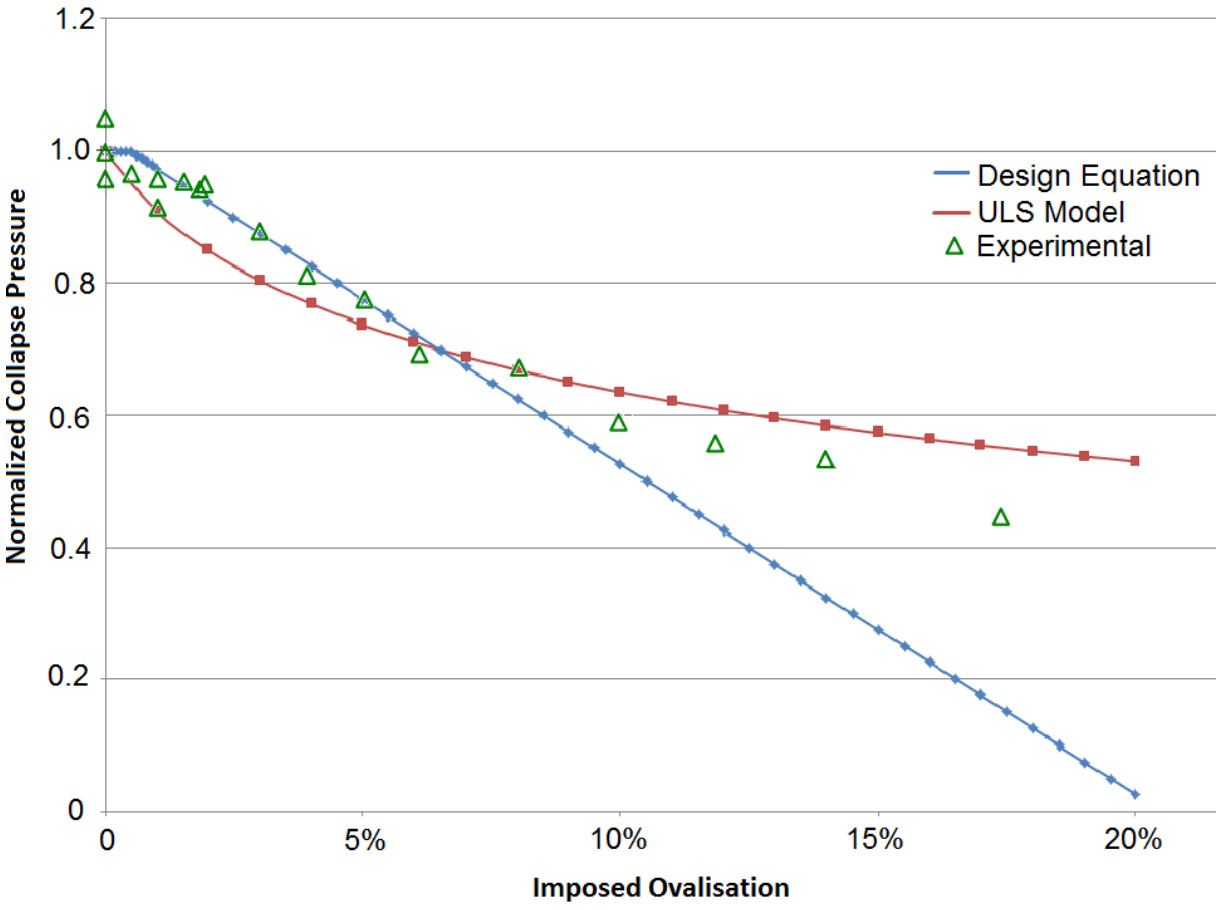

Figure 14: Collapse resistance reduction predicted by the ULS model compared with experimental data from Figure 9 in SPE-74560-MS by Last et al. (2002). The design equation is given in Eq. (25).

Theoretical studies of the effect of ovality on tubular collapse resistance using conventional collapse equations consistently indicate 25% collapse resistance reduction at an ovality of 1-

2%. Empirical investigations indicate a much smaller effect. Ovality is only one of many pipe parameters that influence collapse resistance. Historically ovality has not been singled out as a dominant parameter. In the rare case of ovality exceeding 1% its effect on collapse resistance has been accounted for through the use of minimum performance values (ISO/TR 10400, 2007). If this approach is not selected, e.g. using average values to accurately predict actual strength, a derating function must be applied for imposed ovality.

The calculated collapse pressure for non-ovalised casing should be derated by an ovality factor, $f_{ovality}$ when ovality is imposed. The original decrement function is calibrated by manufacturing ovality up to 1%. A linear derating function has been proposed by Last et al. (2002) which is more conservative than numerical simulations (Last et al., 2002). The threshold for when imposed ovality affects collapse resistance has been set to 0.5%, giving the characteristic initial flat response. The ovality factor is given in Equation (25).

$$f_{ovality} = \begin{cases} 1.0 & ,for\ ovality < 0.5\% \\ 1 - 0.05(ov - 0.5) & ,for\ ovality > 0.5\% \end{cases} \quad (25)$$

4.4 Effect of Casing Wear

Casing wear from drilling operations will reduce collapse strength significantly. Collapse strength ratings are given for factory new casings. In deviated wells the drill string will cause local wall thickness reductions by rotation and drag in contact with the casing wall. Separate models are common in the industry to simulate wear for each drilling operation. Physical measurements may be taken by caliper logs, ultrasonic imaging or similar.

Future casing wear holds great uncertainties. Current collapse strength calculations do not consider casing wear. The industry leading software used for well design performs calculations to indicate maximum allowable casing wear in percentage before collapse is initiated and integrity is lost. However, the reported percentage assumes the casing to be uniformly worn down all along the inner wall. Effectively, the software finds the thinnest casing that, according to the conservative API equation, can withstand the imposed loads even with a design factor applied. In reality casings are not worn uniformly. In fact, the worst case

scenario would be having the tool joint of the drill string concentrated at either the high or low side of casing throughout the entirety of all drilling operations. The tool joint would induce local wall thickness reduction of greater magnitude than a scenario of uniformly distributed wear. In terms of performance 1% uniform wear will reduce collapse strength more than 1% local wear.

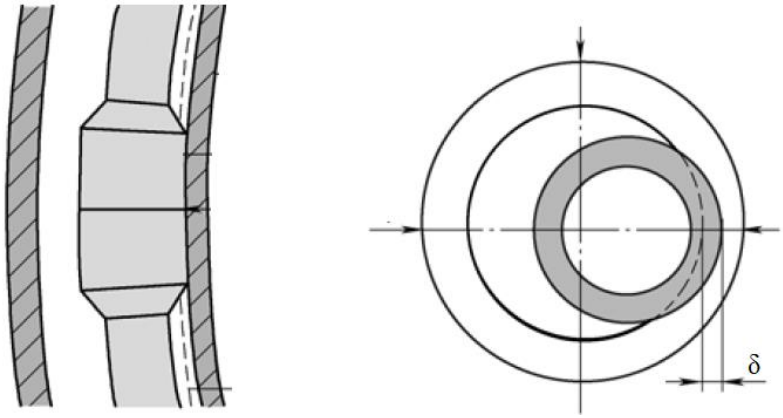

Figure 15: Figure 1 from Liang et al. (2013) shows the mechanism of casing wear where δ is the maximum wall thickness reduction

4.4.1 Physical Experiments

SPE-24597-MS

Through publication of conference paper SPE-24597-MS, Kuriyama et al. (1992) from the former Nippon Steel Corp. and Japan National Oil Corp. investigate the effect of casing wear on the four types of casings listed in Table 18 for three different levels of wear. The wear radius is half of the tool joint outer diameter. The size and capacity of the pressure testing vessel limits the specimens to be tested at 7.0 in outer diameter. The specific wear radius values in Table 18 have been chosen as to represent a 6 ½ in tool joint OD used in a 9 5/8 in casing. The tool joint diameter is roughly 70% of the casing diameter. The wear depth has been limited to 45% of the wall thickness which is sensible for all practical purposes as casing wear will not exceed 50% (Kuriyama et al., 1992)

Table 18: Experimental setup (casing wear) by Kuriyama et al. (1992)

Grade [-]	σ_y [psi]	Weight [ppf]	OD ["]	t ["]	Wear Radius [in]	Wear Depth [%]
S55C	77600	17.00	5,5	0,304	0,5906	0, 20, 35
N80	101200	17.00	5,5	0,304	1,9685	0, 25, 45
N80	91800	29.00	7	0,408	2,4606	0, 20, 40
P110	140650	29.00	7	0,408	2,4606	0, 20, 30

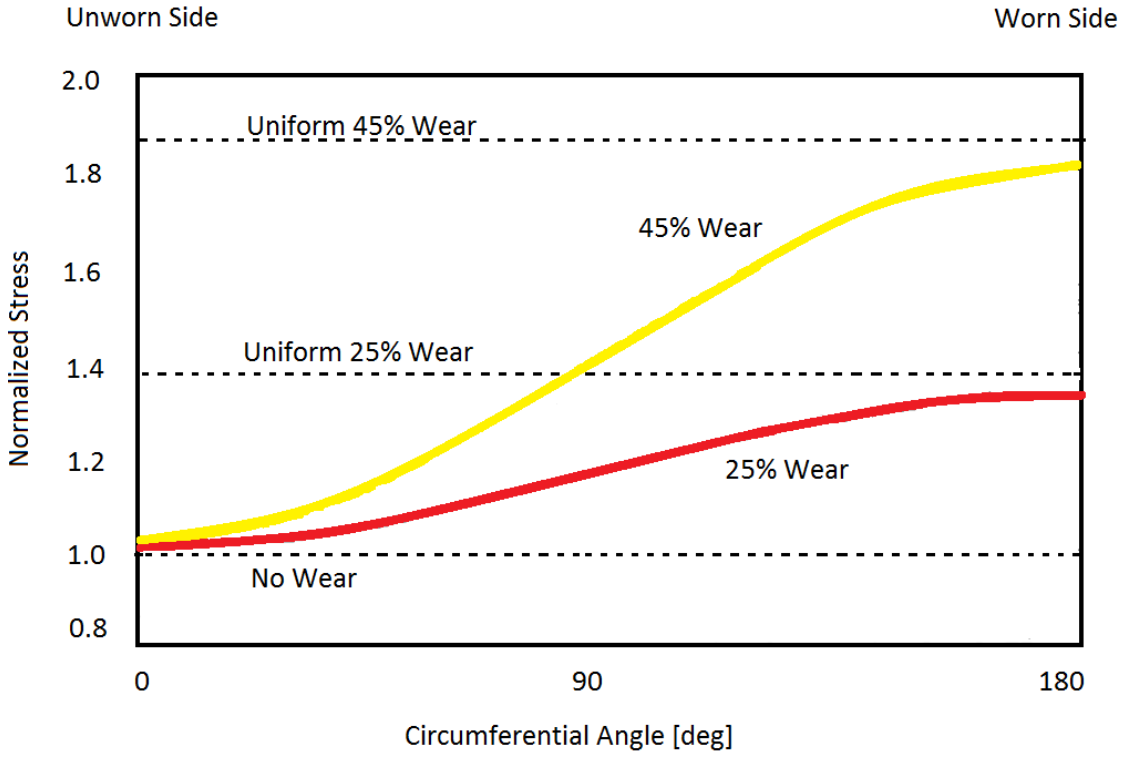

Figure 16: Stress distribution of worn casing normalised by unworn casing stress. Extracted from Figure 8 of Kuriyama et al. (1992)

The worn part of a casing will be exposed to the highest stress levels. Theoretical studies of the circumferential stress reveal the stress state of the casing (Kuriyama et al., 1992). Figure 16 shows constant stress levels all along the inner wall of the casing for uniform wear. If the casing is subjected to local wear, this region will experience the highest circumferential stress at all times. The unworn side of the casing will not experience increased stress levels. Instead a gradual increase in circumferential stress is expected towards the worn side. Even so, analytical studies indicate the maximum stress at the worn side will be slightly less than as if the casing was uniformly worn by the same percentage. It is then obvious the worn side of the

casing will reach onset of yield first and exhibit plastic behaviour, ultimately leading to collapse and loss of integrity. Evaluation of collapse strength of worn casing by uniform wear approximation leads to overestimation of the wear's detrimental effect with regards to collapse strength.

Experimental collapse data of unworn and worn 5 ½ in N-80 casing show a linear reduction of strength as a function of wear (Figure 17). The deviation in collapse strength for equal amounts of wear is believed to be caused by pipe imperfections. With a wear radius of 1.9685 in or 50 mm the collapse strength is reduced slightly less than 1% for every per cent of wear (Figure 17). Using the general approximation of 1% collapse strength reduction for 1% of casing wear will be conservative.

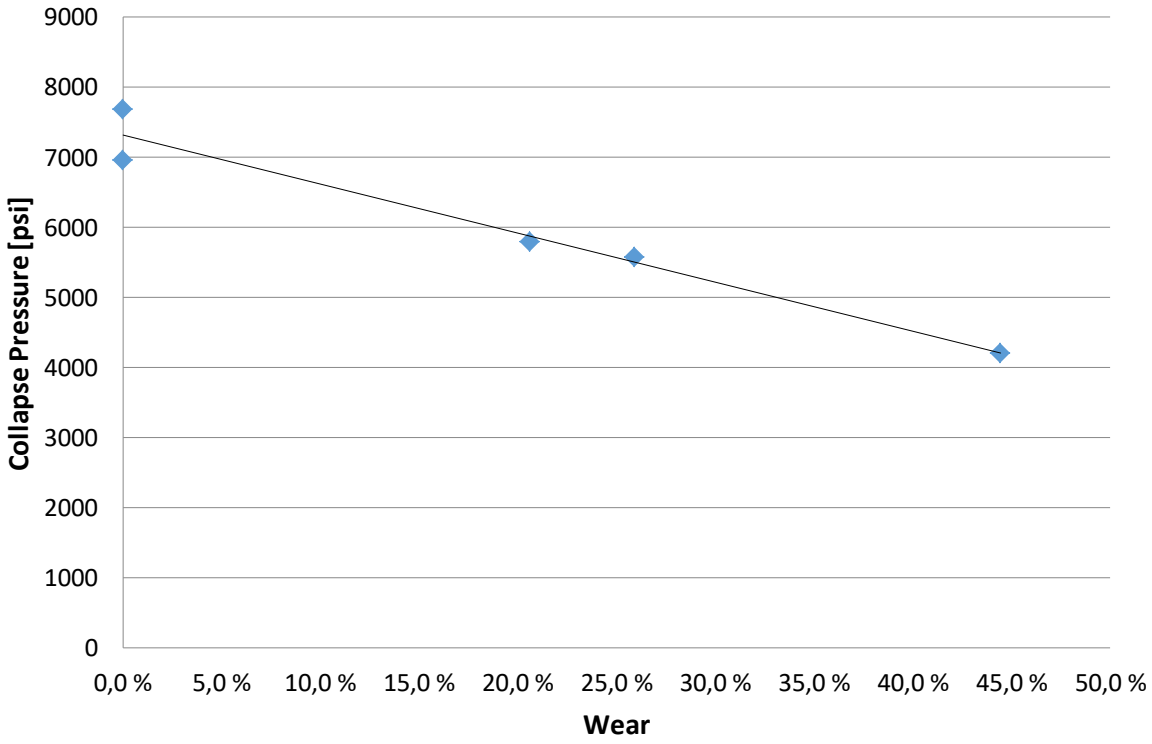

Figure 17: 5.5 in 17.00 ppf N-80 casing performance. Extracted from Figure 3 of Kuriyama et al. (1992)

Kuriyama et al. (1992) also conduct experimental tests on worn and unworn 7 in 29 ppf P-110 casings. Figure 18 summarises the results. The general trend is in accordance with section 4.2 where axially loaded unworn casings were tested. The deviation seen for the casing with 23% wear could be due to pipe imperfections. It is not possible to verify since yield strength is the only measured parameter. In addition the 7 in casings were cut into lengths 6 times greater

than the diameter, less than recommended length according to API. Nonetheless, it is believed that axial loading of worn casing should not be treated as a special case since both effects are accounted for separately.

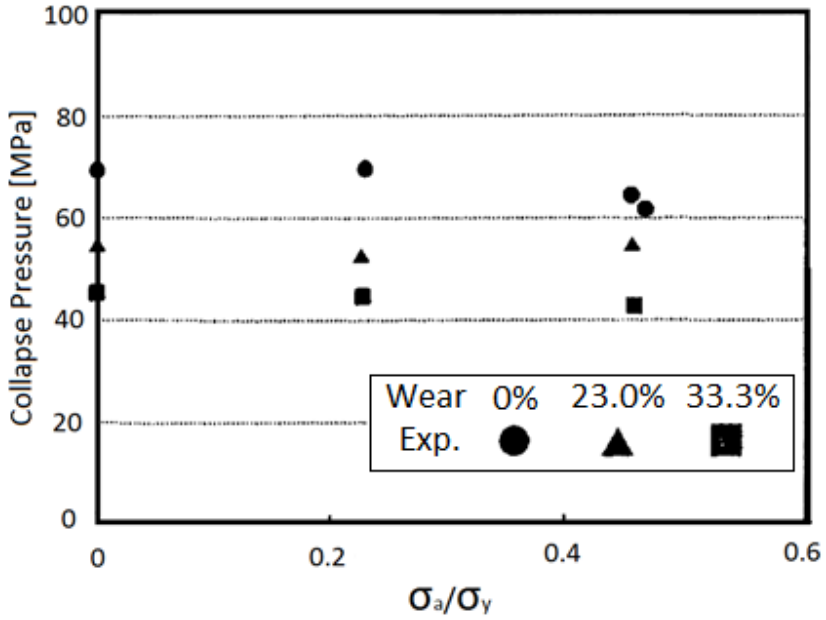

Figure 18: 7 in 29.00 ppf P-110 casing subjected to simultaneous forces. Extracted from Figure 10 of Kuriyama et al. (1992)

Chinese Journal of Mechanical Engineering (2013)

Another technical journal article that also investigates casing wear effect on collapse strength by analytical, FEA and experimental methods was published in Chinese Journal of Mechanical Engineering (2013). Liang et al. (2013) conduct experimental collapse tests on three types of casings according to the set up as described in Table 19. The collapse pressure values are used to verify the accuracy of analytical and numerical methods.

As seen in Table 19 the 9 5/8 in casings are systematically worn by a tool which represents the OD of a drill pipe tool joint of 6.6 in. For production casings in Norway, this would be a typical set up. An unworn casing is used as reference.

All casings are selected from the same furnace or production batch. Only one measurement is taken on a single casing for each parameter. Identical properties are assumed for casings of the same type. Although the parameters are likely to be similar, they are not identical. Each

parameter will have a probability distribution as the statistical analysis in section 3.3.1 revealed. Taking measurements for only one casing will save resources, however, it will be inaccurate.

Table 19: Experimental results of worn casings (Liang et al., 2013)

Grade	σ_y	Weight	OD	t	rs/fy	Wear Radius	Wear Depth	Collapse Pressure
[-]	[psi]	[ppf]	["]	["]	[-]	[in]	[%]	[psi]
S-55C	60900	20.00	5,5	0,394	-0,1190	1,752	20	4930
S-55C	60900	20.00	5,5	0,394	-0,1190	1,752	50	3480
N-80	101200	17.00	5,5	0,304	-0,2149	1,752	25	5800
N-80	101200	17.00	5,5	0,304	-0,2149	1,752	45	4350
P-110	129000	47.00	9 5/8	0,472	-0,2248	3,307	0	8715
P-110	129000	47.00	9 5/8	0,472	-0,2248	3,307	25	6337
P-110	129000	47.00	9 5/8	0,472	-0,2248	3,307	50	4002

For the 5 ½ in S-55C casings, a 30% increase in local wear will reduce collapse strength by 29.4%. Similarly, an additional 20% wear corresponds to 25% strength reduction of 5 ½ in N-80 casings. For the 9 5/8 in P-110 casings, 25% and 50% casing wear reduces collapse strength by 27.3% and 54% relative to the unworn casing.

Only the S-55C tests exhibit the exact linear trend of 1% collapse strength reduction for 1% wear, or the 1%-rule. Where as in Kuriyama et al. (1992) the collapse strength reduction was slightly less than 1%, the results presented by Liang et al. (2013) indicate collapse strength reduction of slightly more than 1%. Since none of the technical papers have measured parameters accurately, it is difficult to make a definitive conclusion.

4.4.2 Numerical Simulations

SPE-74560

Last et al. (2002) analyse the exact same situation as the previous two technical papers: 6 ½ in tool joint wearing down a 9 5/8 in casing. Only numerical simulations, i.e. Finite Element Analysis, are used to analyse the effect of wear. Nodes are placed along the inner casing wall at the contact point with the tool joint.

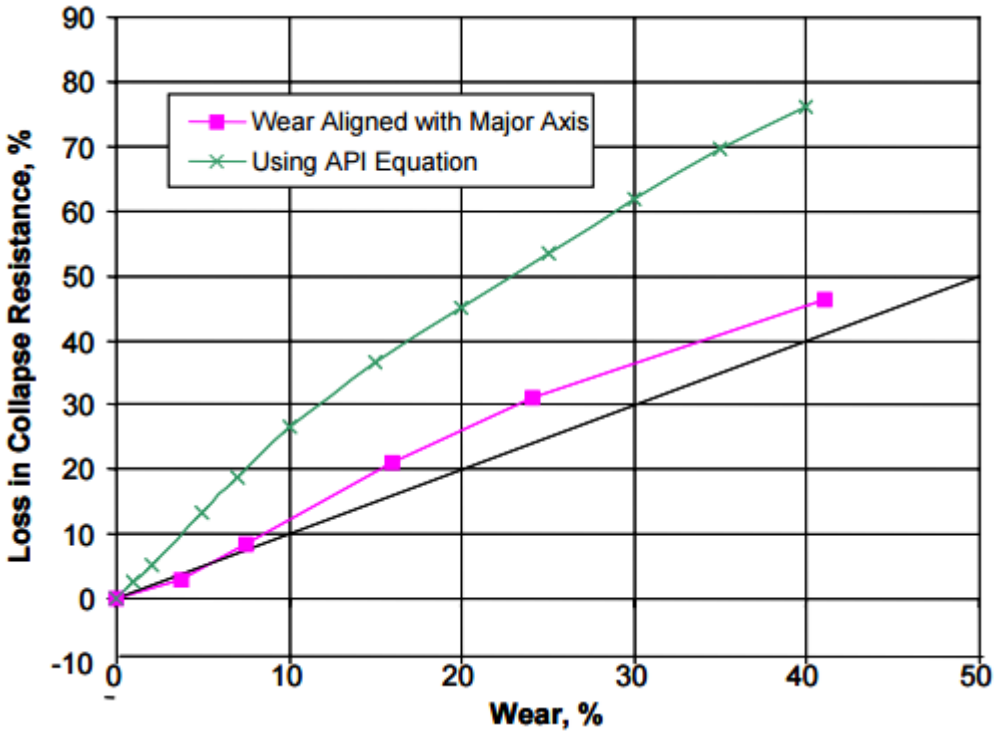

Figure 19: Analytical and numerical simulations of casing collapse strength of worn casing (Last et al., 2002)

Results show deviation from the linear trend at 7% wear. If more severe wear is experienced the loss in collapse resistance is greater than predicted by the 1% rule. This is in line with the experimental results from Liang et al. (2013) but not their numerical results for large OD tool joints in Figure 20. In any way the uniform wear approximation through analytical models is significantly inaccurate.

Chinese Journal of Mechanical Engineering (2013)

Finite element analysis suggests a linear trend in collapse strength with regards to casing wear for large OD tool joints. Smaller wear radius will induce a more curved shape. Figure 6 of Liang et al. (2013) also shows the dependence of wear radius on casing collapse strength for a 7 in 32.00 ppf P-110 casing. Small wear radiuses are more detrimental than larger wear radiuses for the same wear depth. The tool joints used in a 9 5/8 in casing is larger than 5.47 in – the largest wear radius investigated - indicating a linear trend.

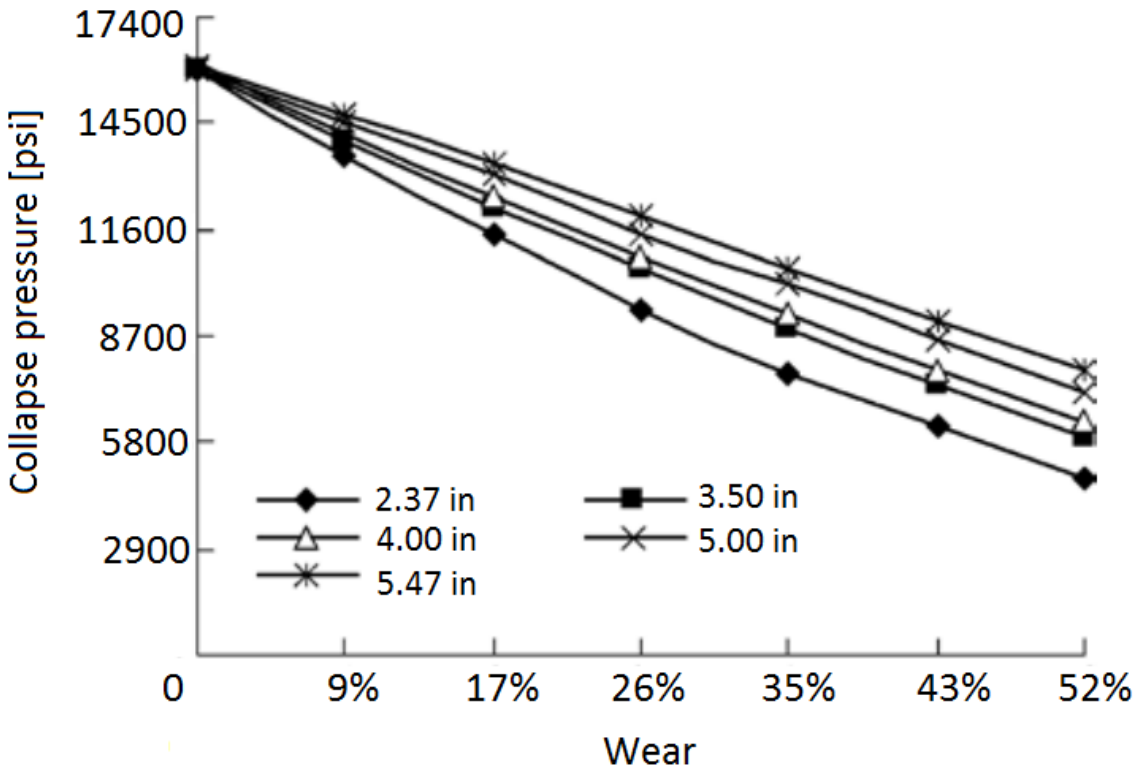

Figure 20: FEA of collapse strength reduction due to wear for various radiuses. Extracted from Figure 6 of Liang et al. (2013).

4.4.3 Recommended Casing Wear Factor

The aim of this chapter is to give an indication of the effect of casing wear on casing collapse resistance rather than predicting the exact consequences of casing wear. All technical documents reviewed are more or less in line with general industry practice governed by the 1% rule, i.e. every per cent of local wear reduces collapse strength by the same magnitude.

Experimental results from Kuriyama et al. (1992) and Liang et al. (2013) are deemed inconclusive due to the lack of parameter measurements. However, the results may still be used as an indication, in addition to verification for numerical and analytical models. Discrepancies will be present when comparing experimental and numerical or analytical results due to uncontrollable imperfections of any pipe.

Last et al. (2002) agrees with Kuriyama et al. (1992) on the proportionality of casing collapse strength and casing wear. Similar results are obtained by Liang et al. (2013) for both experimental research, as well as numerical and analytical modelling.

Although no experimental results can prove exact proportionality, it is more or less sufficient to apply the 1% rule and rather account for inaccuracy through applying a design factor for casing collapse strength. For engineering purposes this is required by governing documentation, where casing wear is one of many uncertainties.

The *wear factor* given in Equation (26), where w is wear given in percentage, must be multiplied by the collapse pressure obtained by the ULS model.

$$\mathrm{f_{wear}} = (100 - w)/100 \tag{26}$$

4.5 Effect of Cement Support

Both the historical API approach and Klever & Tamano models present casing collapse resistance against external hydrostatic fluid pressure. The models assume the annulus to be filled with nothing but fluids. However, casing collapse and/or deformation is commonly caused by formation movement such as reservoir compaction, flowing salt formations, shale swelling, in addition to geotectonic loading. Current collapse ratings are not valid for such scenarios. As the field has not experienced issues related to formation movement, these collapse mechanisms will only be used for discussion and not implemented in the ULS model.

Collapse resistance models do not consider the effect of cement or formation support. In field examples, cement of varying quality will be present throughout parts of the casing string, if not the entire section. Results indicate increased casing strength when the string is uniformly surrounded by cement or formation.

SPE 173069

Klever as co-author of Jammer et al. (2015) study the effect of cement and dual string systems by applying fluid pressure in the annulus between two casings, and/or externally of the outermost casing. The paper focuses on 11 ¾ in 65 ppf P-110 HC casing cemented into a 13 5/8 in 88.2 ppf Q-125 casing. All casings were acquired from a pipe distributor and originate from the same manufacturer. The casing joints were cut into a number of specimens for collapse testing with L/D ratio of 6-8. Numerical simulations aim to provide a strength

prediction but will be ignored in this report. Only the experimental test results will be mentioned.

Relevant parameters were measured and recorded prior to testing. Full details of geometry and material data for each of the pipe test joints can be found in Table 40. Several measurements were taken for the cut pieces of casing. By doing so, multiple measurements for the original joint of casing are obtained and can filter out outliers. For the 11 ¾ in casings, the average normalised yield strength ranges from 1.181 to 1.231 with standard deviations ranging from 1322 psi to 6296 psi. The high yield strengths confirm the high collapse product marking. Similarly, for the 13 3/8 in casings the normalised yield strength varies from 1.006 to 1.086 with standard deviations ranging from as little as 681 psi to 2295 psi. Once again the high collapse nature of the P-110 casings are indicated by having similar yield strengths as Q-125 casings.

The experimental test program consists of three setups. The 1st phase tests five 11 ¾ in specimens for external pressure only. The 2nd phase features 11 casing-cement-casing systems with class H cement cured for 10 days with varying circumferential extent, represented as *void degree*. A perfect cement job is classified by 0 degree void, whereas 300 degree void is a system of largely uncemented parts. External pressure is applied. The annulus between the casings is also pressurised simulating pressure migration into the cement, so called "Annular pressure". The 3rd phase consists of eight tests of similar setup as the previous phase but where only external pressure is applied.

Phase 1 - Pipe Only

The five collapse test of 11 ¾ in 65 ppf P-110 HC casings record external pressure ranging from 6250 psi to 6540 psi. All values are greater than the API minimum rating of 4476 psi. Actual collapse values for these pipes are also 9% to 14% higher than the high collapse manufacturer guaranteed rating of 5740 psi.

For the 13 5/8 in 88.2 ppf Q-125 casings the collapse pressure range from 7260 psi to 7780 psi – all greater than the API rating of only 4801 psi.

Phase 2 - Annular Pressure

Phase 2 applies the same pressure to the annular space between the casings and to the external surface area of the outermost casing. The differential pressure across the 13 5/8 in casing will be zero. The full pressure differential is experienced across the wall of the 11 ¾ in casing as no internal pressure is applied. The collapse mechanism is deformation of the innermost casing in every test, as expected.

Table 20: Experimental test results of annular collapse pressure. Extracted from Table 3 from Jammer et al. (2015)

Test	Pipe inside	Length	Eccentricity	Pipe outside	Length	Cement void	Collapse pressure
[-]	[in]	[ft]	[%]	[in]	[ft]	[deg]	[psi]
0	11 3/4	8	100	13 5/8	7	0	10280
1	11 3/4	8	0	13 5/8	7	0	10390
2	11 3/4	8	0	13 5/8	7	15	10360
3	11 3/4	8	0	13 5/8	7	15	10340
4	11 3/4	8	0	13 5/8	7	30	10080
5	11 3/4	8	0	13 5/8	7	45	10260
6	11 3/4	8	0	13 5/8	7	60	9000
7	11 3/4	8	0	13 5/8	7	60	11130
8	11 3/4	8	0	13 5/8	7	100	10110
9	11 3/4	8	0	13 5/8	7	100	10860
10	11 3/4	8	0	13 5/8	7	200	7900
11	11 3/4	8	0	13 5/8	7	300	7240

The lengths of all 13 5/8 in casings are less than required by API/ISO. Since collapse is initiated only on the innermost casing, this discrepancy can be disregarded.

The 11 test results are shown in Table 20. No significant difference was seen for an eccentric 11 ¾ in casing. When using cement and an outer casing, collapse resistance has increased. For good quality cement up to 45 degrees of void, all collapse pressures are higher than 10 000 psi. This represents at least a 52.9% increase in strength when compared to the best performing single 11 ¾ in casing. Some discrepancies are found above 60 degrees of void but the general trend shows increased strength depends on cement quality. However, even a poor cemented sample has increased strength compared to phase 1 testing of pipe only.

As expected, the results show various performances for the exact same setup. Two samples of 60 degrees void indicate significantly different performance with 9000 psi and 11130 psi. Similarly, two tests with 100 degrees void collapsed at 10110 psi and 10860 psi but are within the normal scatter of casing collapse strength (Jammer et al., 2015). On the contrary, the two tests with 15 degrees void are nearly identical. In addition small errors or factors that are not in control of the author may have played its part. Jammer et al. (2015) investigates the significantly different collapse pressures for systems with 60 degrees of void. The casings were cut open after testing for examination. The location of collapse occurred in the void area for the strongest composite system (dual tubular string), while the significantly different lower pressure collapsed the other composite system about 90 degrees from the void area.

Phase 3 - External Pressure

For all external pressure tests the mode of failure was collapse of the composite pipe-cement-pipe system. For large cement void angles, cascading collapse occurred where the outer casing collapsed first, and then hit and crushed the inner pipe at pressures lower than the collapse pressure of the outer pipe (Jammer et al., 2015).

Since pressure is only applied to the exterior of the composite system, i.e. on the outer wall of the 13 5/8 in casings, collapse values must be compared to that of 13 5/8 in casings only. Maximum collapse strength was recorded at 7780 psi for a 13 5/8 in casing. Installing a smaller casing filled with cement in the annular space vastly improves collapse rating. Test results can be found in Table 21. The assumption is no pressure communication between annulus and the outside of the 13 5/8 in casing. For good cement quality, additional collapse resistance could be well over 20 000 psi. For comparison no standard API casings are listed with a collapse rating that high. Even small OD casings with thick walls do not exceed 20 000 psi. A 5 in P-110 casing with wall thickness of half an inch is listed at 19800 psi. Collapse ratings are naturally reduced with increased outer diameter as the surface area and total force increases. To obtain a pipe only collapse resistance of 26830 psi in the K&T model, the wall thickness must be 1.45 inches. Using a composite system could, according to the experiments from Jammer et al. (2015), have huge benefits in terms of low pressure production well integrity in high pressure areas.

Table 21: Experimental test results of external collapse pressure. Extracted from Table 4 from Jammer et al. (2015)

Test	Pipe inside	Length	Eccentricity	Pipe outside	Length	Cement void	Collapse pressure
[-]	[in]	[ft]	[%]	[in]	[ft]	[deg]	[psi]
0	11 3/4	7,83	100	13 5/8	8	0	24730
1	11 3/4	7,83	0	13 5/8	8	0	26830
2	11 3/4	7,83	0	13 5/8	8	15	24450
3	11 3/4	7,83	0	13 5/8	8	30	22170
4	11 3/4	7,83	0	13 5/8	8	45	21640
5	11 3/4	7,83	0	13 5/8	8	60	17150
6	11 3/4	7,83	0	13 5/8	8	100	10040
7	11 3/4	7,83	0	13 5/8	8	200	9060
8	11 3/4	7,83	0	13 5/8	8	300	7720

SPE 4088

Evans and Harriman (1972) investigate the effect of full cement support on casing collapse resistance. External pressure is applied to the bare cement sheat confining a 2 3/8 in 4.6 ppf tubing. Three different tubing grades are tested. A 1 inch cement sheat of API class A cement is cured and obtains early compressive strength of 2930 psi. The results are reproduced in Table 22.

Table 22: Experimental test results of cemented casings (Evans and Harriman, 1972)

Test conditions	H-40	J-55	N-80
[-]	[psi]	[psi]	[psi]
Not cemented	8200	10250	15000
Full cement sheath	10750	13150	16000
Strength increase	23,5 %	22 %	3 %

For the J-55 tubing various degrees of cement void were reproduced to investigate the effect of cement quality. As expected, increased collapse strength are not realised for poor quality cement.

Dual tubular strings similar to the composite system in Jammer et al. (2015) are also tested. A 5 ½ in 17 ppf J-55 casing in a 8 5/8 in 36 ppf J-55 outer casing with cement in the annular

space exposed to external hydrostatic pressure. No collapse was achieved at the testing machine's pressure limit of 18 000 psi – more than either pipe's collapse ratings. The casings were scaled down while maintaining a constant diameter ratio as to represent 13 3/8 in casing in a 20 in conductor. The curing time for cement was varied to investigate the effect of cement's compressive strength. Figure 7 of SPE-4088-MS (Evans and Harriman, 1972) shows linear increase of collapse resistance with increased cement compressive strength.

Once the strengths of collapse due to hydraulic pressure were obtained, similar casing setups were tested by mechanical point loads. Compressive force was applied and the increase in collapse strength due to cement or dual string was less than that of hydraulic pressure. Point loads are non-uniform and may represent tectonic environments.

The paper was published in 1972. Improvements in the casing manufacturing process and material quality have been made. No effort has been made to verify the magnitude of collapse strength. Nonetheless, the trends are similar to that of Jammer et al. (2015) except for the N-80 casing which only showed 3% increase of collapse resistance. It should be noted that smaller tubulars have higher collapse strengths and more variance compared to large OD casings with identical wall thickness. H-40 and J-55 also feature very high normalised yield strengths compared to N-80, C-110 and P-110.

Support from cement and/or formation is able to hinder ovalisation during yielding. This mechanism is believed to be the main contributor to increased strength.

4.6 Formation Loading

Last et al. (2002) perform a case study of the tectonically active foothills of Colombia motivated by operational challenges. Formation movement is the likely cause of casing deformation or ovalisation of casings making well entry and intervention difficult, if not impossible. Total shut in of the well before reaching end of its design life may be a severe consequence. Ekofisk, Norway, is experiencing the same issues but as a result of compaction.

Monitoring of wells have indicated casing deformation, i.e. ovalisation, accompanying formation movement, not shear as might be expected from fault movement (Last et al., 2002). The orientation of ovalisation aligns with the regional tectonics, and infers a strong link between the observed casing deformations and the rock stresses, Although deformation is small, typically a few millimetres, they are present over long intervals and sufficient to reduce collapse strength as discussed in section 4.3. The initial deformation rate is high, followed by a time-dependence according to formation stresses, implying a squeezing formation. The deformation starts earlier for cemented sections as opposed to sections where the annulus is filled with mud. Deformation is initiated by rock to casing/cement contact. The time dependence will vary according to local or regional tectonic activity. For the field in question, Last et al. (2002) observed single string ovality of 7% and dual string ovality of 5% after 2500 days. The corresponding initial ovality after some weeks was 2% and 3% respectively.

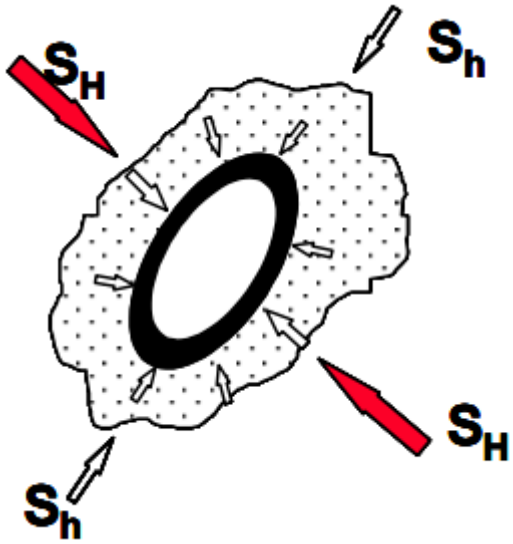

Figure 21: Ovalisation of casing in line with formation stresses (Last et al., 2002)

Numerical analyses on a system of three layers representing casing, cement, and formation, with far field stresses included were conducted. Imposed ovalisation may be as high as 10% before collapse resistance is reduced compared to the minimum API ratings for a single, free pipe. The minimum API ratings were used when designing these wells, so no collapse issues should occur prior to reaching 10% ovalisation. For a well in the tectonically active areas of Colombia, this deformation may take over 10 years to achieve. For further discussion it should be noted that the numerical analyses in Last et al. (2002) not provide actual collapse strength.

5 Case Study

When designing new wells the casing wall thickness may easily be increased to maintain well integrity even when using the conservative API collapse equations. A shift in paradigm towards new ULS models may decrease well cost. When evaluating actual collapse strengths of casings in existing wells the historical API collapse equations should not be used. Only modern collapse formulations are suitable for this purpose.

Advancements in production technology allow the well head pressure to be reduced to greater extents than designed for. Low pressure production implies barrier dependence when using conservative design criteria. The ULS model will be used to evaluate actual collapse strength of the 9 5/8 in 53.5 ppf P-110 production casing in an existing well which is a candidate for prolonged design life. The well is denoted as “Well K”.

5.1 Candidate Well

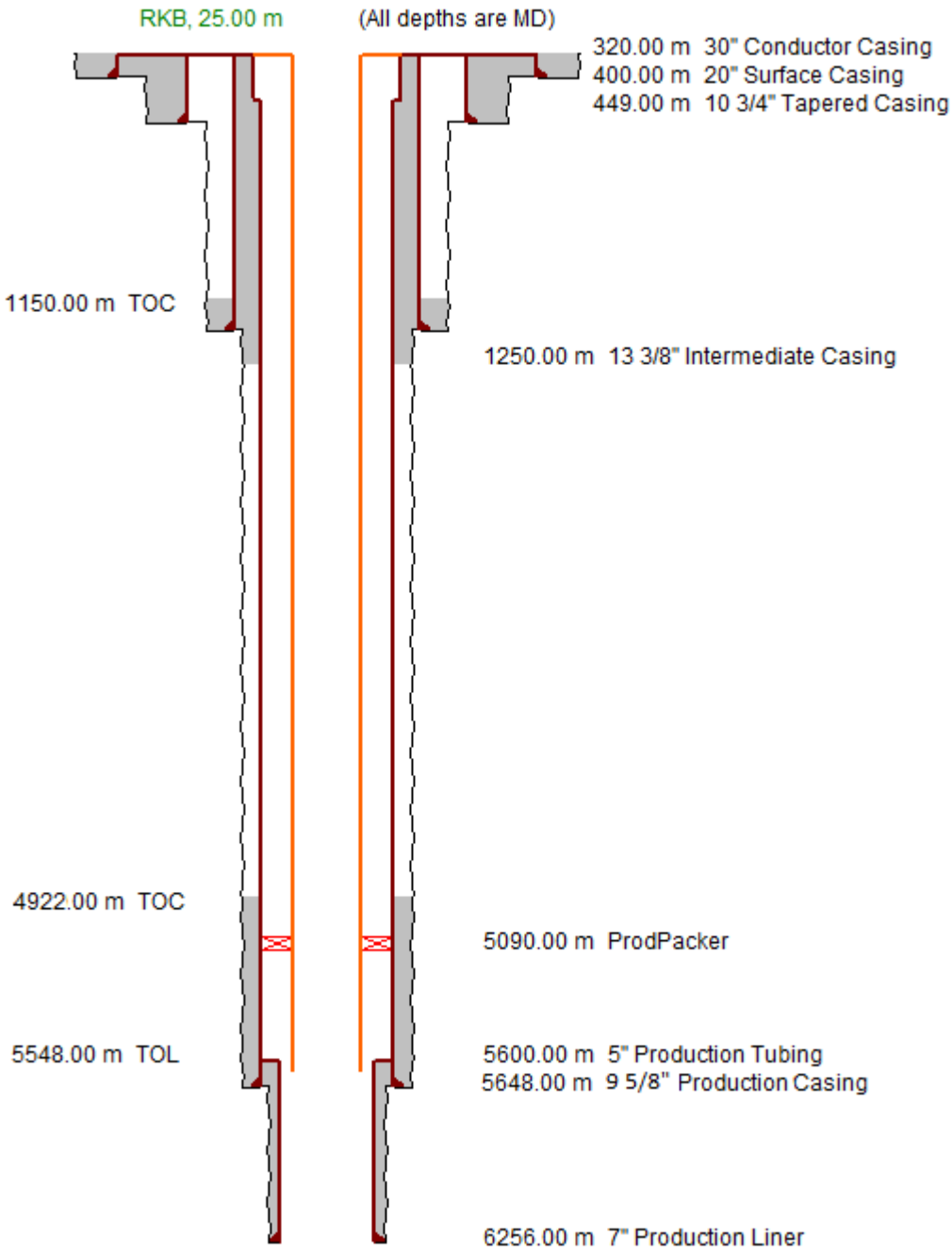

Figure 22: Well Schematic

Table 23: Overview of setting depths for Well K

	TVD [m]	MD [m]
RKB-WH	307	307
13 3/8 in shoe	2078	2088
9 5/8 in TOC Estimated	3760	4922
9 5/8 in TOC Planned	3713	4902
Production Packer	3810	5090
Top of Tiller	3872	5122
Base of Tiller	4015	5460
9 5/8 in shoe	4116	5670

The well is deviated featuring a vertical section and a tangent section which also penetrates the reservoir. The total length of the production casing is 5363 m. The estimated cemented interval length is 748 m based on displacement data and covers the entire length of the high pressure Tiller sandstone formation. The total length of the 13 3/8 in intermediate casing covers 1781 m of the production casing. The remaining 2834 m of production casing string is exposed to the open 17 ½ in hole

.

5.2 Well Integrity

Figure 23 shows the situation of a low pressure production scenario. The presence of a high pressure formation may pose serious integrity challenges. Blue and red colours represent primary and secondary well barriers respectively.

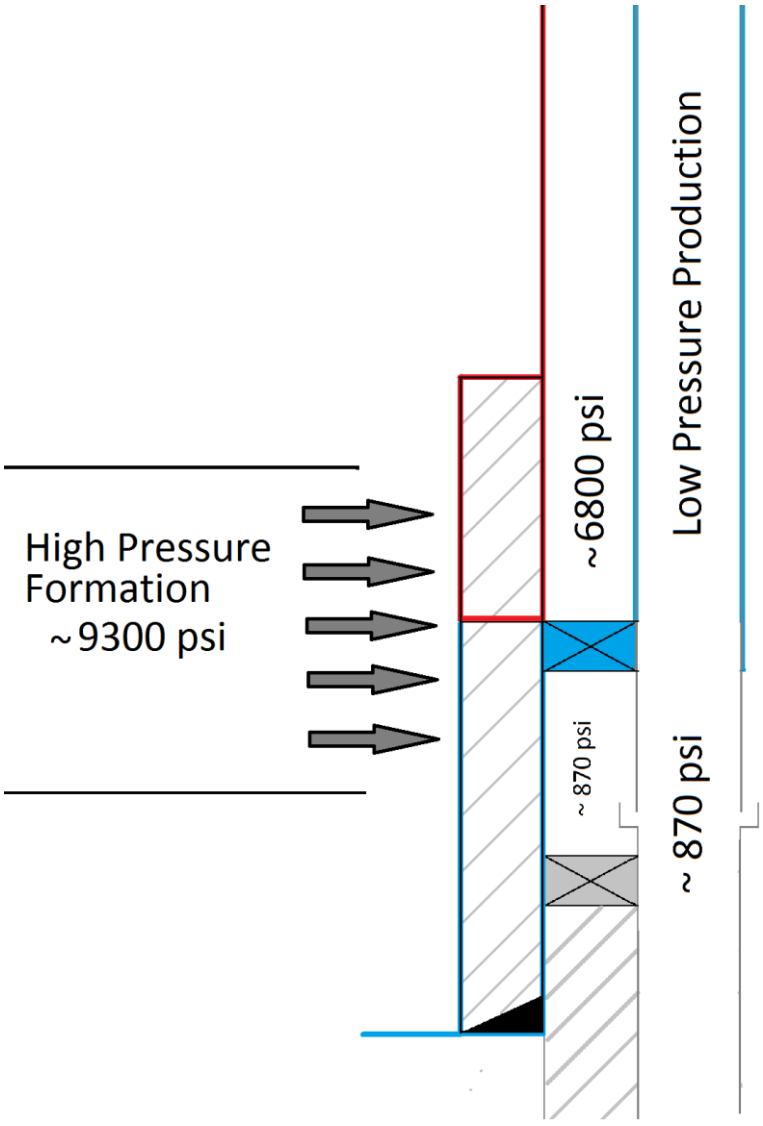

Figure 23: Well Barrier Schematic

Just after completion the well is classified as healthy, i.e. all barriers intact. The differential pressure over the production casing is within design limits. Problems arise when reservoir pressure declines to the lower limit of 870 psi. Assuming pore pressure is dominant throughout the cement, the differential pressure over the production casing below the packer

could potentially be as high as 8430 psi or 581 bar. The 9 5/8 in 53.5 ppf P-110 casing is rated to 7950 psi or 548 bar by default. The design collapse resistance is derated 6% by temperature and with the inclusion of governing design factor of 1.1, the strength would be no more than 6800 psi or 469 bar – before considering casing wear, ovality etc.

Collapse of production casing below the production packer may not necessarily result in leak to surface. If the packer holds and burst strength of the production tubing is deemed sufficient to contain the high pressure, the well can be closed at the DHSV. However, if the primary barrier fails through leakage of production tubing above the packer, full differential pressure of 9300 psi may be experienced across the 9 5/8 in casing. Fracturing of formation below the 13 3/8 in shoe and leak to surface is a likely scenario.

Upon initial casing design conservative methods were used to select appropriate well material and equipment. For the above/below packer criterion, internal pressure profile should be set to hydrostatic column of packer fluid above the packer, and vacuum below the packer. This particular well failed to meet design criteria as seen by the design limits plot (Figure 61) of Appendix F. However, it can be argued this scenario is highly unlikely, if not impossible, thus giving exception of the above/below packer criterion. The minimum well head pressure was set to 70 bar or 1015 psi, and casings were selected thereafter as to withstand all imposed loads throughout the lifetime of the well. New production technology has made it possible to reduce the well head pressure below 70 bar. In fact the flowing bottom hole pressure may be as low as 60 bar. A well not designed for such loads does not meet the current industry standards of well design, also seen by the design limits plot of Figure 61. Since the governing criteria are conservative there are potential hidden safety factors which can be utilised. A goal of this report is to determine the actual risk of well integrity failure.

5.3 Modelling

The casing design software (ILS) will be used to model governing loads and to obtain values for the total axial load throughout the casing string. It uses the historical API equations for casing collapse. The new ULS collapse model will be used for the same loads and compared with the current industry leading software.

5.3.1 Suggested ULS Model

The proposed ULS model is given in Equation (27) if the effective axial force is positive, i.e. tension. Δp_{tc} is calculated by Equation (10).

$$\Delta p = \Delta p c_{tc} f_{ovality} f_{wear} \tag{27}$$

For axial compression, the collapse pressure is given by Equation (28) where $\Delta p_{tc,0}$ is the transition collapse pressure (Equation (10)) of a casing of neutral axial loading.

$$\Delta p = \Delta p c_{tc,0} f_{ovality} f_{wear} f_{compression} \tag{28}$$

Transition collapse pressure is identical to the K&T and ISO models given in Equation (10). Ovality and wear are accounted for through Equation (25) and Equation (26) respectively. For casings subjected to negative axial force, i.e. compression, the transition collapse pressure of a casing of neutral axial loading is used and corrected with the compression factor in Equation (24). All parameters are calibrated as in section 3.1.5.

5.3.2 Industry Practice of Casing Design Simulations

A casing design software shall model all loads throughout the lifetime of the well. Several theories exist in literature with regards to development of external pressure over time. For the production casing, the external pressure profile will initially be that of the mud column used on the section. When cementing, the slurry density will replace mud below TOC often increasing the external pressure. When the cement has set, it is argued that formation pressure

is dominant below TOC. For drilling fluids sagging is initiated and mud is deteriorated to the base fluid density, either water or oil.

Modelling loads in the ILS should according to governing documentation be performed in a pessimistic manner. For all drilling and well operations within 90 days of section completion, the original mud density is used for collapse loads. After 90 days, pore pressure is assumed to be dominant for collapse loads. For burst loads however, deteriorated muds are used in the annulus as it achieves the highest differential pressure during burst.

When reviewing the collapse scenario in a low pressure production well it is clear that the mud is no longer fresh. When sagging is initiated it is common for WBM and OBM to reduce to base fluid densities of 1.03 sg and 0.815 sg. The pore pressure gradient is equal to or higher than that of water. However, some zones are impermeable. The mechanism of fluid interchangeability and sustained casing pressure will not be discussed here. If the mud is deteriorated, the worst case collapse scenario is represented by the use of pore pressure as external pressure, i.e. B-annulus.

5.3.3 Axial Loads

The effective axial load is the sum of all contributions such as buoyed weight of casing, temperature effect, ballooning effect, bending, buckling etc. Appendix B covers the topic of effective axial load. The industry leading software used for casing design calculates the axial load based on some unknown assumptions. It outputs effective axial load with and without bending. These outputs are used in the ULS model for easy comparison. No efforts have been made to replicate the axial load obtained by the casing design ILS by separate calculations.

The effect of bending should only add tension to the total axial forces since it represents reduction of collapse strength. Additional axial compression would increase strength and not be in line with general pessimistic approach. The axial load disregarding bending will feature in the ULS model.

5.3.4 Temperature Derating

Reservoir temperature is set to 150 ^{o}C with linear gradient towards the sea floor at 4 ^{o}C. Temperature is assumed constant. Casing or steel performance is derated by temperature as

properties change Standard measurements are performed at 20 ^{o}C. Collapse resistance is derated 0.046% per degree Celsius above standard temperature of 20 ^{o}C.

5.3.5 Design Factor

Standard design factor for collapse of casing is set to 1.1.

5.3.6 Casing Connections

Casing connections are assumed to be more collapse resistant than the casing itself. Vallourec's data sheets for Vam connections do not provide collapse strength. The casing design software uses casing ratings as design limit for collapse.

5.4 Load 1 - Full Evacuation of Casing

The highest differential pressure is experienced at 5612.6 m MD for full evacuation of casing and low pressure production after tubing leak. For both loads the most compressed joint is, due to bending effects, located at the point of highest differential pressure. Performance is derated by tension and the joint just below the well head is exposed to the highest axial load in the well. The differential pressure at the well head is no more than the normal hydrostatic pressure, rendered not sufficient for casing collapse.

The internal pressure regime will be modelled as vacuum. In order for said scenario to be obtained, loss of all packer fluid from the A-annulus through a hole in the tubing above the production packer must occur and go unnoticed. Once the packer fluid is produced or bull headed into the reservoir, the perforations must be plugged or blocked and the remaining gas must expand to atmospheric conditions. It implies loss of surface pressure control by error or deliberate action. However unlikely, this scenario represents the worst case collapse load case if mud in B-annulus is deteriorated.

The highest differential pressure is 9284 psi and occurs at reference point B; 5612.6 m MD or 4083 m TVD. The most compressed joint is also located at reference point B. Performance is derated by tension and the joint just below the well head is exposed to the highest axial load in the well. The differential pressure at the well head is no more than the normal hydrostatic pressure, rendered not sufficient for casing collapse.

Table 24: Overview of Full Evacuation load scenario

Reference point	MD	TVD	p_i	p_e	Δp	With bending		Without bending	
[-]	[m]	[m]	[psi]	[psi]	[psi]	[lbf]	σ_a/σ_y	[lbf]	σ_a/σ_y
A	313,3	313,3	0,0	459,8	-459,8	547273,0	0,281	384085	0,198
B	5612,6	4083,3	0,0	9284,1	-9284,2	-352985,0	-0,182	-299723,0	-0,154

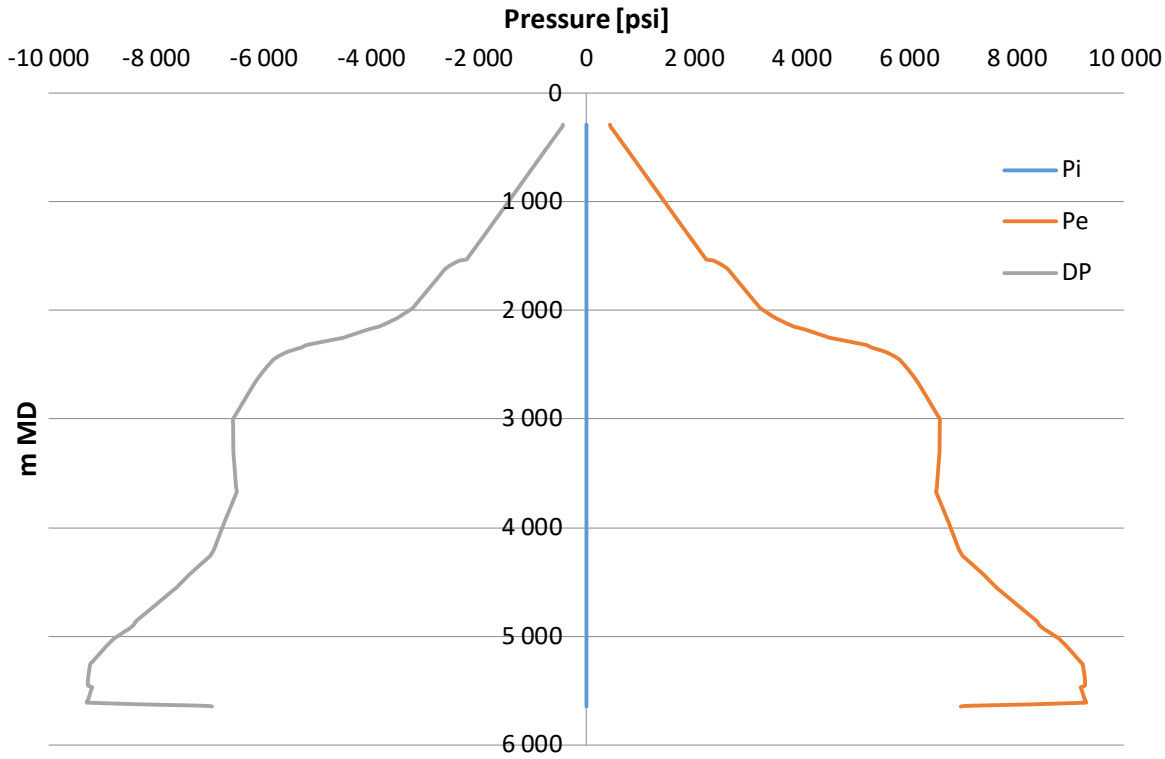

Figure 24: Pressures for fully evacuated casing

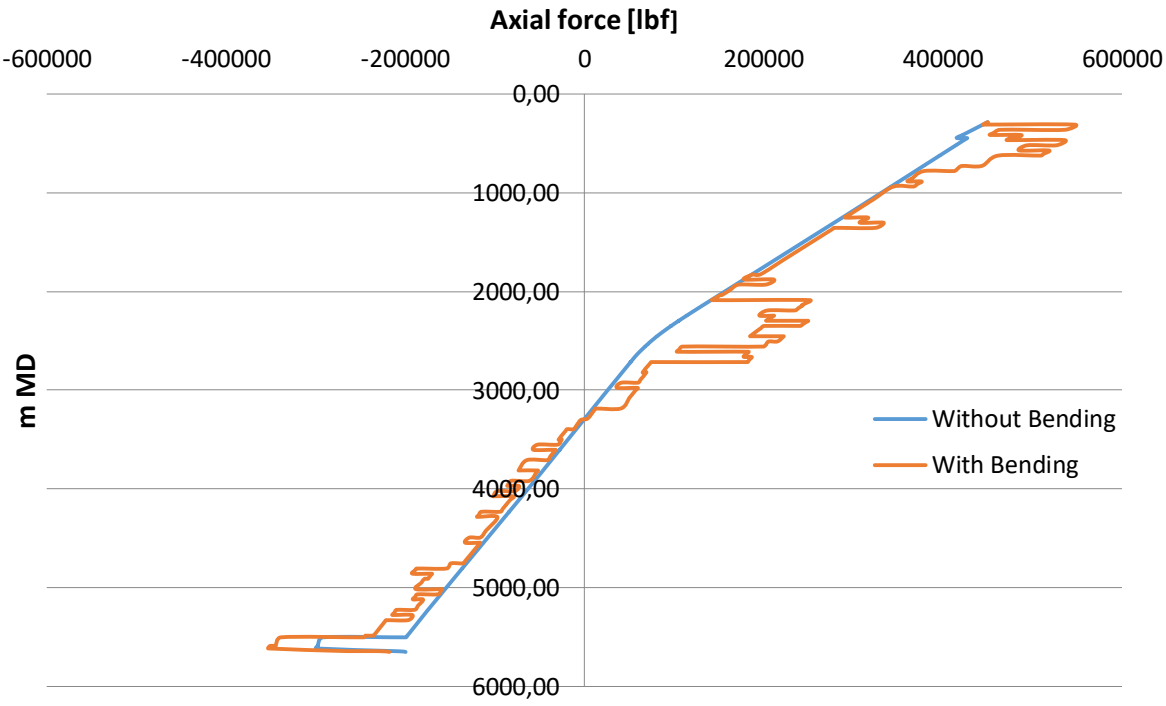

Figure 25: Axial loads for fully evacuated casing

5.5 Load 2 – Low Pressure Production

Full evacuation of the 9 5/8 in production casing after loss of tubing integrity is highly unlikely. A more plausible scenario would be reservoir pressure at total depth with corresponding fluid filling the wellbore. If production is maintained, bottom hole flowing pressure, BHFP, should be applied rather than reservoir pressure. Assuming the reservoir pressure of a mature field to be 90 bar or 1305 psi, the BHFP will be 60 bar or 870 psi with a draw down of 30 bar. The flowing well head pressure is assumed to be 30 bar, equal to the hydrostatic column of sea water at the mud line, as no efforts have been made to estimate the reservoir fluid density profile.

As with full evacuation of casing, reference point A represents the joint exposed to the highest axial load in terms of tension. Reference point B represents the maximum differential pressure of 8444 psi acting on the most compressed pipe.

Table 25: Overview of Low Pressure Production load scenario

Reference point	MD	TVD	p_i	p_e	Δp	With bending		Without bending	
[-]	[m]	[m]	[psi]	[psi]	[psi]	[lbf]	σ_a/σ_y	[lbf]	σ_a/σ_y
A	313,3	313,3	0,0	459,8	-459,8	547273,0	0,281	444554	0,229
B	5612,6	4083,3	840,0	9284,1	-8444,1	-468568,0	-0,241	-415306,0	-0,214

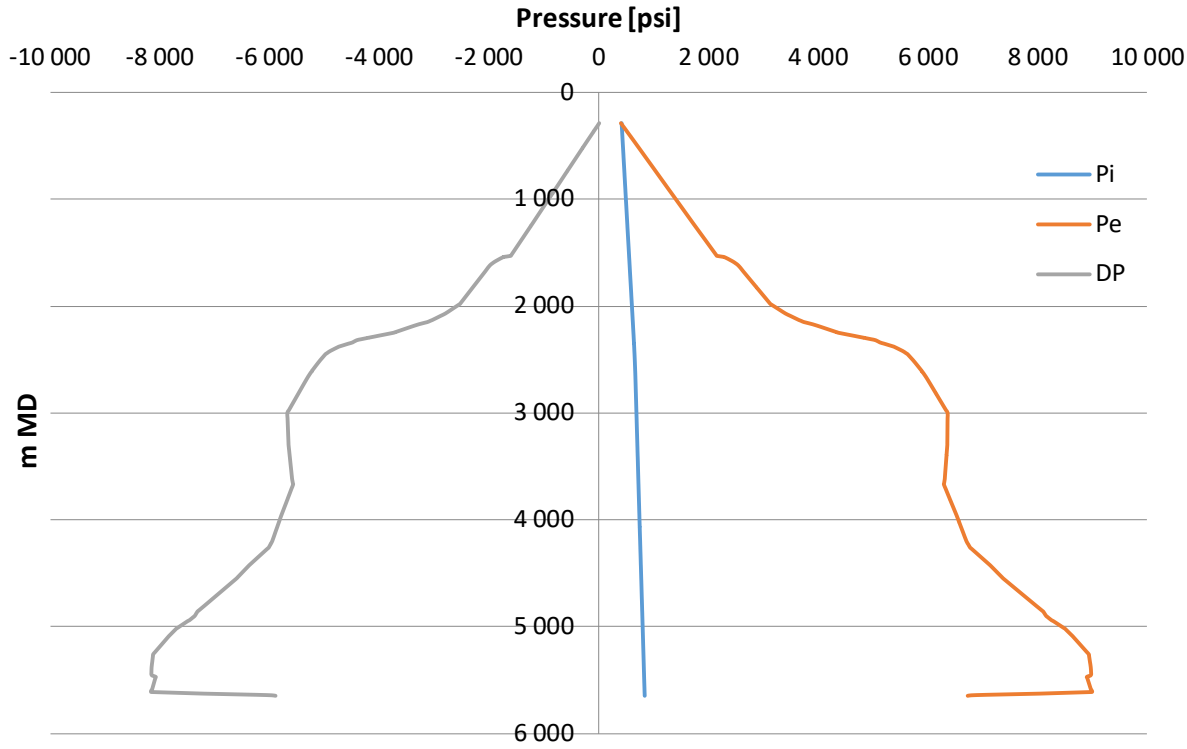

Figure 26: Pressures for low pressure production scenario

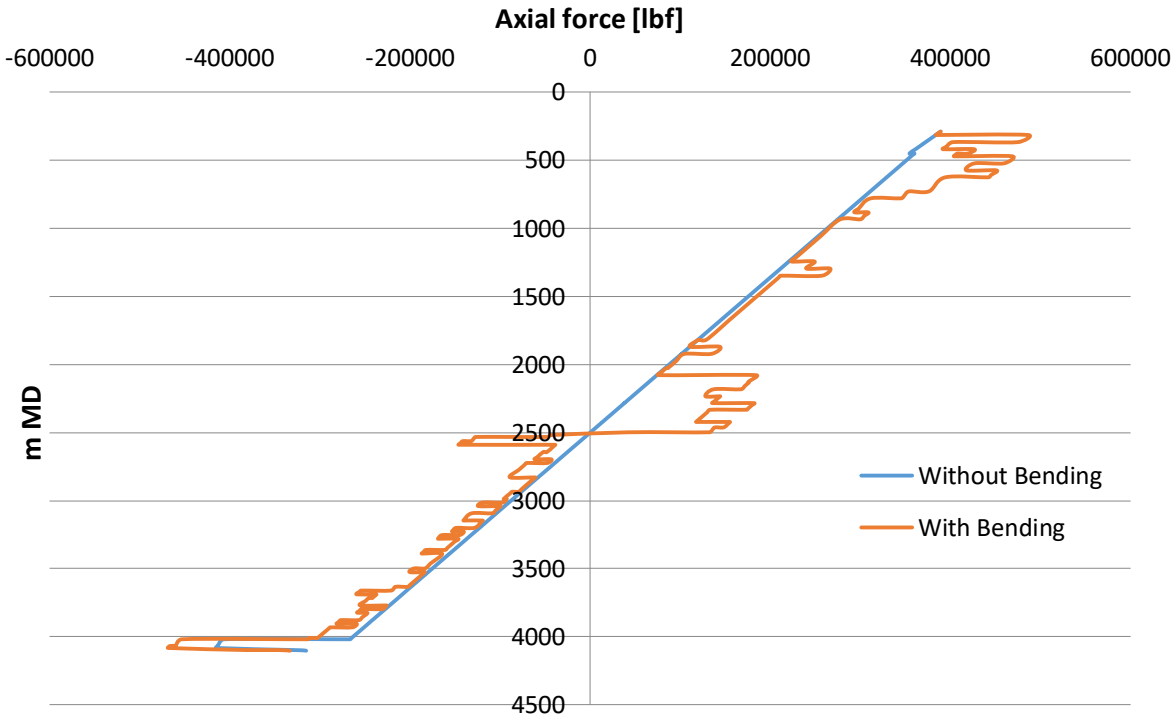

Figure 27: Axial loads for low pressure production scenario

5.6 Casing Collapse Strength Evaluation

The pipes in question, 9 5/8 in 53.5 ppf P-110, are quenched and tempered, seamless and hot rotary straightened. Using the ULS model and actual PDFs from DEA-130 dataset in Monte Carlo simulations, 100 000 values will be obtained with aim to predict actual strength.

5.6.1 Without Axial Effect

Without the effect of axial forces the casing collapse ratings for both scenarios are equal. The difference is mitigated through the internal pressure supporting the casing for a scenario of low pressure production.

5.6.1.1 Base case

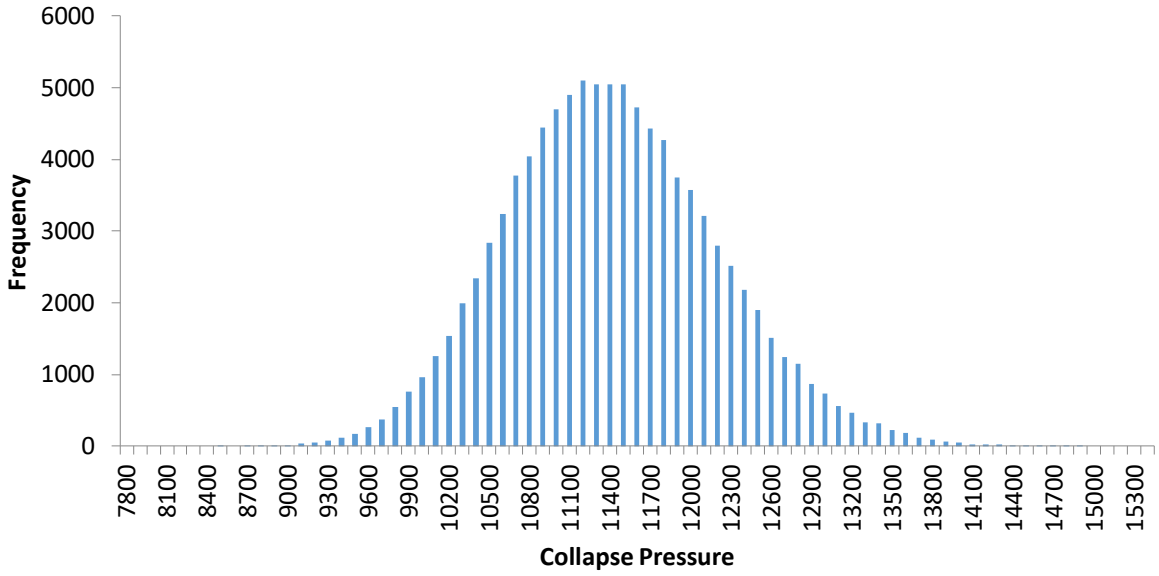

Figure 28: Basic collapse strength predictions for seamless Q&T and hot rotary straightened 9 5/8 in 53.5 ppf P-110 casing

Figure 28 is identical to the analysis performed in section 4.1.1. The average collapse strength of a seamless Q&T and hot rotary straightened 9 5/8 in 53.5 ppf P-110 casing is 11362 psi with standard deviation of 788 psi. The lower bound value at two standard deviations is 9787 psi and should be reproduced by Figure 28. Approximately 2500 predicted collapse strengths are less than 9900 psi meaning 97.5% of the simulations exceed the confidence limit. The best performer, although rare, exceeds the lower limit by more than 4900 psi. Any given casing

will likely perform better than 9900 psi but this value is set to the basic strength for this particular product, higher than its default API rating of 7950 psi.

5.6.1.2 Wear and Ovality

Table 26: Derated collapse strength

Load Case	Basic strength	Temperature derated	DF
[-]	[psi]	[psi]	[psi]
Evacuation	9900	9256,5	8415,0
LPP	9900	9256,5	8415,0

Table 27: Collapse strength matrix including effect of ovality and wear ignoring axial load and cement or formation support.

Ovality / Wear	0%	0,5%	1%	1,5%	2%	3%	4%	5%
0%	8415	8415	8205	7994	7784	7363	6942	6522
2,5%	8205	8205	8000	7794	7589	7179	6769	6359
5%	7994	7994	7794	7595	7395	6995	6595	6196
7,5%	7784	7784	7589	7395	7200	6811	6422	6033
10%	7574	7574	7384	7195	7005	6627	6248	5869
15%	7153	7153	6974	6795	6616	6259	5901	5543
20%	6732	6732	6564	6395	6227	5891	5554	5217

Table 28: Collapse strength as in Table 27 without design factor

Ovality / Wear	0%	0,5%	1%	1,5%	2%	3%	4%	5%
0%	9257	9257	9025	8794	8562	8099	7637	7174
2,5%	9025	9025	8799	8574	8348	7897	7446	6994
5%	8794	8794	8574	8354	8134	7694	7255	6815
7,5%	8562	8562	8348	8134	7920	7492	7064	6636
10%	8331	8331	8123	7914	7706	7289	6873	6456
15%	7868	7868	7671	7475	7278	6885	6491	6098
20%	7405	7405	7220	7035	6850	6480	6109	5739

The matrix from Table 27 indicates the design collapse strength of a casing for an arbitrary combination of wear and ovality using the basic strength of 9900 psi with derated performance in high temperature environment. Design factor for 1.1 has been used. If the

casing is fully evacuated after tubing leak it cannot obtain a satisfactory safety factor against the collapse pressure of 9284 psi. Even if internal pressure is maintained at flowing pressure of 840 psi at reference point B, no wear or imposed ovality is permitted if the casing is to withstand a differential pressure of 8444 psi.

One of the goals of this report is to accurately predict strength. Incorporating a design factor defeats this purpose. If casing design is completed without the aid of a design factor the actual strengths are listed in Table 28. The casing still cannot withstand a pressure regime of internal vacuum. However, more than 7.5% casing wear is allowed for non-ovalised casings if internal pressure is 840 psi.

The matrix also allows for easy identification of minimum internal pressure if casings are to withstand collapse loads. Again, if no design factor is applied the minimum internal pressure must be as according to Table 29.

Table 29: Minimum internal pressure disregarding DF

Wear \ Ovality	0%	0,5%	1%	1,5%	2%	3%	4%	5%
0%	28	28	259	490	722	1185	1647	2110
2,5%	259	259	485	710	936	1387	1838	2290
5%	490	490	710	930	1150	1590	2029	2469
7,5%	722	722	936	1150	1364	1792	2220	2648
10%	953	953	1161	1370	1578	1995	2411	2828
15%	1416	1416	1613	1809	2006	2399	2793	3186
20%	1879	1879	2064	2249	2434	2804	3175	3545

5.6.1.3 With Cement Support

Proper cementing process can support the casing in collapse. As discussed in section 0 the added support may hinder ovalisation of pipes subjected to collapse pressure. A mechanism of collapse is deformation or ovalisation of casings. For simplicity the presence of cement support is assumed to fully restrain ovalisation of the casing string. Section 4.5 indicated increased strengths of 20% for cement-casing composite and 53% for casing-cement-casing composite. The outer casing may represent formation support, however, steel is stiffer than the typical formation. An increase of 53% is thus considered unrealistic for casing-cement-formation which is the composite for parts of this well. Table 4 shows the effect of increased

strength by cement support of non-ovalised casings. Further increase in strength is also an indication of good quality cement.

Table 30: Collapse strength of non-ovalised casing with cement support including DF

Cmt. Support / Wear	0 %	5 %	10 %	15 %	20 %	25 %
0,0 %	8415	8836	9257	9677	10098	10519
2,5 %	8205	8615	9025	9435	9846	10256
5,0 %	7994	8394	8794	9193	9593	9993
7,5 %	7784	8173	8562	8951	9341	9730
10,0 %	7574	7952	8331	8710	9088	9467
15,0 %	7153	7510	7868	8226	8583	8941
20,0 %	6732	7069	7405	7742	8078	8415

5.6.2 With Axial Effect

Table 31: Derated collapse strength

Load Case	Basic Strength	Temperature Derating	DF	Axial effect	Axial effect
[-]	[psi]	[psi]	[psi]	[psi]	[%]
Evacuation	9900	9256,5	8415,0	8622,5	102,5 %
LPP	9900	9256,5	8415,0	8685,2	103,2 %

5.6.2.1 Full Evacuation

The compressional load disregarding bending in a scenario of full casing evacuation yields a 2.5% increase of strength. Still, this is not sufficient for the casing to withstand pore pressure from the formation even when ignoring the design factor. The corresponding matrix for cement support when incorporating axial effect is reproduced in Table 32. Red markings in Table 32 have normalised safety factors below 1.0. Similarly, red markings in Table 33 have absolute safety factor below unity. The difference is the incorporated design factor.

Table 32: Effect of cement support for non-ovalised casing including DF

Wear \ Cmt. Support	0 %	5 %	10 %	15 %	20 %	25 %
0,0 %	8623	9054	9485	9916	10347	10778
2,5 %	8407	8827	9248	9668	10088	10509
5,0 %	8191	8601	9011	9420	9830	10239
7,5 %	7976	8375	8773	9172	9571	9970
10,0 %	7760	8148	8536	8924	9312	9700
15,0 %	7329	7696	8062	8429	8795	9161
20,0 %	6898	7243	7588	7933	8278	8623

Table 33: Effect of cement support for non-ovalised casing excluding DF

Wear \ Cmt. Support	0 %	5 %	10 %	15 %	20 %	25 %
0,0 %	9485	9959	10433	10908	11382	11856
2,5 %	9248	9710	10172	10635	11097	11560
5,0 %	9011	9461	9912	10362	10813	11263
7,5 %	8773	9212	9651	10089	10528	10967
10,0 %	8536	8963	9390	9817	10244	10670
15,0 %	8062	8465	8868	9271	9675	10078
20,0 %	7588	7967	8347	8726	9105	9485

5.6.2.2 Low Pressure Production

With internal pressure of 840 psi and slightly higher compressive force the low pressure production scenario can withstand greater external pressure than vacuum filled casing. With applied design factor the allowable wear is maxed out at 2.5%. Ovality must not exceed 1% for non-worn casing. Disregarding the design factor yields differential pressure limits as in Table 34Table 33. This allows for some combinations of ovality and wear to be sufficiently strong. The maximum differential pressure can be 8444 psi.

Table 34: Effect of wear and ovality excluding DF

Wear \ Ovality	0%	0,5%	1%	1,5%	2%	3%	4%	5%
0%	9554	9554	9315	9076	8837	8360	7882	7404
2,5%	9315	9315	9082	8849	8616	8151	7685	7219
5%	9076	9076	8849	8622	8395	7942	7488	7034
7,5%	8837	8837	8616	8395	8174	7733	7291	6849
10%	8598	8598	8383	8168	7954	7524	7094	6664
15%	8121	8121	7918	7715	7512	7106	6700	6294
20%	7643	7643	7452	7261	7070	6688	6305	5923

Table 35: Effect of cement support for non-ovalised casing including DF

Wear \ Cmt. Support	0 %	5 %	10 %	15 %	20 %	25 %
0,0 %	8685	9119	9554	9988	10422	10857
2,5 %	8468	8892	9315	9738	10162	10585
5,0 %	8251	8664	9076	9489	9901	10314
7,5 %	8034	8436	8837	9239	9641	10042
10,0 %	7817	8208	8598	8989	9380	9771
15,0 %	7382	7752	8121	8490	8859	9228
20,0 %	6948	7296	7643	7990	8338	8685

Table 36: Effect of cement support for non-ovalised casing excluding DF

Wear \ Cmt. Support	0 %	5 %	10 %	15 %	20 %	25 %
0,0 %	9554	10031	10509	10987	11465	11942
2,5 %	9315	9781	10246	10712	11178	11644
5,0 %	9076	9530	9984	10437	10891	11345
7,5 %	8837	9279	9721	10163	10605	11047
10,0 %	8598	9028	9458	9888	10318	10748
15,0 %	8121	8527	8933	9339	9745	10151
20,0 %	7643	8025	8407	8789	9172	9554

6 Discussion

The following chapter will discuss some of the findings of this report. Chapter 4 and Chapter 5 already feature some discussion, and not all of it will be reproduced in this chapter.

Comparison of Models

	API	K&T	ISO	ULS
Collapse Modes				
Elastic	Eq. (34)	Eq. (1)	Eq. (12)	Eq. (12)
Yield	Eq. (31)	Eq. (3)	Eq. (13)	Eq. (13)
Transition	Eq. (33)	Eq. (7)	Eq. (10)	Eq. (10)
Plastic	Eq. (32)	N/A	N/A	N/A
Axial Forces				
Tension	Yes, through equivalent yield strength in Eq. (39)	Yes, through von Mises formulation of yield collapse (or alternative formulation in Eq. (23))	Yes, through von Mises formulation of yield collapse	Yes, through von Mises formulation of yield collapse
Compression	Yes, through equivalent yield strength in Eq. (39)	Yes, through alternative von Mises formulation of yield collapse in Eq. (23)	No	Yes, through compression factor in Eq. (24)
Pipe Imperfections				
H_t	N/A	Not calibrated	Eq. (11)	Eq. (11)
K_e	N/A	Not calibrated	0,825	0,825
K_y	N/A	Not calibrated	0,850-0,910	0,850-0,910
c	N/A	Not calibrated	-0,97 to -0,93	6
Additional Effects				
Imposed Ovality	No	No	No	Eq. (25)
Wear	No	NO	No	Eq. (26)

The ISO model is a simplified version of the original Klever & Tamano model. Most notably is the exclusion of axial compression and parameters to account for pipe imperfections, H_e and H_y. The additional strength of casings in compression is not utilised by the industry. OCTG is assumed to only collapse in the transition region, hence the exclusion of separate elastic and yield decrement functions. Moreover, the model parameter, c, is defined as -1+t/D which ranges from -0.97 to -0.93 for thick walled pipes. The original K&T paper presents all parameters albeit without suggested value.

Further adjustments was introduced and culminated in the ULS model of Equation (27) and Equation (28). It suggests a different calibration of the model parameter c, and includes the effect of compression, imposed ovality and casing wear.

Conservatism of API Equations

It has long been known that the empirical API equations used for collapse prediction of perfect casings are conservative. Minimum performance ratings are used rather than probabilistic values. Modifications to the empirical equations can provide average values of casing collapse pressure but are found to be inaccurate.

The original Klever & Tamano model has been proven to be the most accurate analytical model out of 11 candidates reviewed by the ISO workgroup. For ensemble data of 1138 collapse tests of seamless, quenched and tempered API casings the average actual/predicted collapse pressure was 0.997 with standard deviation of 0.0708. For comparison, average performance ratings from API equations on ensemble data results in average actual/predicted strength of 1.04 with standard deviation of 0.175.

The ULS model used in this report showed similar performance as K&T for 43 samples of seamless, Q&T and hot rotary straightened casings from the DEA-130 dataset. Actual/predicted strength was recorded at 0.999 with standard deviation of 0.0648.

Using calibrated parameters and accounting for pipe imperfections through models based on Klever & Tamano improves accuracy vastly. Elastic collapse is based on thin-walled theory and corrected with the model parameter, c, for thick-walled casings. Yield collapse features a new formulation based on von Mises and Tresca criteria. The mode of collapse in which

OCTG fail is denoted as transition collapse and is a weighted average of elastic and yield collapse pressures. Model parameters are calibrated by empirical data as to best fit the casing reviewed.

With the predictive accuracy of the new ULS model verified, it can be directly compared to the empirical API equations. For a perfect 9 5/8 in 53.5 ppf P-110 casing only exposed to external pressure API predicts collapse at 7950 psi. The more accurate ULS model predicts 12163 psi, an increase of 53%.

Six experimental tests performed on the same type of casing collapsed at 9629 psi, 9879 psi, 10728 psi, 11287 psi, 11640 psi, and 11684 psi – significantly more than the API rating even with pipe imperfections accounted for, all but confirming the conservative nature of API ratings.

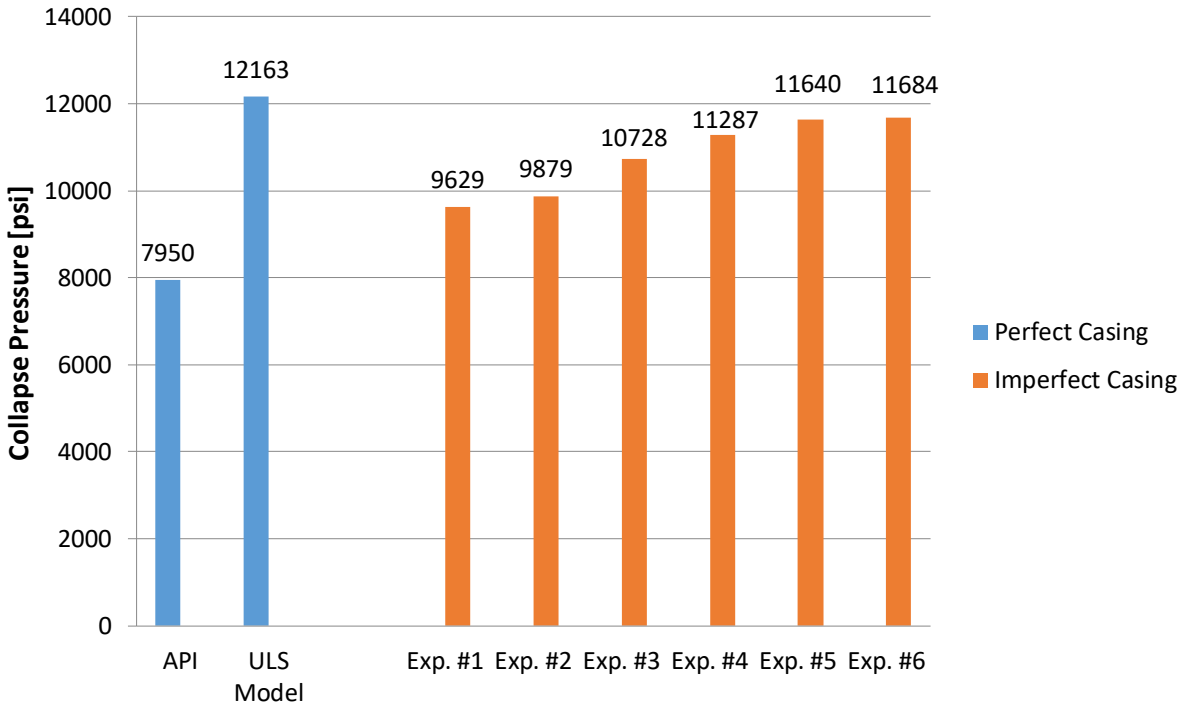

Figure 29: Analytical and experimental results for 9 5/8 in 53.5 ppf P-110

Monte Carlo Simulations

Using random value generators based on PDFs of all input parameters in Monte Carlo simulations resulted in 100 000 collapse strength predictions per casing. The PDFs are obtained by analysing production quality statistics.

Using production data from DEA-130, average strength of seamless Q&T 9 5/8 in 53.5 ppf P-110 casings were found to be 11362 psi for HRS specimens and 10961 psi for CRS specimens. Using ensemble data the corresponding strengths were 10953 psi for HRS and 10468 psi for CRS.

The straightening type affects the residual stress of a factory new casing. Cold rotary straightened casings have elevated stress levels compared to their hot counterparts. As a consequence the tested yield and tensile strengths are reduced – detrimental for collapse resistance. However, the spread is of predicted strength is less for CRS casings seen by lower standard deviations or coefficients of variance.

If the measurements of ovality, eccentricity and residual stress are unknown or minimum performance ratings are desirable, a proposed methodology is to use governing cases. All three parameters feature in the decrement function used derate pipe performance from ideal to actual. The ISO workgroup identified governing cases, e.g. decrement function value of 0.20 for HRS casings. Using the proposed value of decrement function effectively reduces average collapse strength of about 1000 psi using DEA-130 production data. The statistical scatter is naturally less as fewer input parameters are used, locating the 2.5% exceedance level (2σ) at 9200 psi. The absolute minimum predicted collapse strength out of 100 000 simulations was 8139 psi – still more than API's rating of 7950 psi but this approach defeats the purpose of accurate collapse strength prediction.

Using ensemble data and governing cases the 2.5% exceedance level is located at 8900 psi for HRS casings. The absolute minimum value was 7535 psi – even lower than API's rating. The probability of receiving a casing of that minimum performance is 1 in 100 000, or 0.001%. It is clear that minimum performance values represent rare cases and can be regarded as outliers. It is argued that 2.5% confidence limits should be acceptable for engineering applications.

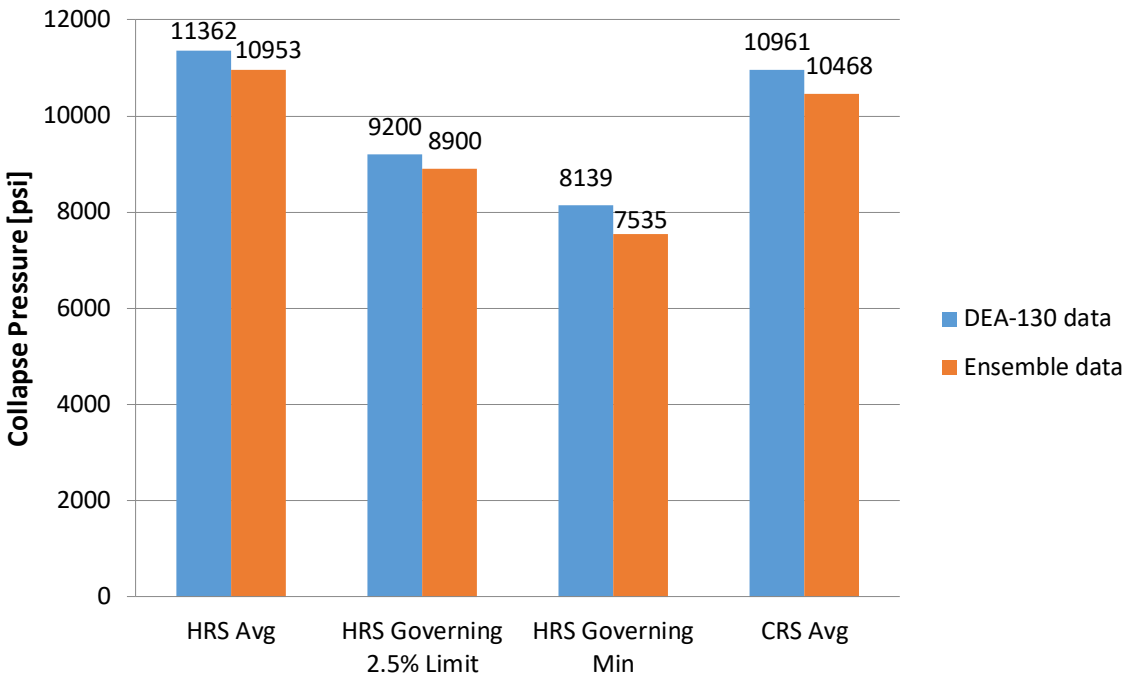

Figure 30: Results from Monte Carlo simulation

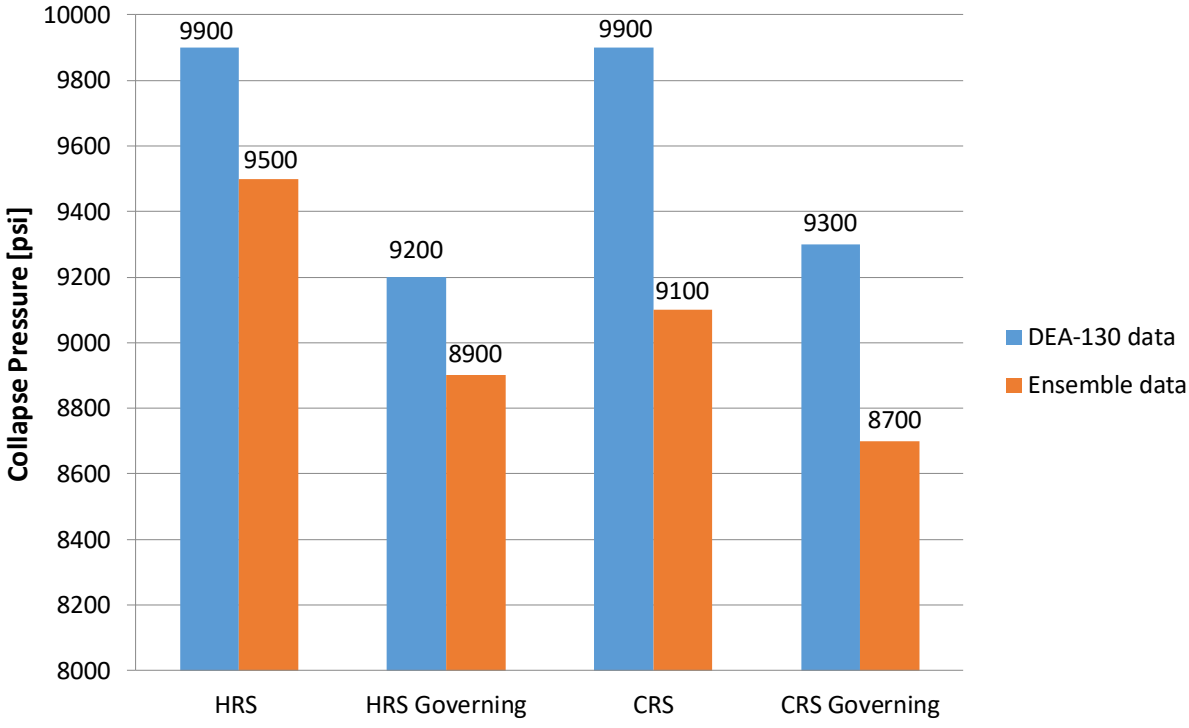

Figure 31: 2.5% exceedance limits. Governing cases use decrement functions of 0.20 and 0.22 for HRS and CRS respectively

If the production quality statistics from DEA-130 is representative of the seamless, Q&T and hot rotary straightened 9 5/8 in 53.5 ppf P-110 casing used in the particular well evaluated, the collapse strength should be more than 9900 psi with a 2.5% lower acceptance limit. That is an increase of 1950 psi or 24.5% compared to API's standard rating.

If governing cases for ovality, eccentricity and residual stress are used, the corresponding value would be 9200 psi – an increase of 15.7%. Collapse strength is then not predicted accurately, but with the aim to provide a minimum guaranteed collapse rating, also called "design strength". Increasing the confidence limits will reduce the design collapse strength towards the standard API rating, and defeats the purpose of accurate strength prediction.

Probability Density Functions

The indirect method of predicting collapse strength through a predictive equation and Monte Carlo simulations requires knowledge of each input parameters probability density function. The probability distribution was revealed by plotting all values and corresponding frequencies. Once the PDF was identified, properties are obtained by equations for mean and standard deviation.

The DEA-130 dataset consists of 151 collapse tests. Filtering by quenched and tempered casings only and removing entries with lack of measurements leaves only 80 collapse tests to be evaluated. Categorising the specimens by forming process and rotary straightening type further reduces the sample size. Only 61 collapse tests are conducted on Q&T seamless pipes, of which 43 are hot rotary straightened. Finding the probability distribution of such small sample sizes could be error prone, especially for the 18 cold rotary straightened samples.

Analyses of individual datasets as stated in Appendix F of ISO/TR 10400 (2007) identifies several trends such as residual stress being dependent upon straightening type. Similarly, ovality and eccentricity are linked with forming process. Similar analyses were desirable in this report but limited access to sufficient number of collapse tests rendered such efforts of little to no use. However, the workgroup of ISO have identified all probability distributions, e.g. Gaussian for wall thickness, two-parameter Weibull for ovality, and so on. Even with small sample sizes these distributions are recognised. Assuming the excellent work by ISO holds true, the properties of all PDFs may easily be obtained. Although the probability

distributions are equal, the properties of each PDF differ slightly when using DEA-130 dataset compared to the whole ensemble of thousands of samples.

The most notable difference between PDFs from DEA-130 dataset and ISO's ensemble is seen by the average values and COV of residual stress for both HRS and CRS samples in Table 37. Residual stress being normalised by yield strength is 27% and 50% higher for HRS and CRS respectively using ensemble production quality statistics. DEA-130 production quality statistics gives 40% and 25% more spread.

Table 37: PDF for HRS and CRS casings using DEA-130 and Ensemble statistics

	DEA-130		Ensemble	
	HRS	CRS	HRS	CRS
Avg	-0,109	-0,158	-0,138	-0,237
Std	0,0774	0,0659	0,0700	0,0787
COV	-0,7082	-0,4165	-0,507	-0,332

Using DEA-130 dataset it should be noted that the PDFs for residual stress was not easily identifiable. The distribution plot for seamless Q&T hot rotary straightened casings is reproduced in Figure 32. If the assumption of Gaussian distribution based on the findings of ISO holds true, the average value of rs/σ_y is -0.109. Only 5 of 43 measurements are found to be within the bin range of -0.10 to -0.14. Most entries are found to be within -0.02 and -0.04. More measurements will hopefully disclose the true distribution. Possible errors in measurements could have occurred. Residual stress have been normalised by actual yield strength in Figure 32. The workgroup of ISO may have normalised by nominal yield strength which would shift data points to lower values, i.e. to the left. By using nominal yield strength, the DEA-130 dataset will have higher frequency of measurements close to the dataset average. Moreover, the high frequency near zero might originate from high collapse casings, i.e. non-API products. High collapse grade casings are recognised by high yield strength and low residual stress. Those properties are correlated and will shift rs/σ_y towards zero.

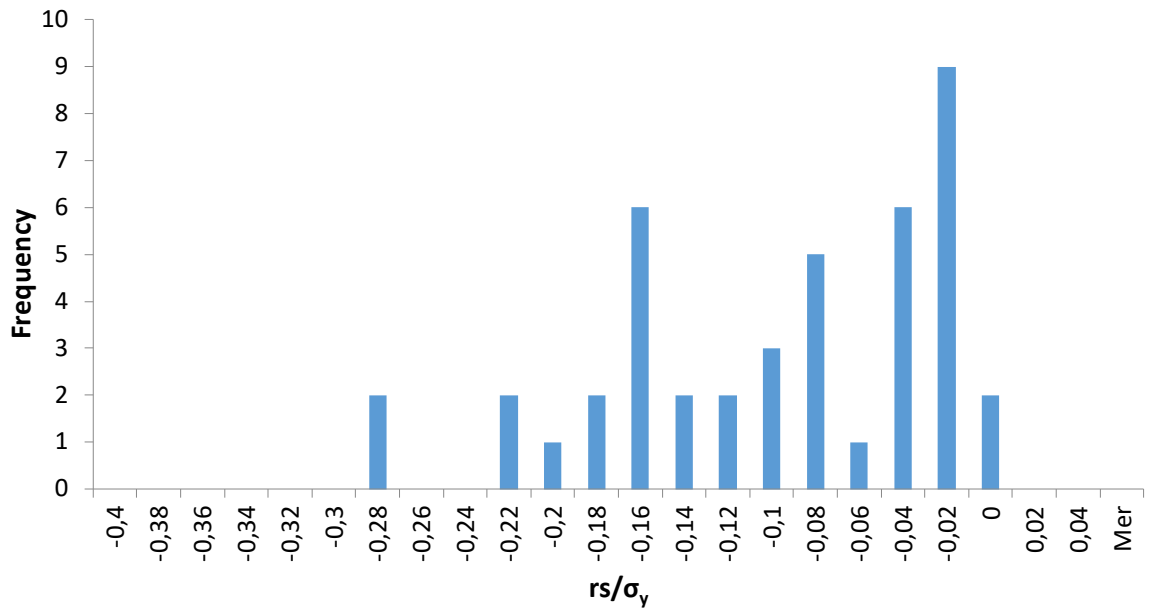

Figure 32: Distribution plot of normalised residual stress for HRS samples of DEA-130

Another problem that arises is the accuracy of the PDFs to replicate variations in production quality. For any determination of collapse strength the dataset(s) used for obtaining PDFs are assumed to be representative of the product itself. Both the DEA-130 dataset and the ISO ensemble feature casings of different size, weight and grade from different mills and batches of several manufacturers – possibly produced over a time span of decades. Ideally only samples from a specific batch should be used to calibrate parameters and should form the basis for PDF representation. This issue is best exemplified by actual yield strength of P-110 casings reported by ISO in Table 11. With average normalised yield strength of 1.10 and standard deviation of 0.05104 the lower limit of 2σ is set to 0.99792 or 109 771 psi. This means more than 2.5% of all P-110 casings have actual yield strengths less than the specified absolute minimum of 110 000 psi. No API casings have yield strengths below the specified minimum.

High Collapse Pipes

High collapse performance is normally a result of exceptional geometric properties such as low eccentricity, ovality, and wall thickness variation. Yield strength is correlated and should be correspondingly high.

The empirical API equations are not compatible with high collapse products (ISO/TR 10400, 2007). The workgroup of ISO have identified Klever & Tamano as the best predictor of strength for HC casings too with average actual/predicted ratio of 1.001 and standard deviation of 0.064 – similar accuracy as regular API casings where the average was 0.997 with standard deviation of 0.071. It seems like the original K&T equation is even more accurate for HC products.

Filtering out high collapse products from the DEA-130 dataset does not result in any noteworthy change of actual/predicted collapse strength. However, the variation may be affected through Monte Carlo simulations where input parameters feature by probability density functions from actual measurements. Since HC products normally have excellent properties, including these measurements in representation of API casings could lead to loss of predictive accuracy of collapse strength. The DEA-130 dataset is listed with 26 high collapse products. Some were used to verify model accuracy and in the process of identifying the PDFs. The results obtained are similar to Table F.4 of ISO/TR 10400 (2007) where HC products are included. Reviewing API casings and HC products separately for a large dataset or an ensemble of datasets would be interesting. Further investigations are needed.

Since Klever & Tamano was proven to be the best predictor of strength for API casings and high collapse products separately, it is believed the ULS model will be a good predictor for both API and HC casings. Obtaining probability density functions based on measurements from a mixture of both API and HC casings could possibly lead to higher variation even though the overall average is not changed. Assuming those PDFs to be representative of either API casings or HC casings could be misleading. As mentioned, only samples from a specific batch should ideally form the basis for obtaining PDFs.

Imposed Ovality

Ovality is a feature of imperfect pipes and disregarded in the empirical API equations. Ovality is accounted for in the decrement function of K&T based models, albeit designed or calibrated by only manufacturing ovality up to 1%. Imposed ovality may be of far greater extent only limited by physical properties. In field examples tectonic loads, flowing or swelling formations, and reservoir compaction are common causes of imposed ovality – all factors of limited control. Field handling by pipe stacking may also induce ovality to

detrimental effect and is more easily controllable. It is therefore important to regularly measure casing diameter and wall thickness as collapse resistance is greatly affected by imposed ovality.

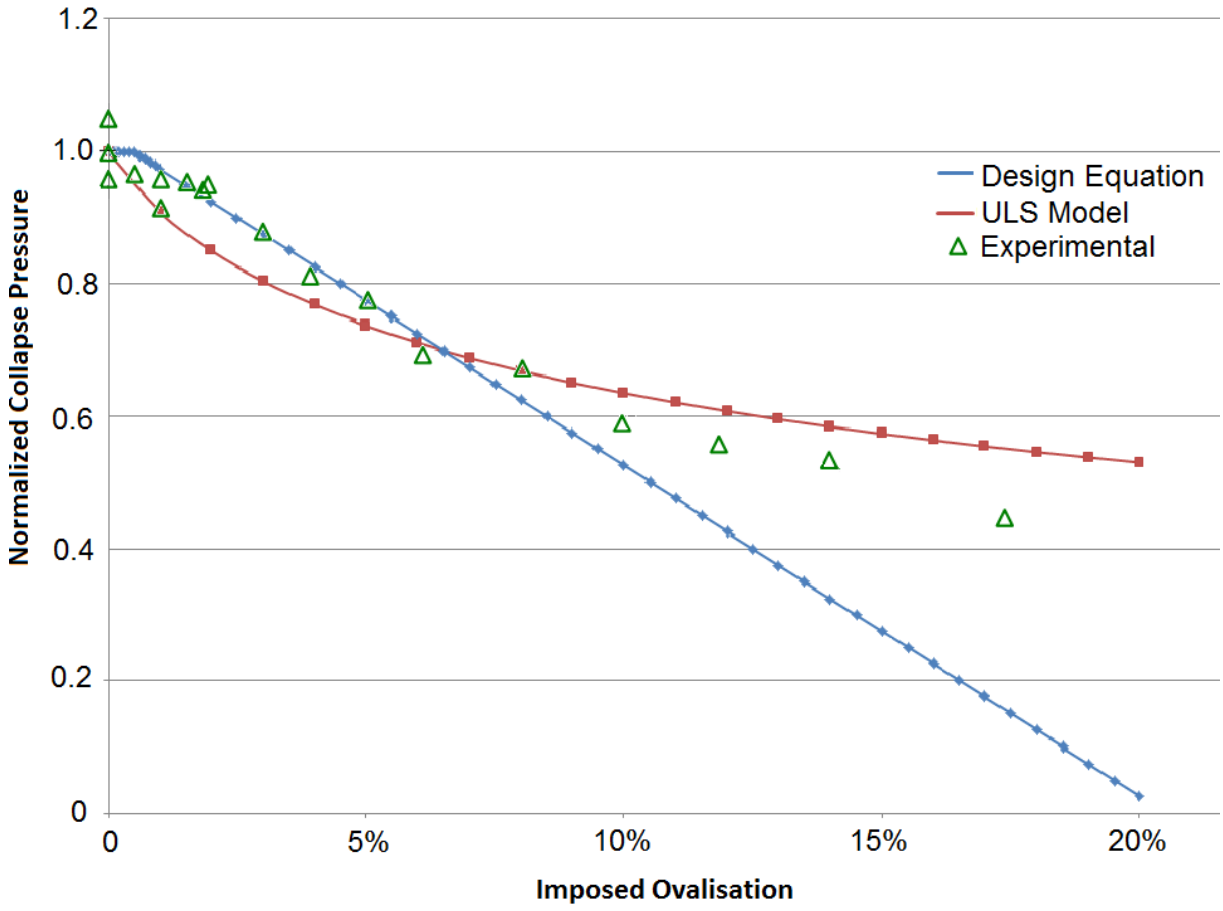

Figure 33: Design equation featuring ovality factor and ULS model compared with experimental data

The proposed design equation or ovality factor reduces collapse resistance linearly from 0.5% imposed ovality. It was chosen as to best represent actual casing performance since analytical models consistently underpredict strength. However, after reaching about 6% ovality the linear ovality factor predicts far greater loss in strength than the ULS model. The limited amount of experimental data available exhibits the same trend as the analytical model. After, say, 10% ovality, it is clear the design equation is pessimistic and not accurate. A suggestion could be to use the ULS model for ovality greater than a certain percentage. The ovality factor was introduced by Last et al. (2002) based on comparison with numerical analyses and the

analytical Tamano model which is extremely sensitive to ovality, e.g. 60% loss in collapse strength at 5% ovality. The ULS model based on Klever & Tamano with its decrement function calibrated by ISO have seemingly accounted for ovality as indicated by the similarities of the curve in Figure 33 compared to experimental data, even though it slightly underpredicts strength at low ovality and overpredicts strength at high ovality. Uncertainties in actual performance at high degrees of ovality lead to the sensitivity analysis in section 5.6 being limited to 5% imposed ovality.

The possibility of casings being ovalised to such great extents must be investigated, and maximum ovalisation should be differentiated by the cause of ovalisation, e.g. hydrostatic pressure or non-uniform loading,

The validity of the experimental data may be questioned. The results originate from collapse tests of multiple welded 4 ½ in P-110 casings of various pipe geometry. Its representation of 9 5/8 in P-110 casings cannot be verified without further testing.

Ovality has historically been disregarded by API as a separate factor that needed singling out. Literature review shows the importance of imposed ovality and culminated in an ovality factor. The well evaluated in this report is located in an area of uniform stress levels. Since severe ovality is usually caused by non-uniform formation stress levels it is not considered important.

Axial Tension Loads

Of all sources reviewed in this project only Jammer et al. (2015) and the DEA-130 dataset provide measurements of all required parameters in the ULS model. None of the casings tested are subjected to simultaneous forces. Verification of the ULS model for casings with axially induced stresses ought to be done in conjunction with testing machines capable of applying axial loads. Some technical papers exist in literature but fail to report the needed measurements for model verification.

Usually only actual yield strength is measured and reported. Using nominal values and governing cases for the decrement function, the analytical collapse resistance of the best and worst performing casing subjected to axial loads can be determined. Experimental test results

should plot anywhere in between those performances. Figure 7 and Figure 8 confirm the plausibility of the experimental test data from Kyogoku et al. (1982).

The difference between the best and worst performing casing according to the ULS model may be as much as 38%. Bear in mind only the decrement function consisting of ovality, eccentricity and residual stress is affecting the three curves of the figures mentioned. It is a huge spread and the model accuracy is not verifiable by the experimental data without geometric and residual stress measurements.

Assuming all casing samples are obtained from the same batch, properties will most likely be similar. If so, the ULS model predictions of average decrement function values seem to be of best fit. It is then likely that the pipes tested by Kyogoku et al. (1982) are average. Experimental data exhibit the same trend as the ULS model when axial tension load is increased.

Axial Compression Loads

The analytical models based on von Mises yield criterion referred to in this report show increased collapse strength of compressed casings.

ISO simplifies the K&T model and denotes axial loading exclusively as tension. The calibrated parameters as presented by ISO are not compatible with the original Klever & Tamano model that differentiates tension and compression. Casing performance in compression is consequently a mere image of performance in tension. The ISO workgroup are in possession of several classified databases of collapse of casings subjected to simultaneous loading. It is not specified if the axial load is tension or compression.

Few technical papers evaluate casing performance when subjected to compressional loads. Previously the industry only used standardised ratings for casing strength which did not account for axial loads. The detrimental effect of tension to collapse resistance was identified resulting in the equivalent yield strength formulation. Tension and compression are differentiated by a term in the von Mises equation not present in the model presented by ISO. By plotting collapse strength of casings subjected to axial loads by using equivalent yield strength and the empirical API equations, performance is seen to be increased by

compression. However, general industry practice is not to utilise the added benefit. The absolute maximum collapse strength of a casing is its standardised API rating at standard temperature, e.g. 7950 psi for 9 5/8 in 53.5 ppf P-110 casing.

The effect of axial compression must be accounted for when evaluating actual collapse resistance. The use of a compression factor was proposed by polynomial approximation based on pessimistic analysis. It effectively increases the collapse strength at neutral axial loading by a certain percentage. Indicated by Figure 9 it was deemed more conservative than other analytical models.

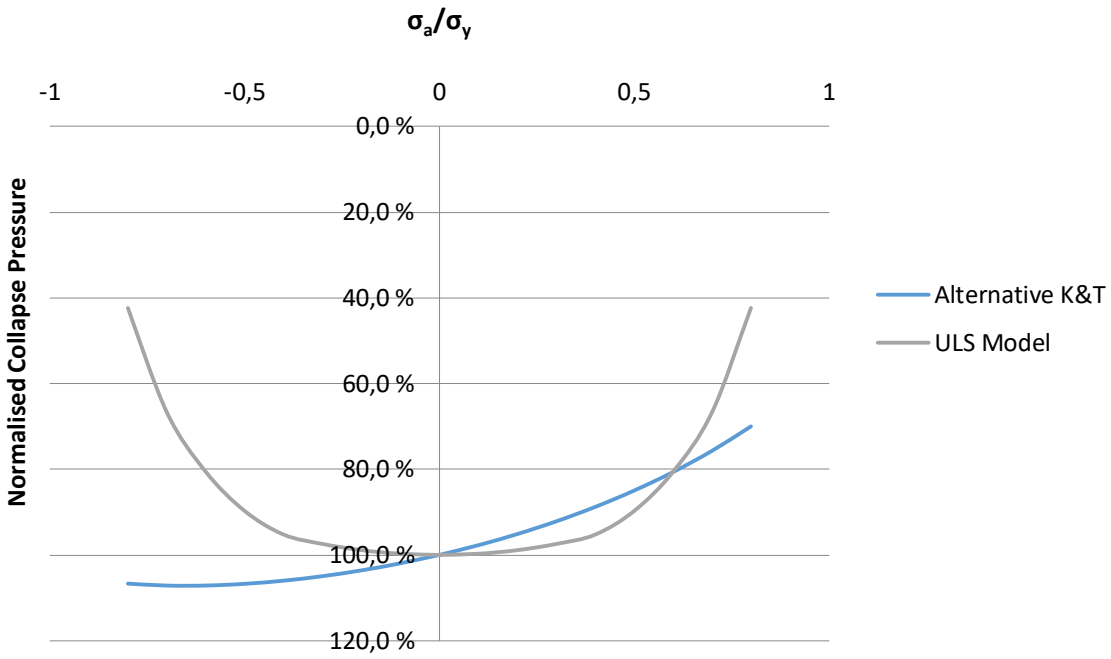

Figure 34: 9 5/8 in 53.5 ppf P-110 performance according to the ULS model and alternative K&T formulation

Figure 34 shows the predicted collapse pressure for the typical casing in question. If using the suggested equations and parameters by ISO, the ULS model mirrors performance in tension and compression. Section 4.2.1 evaluated the accuracy of this model of casings in tension. The predicted collapse strengths matched the trend line of experimental data accurately if the pipes were of similar geometric properties. The alternative K&T formulation predicts strength in tension differently. Which model is the best predictor of strength is unknown. A possible suggestion for further discussion may be to calibrate parameters exclusively for the original Klever & Tamano model. No such effort has been made in this report.

For performance of compressed pipes the two models are vastly different. The ULS model (prior to implementing the compression factor) indicates reduction of strength as axial compression increases. The alternative K&T formulation shows increased strength, in line with API and Tamano. Only experimental test data will verify the accuracy of these models. Experimental test data are, however, limited. Only 9 collapse tests were available to the author. The tests show various degrees of accordance with von Mises yield criterion and are deemed inconclusive. Systematic testing of pipes in compression is needed to verify the model. The highest increase of collapse strength of compressed casings was 12% for a perfect pipe according to the original Tamano equation. For design purposes, it requires great amounts of resources to verify or develop models to prove the benefits of axial compression. Even a greater deal of effort is needed to change internal practices and widely accepted industry standards. It is, as with casing wear, much simpler to increase grade or wall thickness.

Casing Wear

Casing wear is predominantly critical for multilateral wells of high deviations. The well in question is somewhat unusual for modern wells with only a tangent section of 60^{o}. Nonetheless typical wear for a production casing could be 10-20% depending on the scale of operations and material quality of the casing itself.

The location of highest wear is expected to be at the build section due to high dog leg severity. Key seating could potentially be an issue to which increased wear is experienced. For the Well K the differential pressure across the casing wall is significantly lower at kick off point than at the vicinity of Tiller sandstone formation. However, casing wear should not be ignored in the tangent section. Especially since applying weight on bit causes compression of the drill string which pushes it against the low side of the casing. Efforts should be made to obtain USIT logs of the production casing.

The analytical models mentioned in this report do not consider casing wear. Its impact is reviewed separately. Current industry practice assumes uniformly distributed wear. The industry leading software used for well design performs calculations to indicate maximum allowable casing wear in percentage before collapse is initiated and integrity is lost. Effectively, the software finds the thinnest casing of same grade that, according to the

conservative API equation, can withstand the imposed loads even with design factor applied. In reality casings are not worn uniformly. In fact, the worst case scenario would be having the tool joint of the drill string concentrated at either the high or low side of casing throughout the entirety of all drilling operations. The tool joint would induce local wall thickness reduction of greater magnitude than a scenario of uniformly distributed wear. In terms of performance 1% uniform wear will reduce collapse strength more than 1% local wear.

As discussed in section 4.4 the 1% rule is not agreed upon by all technical papers. There are great uncertainties related to derating collapse strength by a certain percentage. The wear radius, or tool joint OD, is of importance to the linearity of collapse strength reduction due to casing wear. Proposed further work is to analyse the effect of local casing wear by FEA and/or more experiments and propose an analytical formulation. The extra hassle of incorporating analytical solutions with regards to casing wear is acknowledged, especially due to all the uncertainties related to casing wear models. Using the 1% rule is an approximation for engineering applications but more precisely analyses are needed for accurate collapse strength predictions.

Cement Support

All experiments showed increased collapse resistance with support of cement. Casing-cement-casing composite showed greater increase than only casing-cement composite. The increased collapse resistance is believed to be caused by deformation constraint. Ovalisation is hindered by the confining cement and another mode of collapse is initiated as seen by the numerical modelling in Figure 35.

For all experiments the cement has been taken the same for all cases, valid for ambient temperature and not HPHT wells of 150 ^{o}C. The effect of temperature on cement properties is not evaluated.

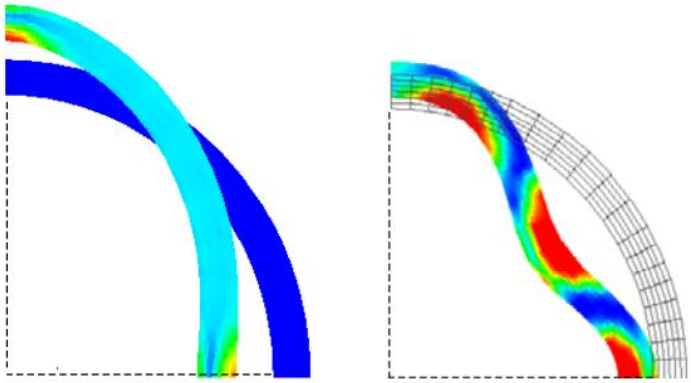

Figure 35: Casing deformation with and without support of cement. Extracted from Figure 11 of Last et al. (2002). Initial state of casing is the dark blue quarter. Red colour represents maximum strain.

In field examples it is likely that only parts of the casing string is cemented inside another string of casing. The production casing length tends to be some thousand meters long. Norsok D-010 requires 100 or 200 meters of planned cemented interval above a zone of potential inflow or cross flow of hydrocarbons. The actual required length of cemented interval is even reduced if integrity is verified by logging tools. In other words it is unlikely the entire production casing is supported by cement. Even if the entire string was cemented in place, it would still miss the support of an outer casing for major parts of the section. The pipe-cement-pipe system tested by Jammer et al. (2015) may represent field cases in some instances. For numerical modelling, three layers are applied to the software model. The outermost casing is not representative of formation support, i.e. formation closure around the circumference of the casing or cement sheath, since Young's modulus of steel is far greater than that of typical rocks. It is rather unlikely the 52.9% increase in strength is realised in a pipe-cement-formation system. For experimental testing purposes it is recommended to replace the outermost steel casing with an aluminium casing, which is more representative of the ductile behaviour of formations.

Cement support may hold the key to counter high pressure formations in deep wells. Cement is already used for zone isolation, i.e. isolate and seal high pressure formations of potential influx or cross flow. Not utilised in design of wells is the deformation hindrance cement introduces. Literature search returns few scientific papers investigating collapse of cemented casings, and understandably so. To quantify the strength increase by presence of cement requires verification of its quality, e.g. by USIT logs or CBL tests. Cement is used for well integrity as a barrier element and quality verification through logging is not necessarily

required. Integrity of cement sheath may be verified by returns during cementing and pressure testing. With varying wellbore geometry and the use of excess cement, pin pointing the exact location of top of cement, i.e. actual length of cemented interval, holds great uncertainty.

Cement jobs are completed with various degrees of success. Consequently cement quality differs. Suggesting a universal analytical or empirical equation for collapse strength of cemented casings would be difficult to implement. It would possibly require mandatory secondary logging of all cemented intervals even though full returns during cementing would be sufficient to qualify as barrier element. Designing new wells, it is much easier to simply increase grade or weight of casing. However, in a scenario of risk assessment of an existing well an analytical or empirical equation could be introduced as long as uncertainties are accounted for.

Even poor quality cement showed increase of collapse resistance for the experimental tests as presented in section 4.5. More tests are required to confirm numerical simulations and/or develop an analytical model.

Well Integrity

Section 5.6 analysed the well integrity challenges of asset life extension (low pressure production) of a subsea well. Two scenarios were modelled, only differentiated by internal pressure. The main issue for this particular well is the collapse strength of the 9 5/8 in 53.5 ppf P-110 production casing. The presence of a high pressure formation will, according to current governing documentation, collapse the production casing if the internal pressure is reduced sufficiently.

The main goal of the case study in this project was to utilise the hidden safety factor for collapse strength due to conservative estimations upon initial design. The basic strength of the casing was found by Monte Carlo simulations and effects of temperature, axial loading, ovality, casing wear, cement support was evaluated with and without design factor applied.

The basic strength of the casing was estimated to be at least 9900 psi with 97.5% confidence. Derating strength due high temperatures and applying design factor of 1.1 leads to the design strength of 8415 psi before considering casing wear – not sufficient to withstand the collapse

pressure of either load: full evacuation or low pressure production. Even when excluding the use of design factor, the casing is still predicted to fail under full evacuation with collapse pressure of 9284 psi. It is then obvious Well K still would need exemption from the above/below packer criterion even when replacing the empirical API equations with the ULS model, all things equal.

In order to ensure safe operation of Well K the beneficial effects of axial compression, cement support or internal pressure must outweigh the detrimental effects of wear and ovality when exposed to the full 9284 psi of Tiller formation. By conservative approximation, the axial effect increases collapse resistance by 2.5% and 3.2% for Full Evacuation and LPP respectively. Since the Tiller formation is present in the cemented interval of the 9 5/8 in casing at a uniform stress field location, the assumption of non-ovalised casing was applied. Full evacuation of casing is still an issue. The collapse resistance needs to be improved vastly by cement support. If internal pressure is maintained the maximum allowable wear of a non-ovalised casing is 2.5% when including the design factor. Every per cent increase in collapse resistance due to cement support can counter an additional per cent of casing wear as seen in Table 34. Ignoring the design factor, the casing could allow for up to 10% wear even without support of cement. The main uncertainty is the quality of cement and its effect on collapse resistance.

According to current governing documentation and industry practice the minimum internal pressure, i.e. reference point B (5613 m MD), bottom hole flowing pressure minus hydrostatic gradient and friction loss, should be 2490 psi. In fact, since using the empirical API equations, it should be slightly more since the support of internal pressure is not fully added to the collapse strength. The minimum BHFP can be converted to well head pressure but it requires knowledge of the produced fluid. Minimum internal pressure of approximately 2500 psi is required to maintain well barrier independence for a casing of no wear and imposed ovality. This requirement is nowhere near the suggested lower limit of BHFP of 870 psi. The well must be shut down, reservoir pressure maintained, or secondary modifications such as scab liner or recompletion with replacement of the production packer – any option must be considered for safe operations according to current collapse strength formulations.

Even if the cemented interval is resistant to collapse, the uncemented parts of the casing string must still withstand a high pressure differential. The highest pressure differential in the uncemented string would be at top of cement. The external pressure is 8525 psi or 588 bar.

Ignoring the small benefits of axial compression, Table 27 and Table 28 allow for easy identification of allowable wear as for ovalised casings. Many combinations of wear and ovality are allowed if internal pressure is maintained at, say, 870 psi – especially if design factor is ignored or lowered.

Introducing the ULS model to casing designers will for some combinations of wear and ovality or cement support – especially when internal pressure is maintained – allow for safe operating. The hidden safety factor as a result of conservative estimations may be utilised after completing the well. Even if the above/below packer criterion still is not fulfilled, the required internal pressure limit can be decreased as to allow for greater recovery than originally planned.

Uncertainties

The uncertainty of the predictive equation was explained in section 3.1.3. The model uncertainty is the statistical variation due to errors and/or limitations in the model. Treating all input variables as independent the effect of each parameter may be filtered out leaving the remaining variability as the model uncertainty. When incorporating other effect, e.g. imposed ovality and casing wear, the uncertainty is greatly increased.

The casing in question, 9 5/8 in 53.5 ppf P-110, is assumed to be representative of the production quality statistics from DEA-130 dataset. This dataset contains measurements from 43 seamless Q&T HRS casings of different size, weight and grade from different batches, mills and manufacturers. An example of inaccurate PDF representation is the output of yield strengths less than the specified minimum of 110 000 psi for P-110 casings. In addition, errors in measurements may have occurred, though outliers are removed. This is not in control of the author.

The pipe dimensions and stress statistics of the ensemble of 2986 Q&T specimens used to calibrate parameters by ISO were manufactured from 1977 to 2000 from at least 14 different API mills worldwide (ISO/TR 10400, 2007). It is believed that a single batch or any individual mill may have less variability in production quality than the ensemble average.

The predictive accuracy of the design ULS model for collapse strength of pipe only was identified. With Gaussian distribution, the average actual/predicted strength was 0.999 with corresponding standard deviation of 0.0648. The worst predictions were 11.3% below and 14.1% above actual strength.

The effect of axial compression was modelled after current analytical models and an equation was conservatively suggested based on the worst performing model.

The suggested use of an ovality factor for imposed ovality was fitted to experimental test data of a non-representative casing. It is more conservative than the experimental and numerical results but not the decrement function for up to 6% ovality.

Linear trend, or the 1% rule, was used to account for casing wear. It is less detrimental than current practice of uniform wear approximation. Literature review returned results which indicated both more and less collapse strength reduction than the linear suggestion.

The effect of cement support was discussed qualitatively. No equation was given for collapse strength increase. The 52.9% increase in strength by experimental results was considered too much. There are great uncertainties in both the actual increased strength of cement support, and which properties of cement influence collapse strength increase.

For Well K, the axial loads were extracted from industry leading software using unknown assumptions. The ILS is usually conservative. Regarding bending, only tension was added to the total axial force – detrimental for casing collapse resistance.

No effort has been made to evaluate the effect of temperature. Standard derating of 0.046% per ^{o}C above 20 ^{o}C was used.

Assumptions

ULS Model

- All OCTG are thick walled meaning the mode of collapse is in the transition region
- Fluid pressure is the mechanism of collapse
- The ULS model is for ultimate collapse strength; that is, they predict when the casing actually fails
- All calibrated parameters by ISO except the model parameter, c, is representative of casings used in analyses
- Probability density functions reproduce the actual spread of input variables
- All parameters are treated as independent
- All casings are seamless and quenched & tempered
- Casing connections do not collapse
- Residual stress is normalised by actual yield strength
- Temperature is constant
- Performance is derated by 0.046% per ^{o}C above 20 ^{o}C
- All casings are made of steel with Young's Modulus of 30 000 000 psi and Poisson's ratio of 0.28
- Hot rotary straightened casings feature sharp knee stress-strain curves
- Cold rotary straightened casings feature round knee stress-strain curves

Case Study

- Production quality statistics from the various casings of the DEA-130 dataset is representative of the 9 5/8 in 53.5 ppf P-110 casing used in the case study
- A confidence of 97.5% is sufficient for engineering applications
- Temperature is 150 ^{o}C
- Pore pressure is dominant throughout B-annulus and cement
- For full evacuation of the casing a leakage through the production tubing, blocking of perforations and continued production of wellbore fluids are assumed
- No ovalisation of casing joints in cemented interval
- All axial loads are calculated by ILS

7 Further Work

- Verify the model by comparison with more collapse tests
- Evaluate the predictive accuracy of the ULS model for other types of forming processes and straightening methods
- Perform physical experiments and finite element analysis to review all secondary effects such as casing wear, ovality, axial compression and cement support. Especially cement support is important
- Perform collapse tests with various types of casing connections to see if they are more resistant to collapse than casings
- Filter out high collapse products prior to obtaining probability density function of a parameter
- Propose a design model which outputs collapse strength with a certainty even when not all input parameters are available
- Propose a standardised system of measuring geometrical properties and stress levels of casings
- Investigate the effects of temperature
- Evaluate other candidate wells for asset life extension
- Obtain pipe certificates of casings used in specific wells to accurately estimate properties
- Obtain analysed casing wear logs
- Measure ovality of casings used in actual wells
- Gain knowledge of fluid interchangeability in B-annulus of Well K to estimate the probability of pore pressure being dominant as external pressure
- Perform risk evaluation and probabilistic analysis of well failure of Well K

8 Conclusion

Basic Strength

- The ULS model was found to be very accurate when compared to actual collapse tests from the Drilling Engineering Association project DEA-130. Actual/predicted collapse strength feature a Gaussian distribution, and for seamless Q&T and hot rotary straightened casings the average actual/predicted strength was 0,999 with standard deviation of 0,0648.
- The model parameter, c, greatly affects the predictive accuracy. Using the suggested value of -1+t/D by ISO increases the average actual/predicted collapse strength ratio and standard deviation.
- The indirect method used to estimate collapse strength requires only knowledge of the probability density function of each parameter. With production quality statistics from DEA-130 the average strength of seamless Q&T 9 5/8 in 53.5 ppf P-110 casings was 11362 psi for hot rotary straightened specimens. The 2.5% acceptance limit was 9900 psi – 24.5% more than API's standard rating of 7950 psi.
- With governing cases the average strength was 10269 psi with the 2.5% limit at 9200 psi. This provides minimum performance ratings or design strengths. It defeats the purpose of accurate collapse strength prediction and will add an extra safety factor
- Similar PDFs are presented by ISO from an ensemble of 20 datasets. The corresponding collapse strengths are 10953 psi and 9500 psi using all PDFs, and 9979 psi and 8500 psi using governing cases.

Secondary Effects

- Including the effects of axial loads, internal pressure, imposed ovality, casing wear, cement support, and formation loading will require assumptions – in turn increasing uncertainty.
- Internal pressure supports the casing wall and is simply added to the total collapse pressure differential.
- Axial tension load reduces collapse strength. The ULS model was compared with experimental data for two 9 5/8 in P-110 casings (58.4 ppf and 47.0 ppf). Direct

comparison was not possible due to lack of property measurements but the general reduction of collapse strength with induced axial tension was confirmed.

- The ISO model is not applicable for casings subjected to axial compression
- The increased collapse strength of compressed pipes were conservatively approximated by polynomial curve fitting of an alternative formulation of yield collapse strength which features the same trends as Tamano (1983) and the equivalent yield strength approach by API.
- A factor for imposed ovality was added to the ULS model. For any ovality greater than a threshold of 0.5%, collapse strength is derated linearly. It was suggested by Last et al. (2002) as to best fit experimental data while simultaneously being more conservative than numerical simulations.
- The decrement function was calibrated by ISO based on manufacturing ovality up to 1%. It seems to also be applicable for imposed ovality with the general trend of experimental data being reproduced for ovality above 6%.
- Three technical papers that perform physical collapse tests of worn casings were reviewed. None of the papers have measured the required input parameters of the ULS model accurately, making a direct comparison between experimental results and analytical predictions impossible. The 1% rule is not agreed upon by all papers but without measurements of the required parameters it is difficult to filter out the effect of pipe imperfections to isolate and evaluate the effect of casing wear. Using the 1% rule with a design factor is deemed appropriate and was incorporated to the ULS model.
- Experimental test results from two technical papers showed increased in composite collapse resistance even with poor quality cement. Casing-cement-casing composite showed the greatest increase in strength compared to casing only.
- Cement support may hold the key to counter high pressure formations. Not utilised in design of wells is the deformation hindrance cement introduces. To quantify the strength increase by presence of cement requires verification of its quality, e.g. by USIT logs. Logging of cement is currently not necessarily required. Proposing an analytical and universal equation to accurately predict the effect of cement support would require secondary logging of cement quality which differs vastly.

Caste study well

- With the current industry practice, minimum internal pressure at the depth of the high pressure formation needs to be 2500 psi, significantly more than the suggested design life extension pressure 870 psi.
- The above/below packer criterion is not fulfilled even when replacing the empirical API equations with the Klever & Tamano based ULS model. Support from internal pressure or cement is required.
- Axial compression increases collapse strength by 2.5% with full evacuation of casing. Similarly, the increased strength is 3.2% for a low pressure production scenario. The difference is due to ballooning effect.
- With support from internal pressure of 840 psi, non-ovalised casings may allow up to 2.5% casing wear. Ignoring design factor, wear may be as high as 10%
- Moderate strength increase due to support from cement allows for safe operation even when including design factor of 1,1. The critical point would then be at top of cement.

This project proved the feasibility of indirect collapse strength predictions when using production quality statistics and an accurate predictive equation of strength. The case study of Well K is summarised by the following statement: “With some support of internal pressure and/or cement, maintaining well integrity at low pressure production is plausible but cannot be guaranteed”.

In conclusion, the basic strength of a casing is of all likelihood greater than predicted by the empirical API equations. The ULS model was proven to be a good predictor of strength for a small sample size of casings. The detrimental effects of casing wear and ovality can be implemented directly to a collapse strength model, however, accuracy is reduced. The benefit of axial compression needs to be verified by collapse test data. Cement support is likely to increase composite collapse resistance and could be, for special applications, utilised in integrity evaluation. The uncertainties of implementing secondary effects to collapse strength evaluation are acknowledged and the need for a design factor is still viable.

For new wells the Klever & Tamano based model can easily replace the empirical API equations. Other options include increasing weight and/or grade. A shift in paradigm towards more accurate prediction of collapse strength should be pursued. ISO presented the simplified K&T model in 2007 – 10 years later the current industry standards have not yet changed.

9 References

BELLARBY, J. 2009. *Well completion design,* Amsterdam, The Netherlands, Elsevier.

BOURGOYNE, A. T., MILLHEIM, K. K., CHENEVERT, M. E. & YOUNG, F. S. 1986. *Applied drilling engineering,* Richardson, TX, Society of Petroleum Engineers.

CONTINENTAL, A. & S. *P110 - Chemical Composition* [Online]. Available: http://www.contalloy.com/products/grade/p110 [Accessed Dec 15 2016].

DEA-130 2002. *DEA-130 Modernization of Tubular Collapse Performance Properties*, Drilling Engineering Association.

ECONOMIDES, M. J., WATTERS, L. T. & DUNN-NORMAN, S. 1998. *Petroleum well construction,* Chichester, UK, Wiley.

EVANS, G. W. & HARRIMAN, D. W. 1972. Laboratory Tests on Collapse Resistance of Cemented Casing. Society of Petroleum Engineers.

GREENIP, J. F. 2016. Collapse Strength of Casing Subjected to Combined Load. *IADC/SPE Drilling Conference and Exhibition.* Fort Worth, Tx: Society of Petroleum Engineers.

ISO/TR 10400 2007. *Petroleum and Natural Gas Industries - Equations and calculations for the properties of casing, tubing, drill pipe and line pipe used as casing or tubing,* Genève, Switzerland, ISO.

JAMMER, P., HARIHARAN, H. & KLEVER, F. J. 2015. Casing Collapse Strength Enhancement Due to Cement and Pipe Support via Modelling and Testing. Society of Petroleum Engineers.

KLEVER, F. J. & TAMANO, T. 2006. A New OCTG Strength Equation for Collapse Under Combined Loads. *SPE Annual Technical Conference and Exhibition.* Houston, TX.

KORNBERG, E. & STAVLAND, S. 2016. Special Considerations in Casing and Tubing Design for Hydraulic Fracturing Operations. *TPG4560 Petroleum Engineering Specialization Project.* Trondheim: NTNU.

KURIYAMA, Y., TSUKANO, Y., MIMAKI, T. & YONEZAWA, T. 1992. Effect of Wear and Bending on Casing Collapse Strength. Society of Petroleum Engineers.

KYOGOKU, T., TOKIMASA, K., NAKANISHI, H. & OKAZAWA, T. 1982. Experimental Study on the Effect of Axial Tension Load on the Collapse Strength of Oilwell Casing. *OTC 4108.* Houston, TX: SPE-11238-PA.

LAST, N., MUJICA, S., PATTILLO, P. & KELSO, G. 2002. Casing Deformation in a Tectonic Setting: Evaluation, Impact and Management. Society of Petroleum Engineers.

LIANG, E., LI, Z., HAN, Y., LI, G. & GUO, P. 2013. Analysis on Collapse Strength of Casing Wear. *Chinese Journal of Mechanical Engineering,* 26**,** 613-619.

MITCHELL, R. F. & LAKE, L. W. 2006. *Petroleum Engineering Handbook: Driling Engineering*, Richardson, TX, Society of Petroleum Engineers.

PATTILLO, P. D., LAST, N. C. & ASBILL, W. T. 2003. Effect of Nonuniform Loading on Conventional Casing Collapse Resistance. Society of Petroleum Engineers.

RAHMAN, S. S. & CHILINGARIAN, G. V. 1995. *Casing Design-Theory and Practice*, Burlington, NH, Elsevier.

TAMANO, T., MIMAKI, T. & YANAGIMOTO, S. 1983. A New Empirical Formula for Collapse Resistance of Commercial Casing. *Journal of Energy Resource Technology*.

TØIEN, M., BRECHAN, B. A. & SANGESLAND, S. 2015. Modell for casing design.

Appendix A Historical API Approach for Collapse Strength Determination

The following chapter in its entirety is extracted from Kornberg and Stavland (2016) - a specialisation project in Petroleum Engineering at NTNU, Trondheim, forming the basis of this report. The purpose of this chapter is to provide background for the reader.

Burst, collapse and tensile ratings at standard temperature will be given for any casing with a specific API grade, albeit based on a uniaxial stress state in which only one of the three principal stresses is nonzero. For scenarios of combined loads, tri-axial rating should be used. These fundamental loads and corresponding API requirements are explained in the following segments. The effect of temperature is explained in Appendix B.3.

A.1 Tubular Ratings

The American Petroleum Institute, API, have introduced industry accepted standards by providing several quality test methods and standardization of measurements. The grading system consists of a letter which represents the type of steel in use, and a number which corresponds to the minimum yield strength in ksi. An example could be P-110 where the letter P limits the amount of phosphor and sulfur of the steel composition, and 110 indicates a minimum yield strength of 110 000 psi (Continental and S). Yield strength is defined by API as the tensile stress required to produce a total elongation per unit length of 0.005 on a standard test specimen. The test results will vary as the required elongation exceeds the elastic limit of steel, hence the need for considerable test data. The minimum yield strength has been defined as 80% of the average yield strength obtained from the aforementioned tests (Bourgoyne et al., 1986). Other properties are also reported based conducted tests and measurements within standard criteria. Please note that many steel grades do not comply with all of API's standards. Such grades are referred to as 'non-API' and will not be used in this project.

A.2 Tension

If a pipe body is subjected to axial loading it can undergo three types of deformation: elastic, elasto-plastic (transition) or plastic. *Figure 36* plots a typical curve for steel where the straight line up to P represents the elastic range. No permanent deformation is experienced in this

region as the pipe body will always regain its initial form. However, when point P is exceeded, the steel body will undergo permanent deformation, as seen by the deviation from the linear trend. Loss of strength will most likely be a consequence. Point Q on the curve is defined as the yield strength, whilst point R in the plastic region defines the ultimate tensile strength. Axial loads should preferably only induce elastic deformation, and least of all exceed the material yield strength as required by API.

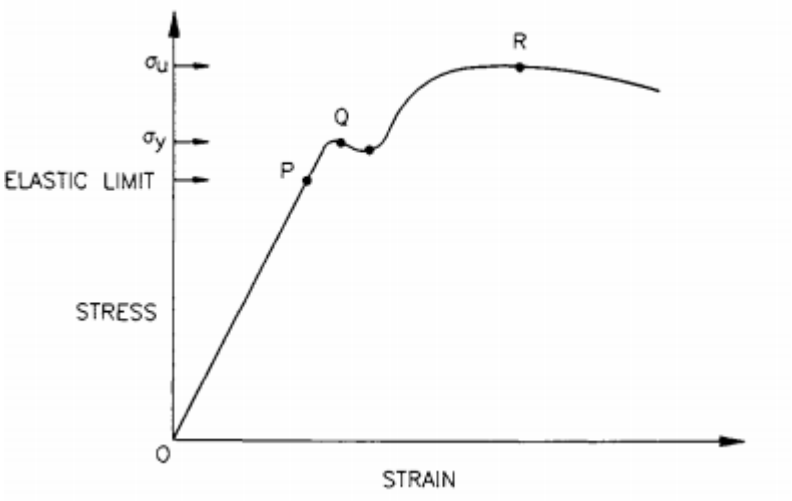

Figure 36: Typical stress-strain relationship for a metal (Rahman and Chilingarian, 1995) Fig 2.1

When there is no differential pressure across the wall, the minimum axial force needed in order to inflict permanent damage to a pipe body is defined as:

$$F_a = \frac{\pi}{4}\sigma_y(D^2 - d^2) \tag{29}$$

A.3 Collapse

Collapse of a pipe may occur when the external pressure is greater than the internal pressure. This is exactly the opposite of burst, yet the collapse phenomenon is much more complex. As a theoretically rigorous equation for collapse does not exist, classic elasticity theory can be combined with numerical and statistical tools to establish the API minimal collapse resistance formulas, given in ISO/TR 10400 (2007) which is identical to API bulletin TR 5C3.

There are four different modes of collapse: yield strength, plastic, transition, and elastic. Collapse strength is primarily a function of the material's yield strength along with the outer diameter to wall thickness ratio, d_n/t, of the pipe body subjected to collapse loads. The ISO

standard presents an equation for each mode of collapse, and specifies applicable D_n/t-ranges.

Historically, the collapse formulas, equation (31) through (34), have used the specified minimum yield strength. If replaced by the equivalent yield strength, $\sigma_{yield,e}$, equation (30), the effect of combined loads according to von Mises may be incorporated to the collapse formulas. The internal pressure has recently been introduced to equation (30) which is the recommended formula for equivalent yield strength.

$$\sigma_{yield,e} = \sigma_{yield}\left(\sqrt{1 - \frac{3}{4}\left(\frac{\sigma_z + p_i}{\sigma_{yield}}\right)^2} - \frac{1}{2}\frac{\sigma_z + p_i}{\sigma_{yield}}\right) \tag{30}$$

Yield collapse rating, p_{yc}, is given by

$$p_{yc} = 2\sigma_{yield,e}\frac{d_n/t - 1}{(d_n/t)^2} \tag{31}$$

Plastic collapse rating, p_{pc}, is given by

$$p_{pc} = \sigma_{yield,e}\left(\frac{F_1}{d_n/t} - F_2\right) - F_3 \tag{32}$$

Transition collapse rating, p_{tc}, is given by

$$p_{tc} = \sigma_{yield,e}\left(\frac{F_4}{d_n/t} - F_5\right) \tag{33}$$

Elastic collapse rating, p_{ec}, is given by

$$p_{ec} = \frac{46.95 \cdot 10^6}{(d_n/t)(d_n/t - 1)^2} \tag{34}$$

For simplicity the equivalent yield strength is denoted as Y. The historical empirical constants, F_1 to F_5, are then given by

$$F_1 = 2.8762 + 0.10679 \cdot 10^{-5}Y + 0.21301 \cdot 10^{-10}Y^2 - 0.53132 \cdot 10^{-16}Y^3$$

$$F_2 = 0.026233 + 0.50609 \cdot 10^{-6}Y$$

$$F_3 = -465.93 + 0.030867Y - 0.10483 \cdot 10^{-7}Y^2 + 0.36989 \cdot 10^{-13}Y^3$$

$$F_4 = \frac{46.95 \cdot 10^6 \left(\frac{3F_2/F_1}{2 + F_2/F_1}\right)^3}{Y\left(\frac{3F_2/F_1}{2 + F_2/F_1} - F_2/F_1\right)\left(1 - \frac{3F_2/F_1}{2 + F_2/F_1}\right)^2}$$

$$F_5 = F_4F_2/F_1$$

The mode of collapse is determined by the outer diameter to thickness ratio, d_n/t. This value should be compared to three criteria. Equation (35) is the upper limit of yield collapse, equation (36) is the upper limit of plastic collapse, and equation (37) is the upper limit of transition collapse. This implies that yield collapse is used for very thin-walled pipe and elastic collapse is applicable for very thick-walled pipes. Most oilfield tubulars are thick-walled.

$$\left(\frac{d_n}{t}\right)_{yc} = \frac{\sqrt{(F_1 - 2)^2 + 8\left(F_2 + F_3/\sigma_{yield,e}\right)} + F_1 - 2}{2\left(F_2 + F_3/\sigma_{yield,e}\right)} \tag{35}$$

$$\left(\frac{d_n}{t}\right)_{pc} = \frac{\sigma_{yield,e}(F_1 - F_4)}{F_3 + \sigma_{yield,e}(F_2 - F_5)} \tag{36}$$

$$\left(\frac{d_n}{t}\right)_{tc} = \frac{2 + F_2/F_1}{3F_2/F_1} \tag{37}$$

A.4 Triaxial

As mentioned, the ratings supplied by API do not consider simultaneous forces. Many of the casing performance properties are altered significantly by axial tension or compression. To evaluate the pipe performance under realistic loading conditions, the uniaxial yield strength should be compared with a yielding criterion. API suggests the use of Huber-Hencky-Mises yield criterion, or simply von Mises, which is based on the maximum distortion energy theory.

$$\left(\frac{\sigma_t + p_i}{\sigma_{yield}}\right) = \pm\sqrt{1 - \frac{3}{4}\left(\frac{\sigma_z + p_i}{\sigma_{yield}}\right)^2} + \frac{1}{2}\left(\frac{\sigma_z + p_i}{\sigma_{yield}}\right) = 0 \qquad (38)$$

Equation (38) defines the combinations of internal pressure, external pressure, and axial stress that will result in a yield strength mode of failure (Bourgoyne et al., 1986).

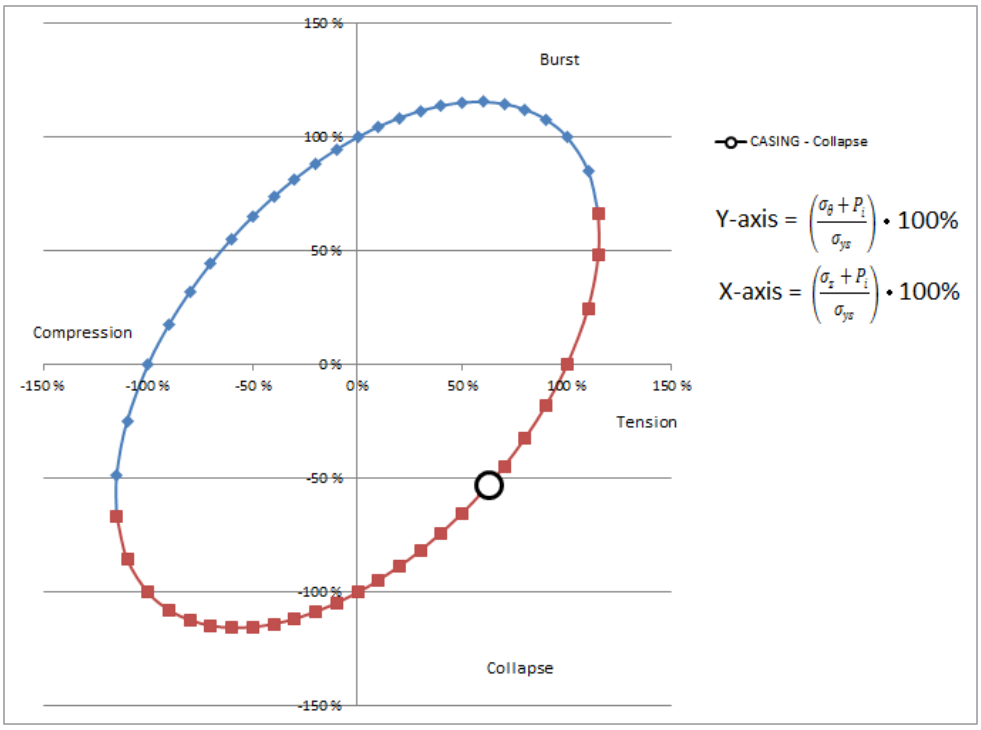

Figure 37: Ellipse of Plasticity

The triaxial stress or equivalent stress is not a real or physical stress. It is only a theoretical term which allows a generalized 3D stress state to be compared to the uniaxial value of yield strength. Any point outside the ellipse will cause yield failure.

A.4.1 Combined Collapse and Tension Loading

By rearranging equation (38) the equivalent yield strength may be expressed as:

$$\sigma_{yield,e} = \sigma_{yield}\left(\sqrt{1 - \frac{3}{4}\left(\frac{\sigma_z + p_i}{\sigma_{yield}}\right)^2} - \frac{1}{2}\left(\frac{\sigma_z + p_i}{\sigma_{yield}}\right)\right) \quad (39)$$

This equation plots the red lower half of the ellipse shown in *Figure 37*, and is applicable for the whole of the 2nd quadrant, which represents a combination of collapse and tension stresses.

With tension of the pipe, the collapse rating is lower than the uniaxial rating. API recommends the use equivalent yield strength for all equations, empirical coefficients and d_n/t criteria range discussed previously when determining the collapse pressure rating.

However, Economides et al. (1998) states that collapse of most oil field pipes is either an inelastic stability failure or an elastic stability failure independent of yield strength. Von Mises criterion is based on elastic behavior and yield strength and should not be used with collapse loads since the collapse pressure rating will be overly conservative. The exception is thick-wall pipes (low d_n/t ratio) where the lower right quadrant of ellipse of plasticity is essentially equal to the uniaxial API criterion.

A.4.2 Combined Collapse and Compression Loading

Compression and collapse loads may induce a failure mode of permanent corkscrewing as a result of helical buckling. This combination is typically experienced in wells where production induces a large temperature increase which also causes reverse ballooning (Economides et al., 1998). The result is increased compression in the string which is not fixed.

Appendix B Axial Load

The following chapter in its entirety is extracted from Kornberg and Stavland (2016) - a specialisation project in Petroleum Engineering at NTNU, Trondheim, forming the basis of this report. The purpose of this chapter is to provide background for the reader.

Axial loads act along the length of the tubing. Several factors, including pressure and temperature, contribute to axial loads so that a pipe may either be in tension or compression. The transition between tension and compression of a string will include a neutral point of zero axial load. Tension will be defined with positive values throughout this report. The following chapter is based on Well Completion Design (Bellarby 2009).

B.1 Weight of Casing

The unit weight of any casing is listed as a property. It includes nominal threaded and coupled connections as defined by API. The total weight of the string may be obtained by multiplying weight per foot by the length of the string. The value obtained is dry weight and would represent the hook load in a drained, vertical well.

In deviated wells only the vertical component of the weight is contributing to the recorded hook load at RKB. The horizontal component is said to be resting on the low side of the hole. By correcting for hole inclination the axial force will be given by:

$$F_w = W\cos\theta \tag{40}$$

where F_w is axial force, W is the weight of the string, and θ is hole inclination.

The weight of the string in a horizontal section will not contribute to axial forces, as seen by setting θ equal to 90^o in the equation (40). It leads to some operational issues such as using drill collars for WOB further up the wellbore.

B.2 Buoyancy

The weight of casing must be corrected for buoyancy effect. Any object immersed in any fluid will be subjected to a buoyancy force acting in the opposite direction of gravity. This effect is largely determined by the fluid density and object volume or surface area. The term

fluid includes gas and liquids. Since the unit weight of casing is measured in air, the buoyancy force is already accounted for. In addition, the buoyancy effect in low density gas is very small. It is therefore more convenient to speak of submerged objects in liquids.

There are two ways in which the buoyed weight of an object can be obtained. Both will be presented here since opinions are divided regarding which method is correct. However, Tøien et al. (2015) indicates that the ILS uses the latter method.

B.2.1 Archimede's Principle

Archimede's principle indicates that there will be a buoyant force exerted on a body immersed in a fluid which will act in the opposite direction of gravity. A buoyancy factor is obtained by:

$$\beta = 1 - \frac{\rho_o + \rho_i \left(\frac{{d_i}^2}{{d_n}^2} \right)}{\rho_s \left(1 - \frac{{d_i}^2}{{d_n}^2} \right)} \tag{41}$$

where β is buoyancy factor, ρ_o is fluid density outside of the pipe, ρ_i is fluid density inside of the pipe, ρ_s is density of steel and d_i is inner pipe diameter

The dry weight of the casing string must be multiplied by the buoyancy factor in order to find the net sum of gravitational force and buoyant force.

B.2.2 Piston Force

Buoyancy, in terms of piston force, will be modeled as fluid pressure acting directly on the exposed pipe cross section, as seen in *Figure 38*. The net axial load is obtained by subtracting the buoyancy force from the dry weight of the casing string. The exposed area will be dependent upon closed end or open end displacement. Buoyancy force is given by:

$$F_p = \rho_f g Z A \tag{42}$$

where F_p is buoyancy force, ρ_f is fluid density, g is the gravitational acceleration, Z is true vertical depth, and A is either closed end area or open end cross sectional area of the pipe.

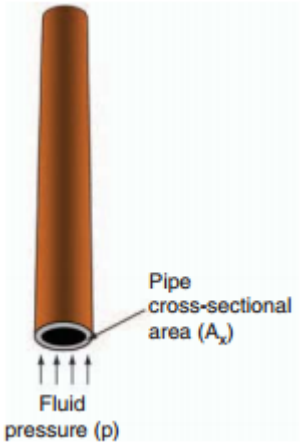

Figure 38: Buoyancy force as piston force acting on the cross sectional area (Bellarby, 2009)

B.3 Temperature Effect

Metal expands when heated, and contracts when cooled. If the casing is fixed in the casing hanger at the well head and at the bottom by cement, such processes will cause compressive and tensile stresses respectively.

Axial stress contribution caused by temperature change is given by:

$$F_T = -C_T E \Delta T (A_o - A_i) \tag{43}$$

where F_t is axial force due to temperature change, C_T is the coefficient of thermal expansion, E is Young's elastic modulus, A_i is the inner area, A_o is the outer area, and ΔT is temperature change (Bellarby, 2009).

As a general rule, heating is caused by production and cooling is caused by injection, either by drilling operations or by enhanced oil recovery methods (Bellarby, 2009). Production of hot reservoir fluids will often be the most extreme case in terms of steel expansion. Occasionally gas injection at high pressures and/or high rates will also increase the temperature as the compressors will heat the gas. Friction caused by fluid flow will also cause

heat development, but the effects are negligible in terms of metal expansion thus axial stresses (Bellarby, 2009).

Temperature change will also influence the load resistance as the material's yield strength is temperature dependent. Heating of steel pipe will reduce the burst, collapse, axial and triaxial ratings given by API (Mitchell and Lake, 2006).

B.4 Ballooning Effect

The relationship between radial strain and axial strain is given by Poisson's ratio, equation (44), and is considered to be a material property. These two strains are proportional to each other in the elastic region.

$$\nu = -\frac{\varepsilon_r}{\varepsilon_a} \tag{44}$$

where ν is Poisson's ratio, ε_r is radial strain, and ε_a is axial strain (Bellarby, 2009).

Radial strain as a result of change in pressure will induce axial strain, or axial stress if the tubing is fixed in both ends, an effect known as ballooning. A change in pressure either outside or inside of the casing or tubing (i.e. burst or collapse loads) will generate an axial tension or compression respectively. The resulting force can be obtained by

$$F_b = 2\nu(A_i \Delta p_i - A_i \Delta p_o) \tag{45}$$

where F_b is the ballooning effect force and Δp is the change in pressure relative to the pressure at time of completion or cementing.

B.5 Bending and Buckling

Bending can be caused by doglegs of the well trajectory and by buckling, both of which give important effects on axial loads. Bending will result in increased axial tension on the convex side and increased axial compression on the concave side. Unlike the previously mentioned contributors to axial loads, the bending loads caused by doglegs are local. Consequently a bend will not affect the stresses anywhere else in the pipe. The bending stresses are either

tension or compression and should be added to the existing stress profile. Common practice is to apply worst case scenario. If the existing stress profile due to weight, temperature and ballooning indicate tension, only the tensile contribution of bending should be added. Similarly, if the pipe is in compression, only the compressive contribution of bending is included.

Beam theory can be applied to calculate bending stresses given in field units by:

$$\sigma_b = \pm \frac{ED\pi\alpha}{360 \cdot 100 \cdot 12} \tag{46}$$

Where σ_b is stress due to bending. In addition, the dogleg severity, α, is given in ^{o}/100 ft and diameter is given in inches (Bellarby, 2009). The ± sign is because tension on the outside of the bend is given by positive values, and compression on the inside of the bend should have negative values.

Buckling may occur when the pipe is under sufficient compressional load. Buckling is a deformational process in which the pipe reaches a more stable state upon compression. There are two modes of buckling; sinusoidal and helical. Sinusoidal buckling is also known as lateral buckling since its S-shaped deformation is not a true sinusoid (Bellarby, 2009). Helical buckling takes the form of a coil. The effective force under buckling is given by:

$$F_{eff} = F_{tot} + (p_o A_o - p_i A_i) \tag{47}$$

where F_{tot} is the total axial force disregarding buckling.

The pipe will tend to buckle if F_{eff} is less than the critical force F_c, which in a deviated wellbore is given by:

$$F_c = K' \sqrt{\left(\frac{4EI\omega sin\theta}{r_c}\right)} \tag{48}$$

where I is the moment of inertia, equation (49), ω is the buoyed pipe weight, and r_c is the radial clearance. K' is a constant and equal to 1 for sinusoidal buckling and 1.41-1.83 for helical buckling (Bellarby, 2009).

$$I = \frac{\pi}{64}(D^4 - d^4) \tag{49}$$

Buckling is also affected by the internal and external pressure as seen by equation (45). As mentioned in previously, burst pressure will cause ballooning of the pipe. This effect reduces the axial compression and hence the effective buckling force. However, the latter term of equation (45) is increased so that ultimately the effective buckling force increases (Mitchell and Lake, 2006).

The mode of buckling is dependent upon several factors, such as wellbore deviation, connections, centralizers, radial clearance amongst others. They are thoroughly discussed in Bellarby (2009) section 9.4.8 and will not be presented here. However, a general buckling mode criteria can be used and is summarized in the table below.

Table 38: Buckling criteria (Mitchell and Lake, 2006)

Buckling Force Magnitude	Result
$F_{eff} < F_c$	No buckling
$F_c < F_{eff} < \sqrt{2}F_c$	Sinusoidal buckling
$\sqrt{2}F_c < F_{eff} < 2\sqrt{2}F_c$	Sinusoidal or helical buckling
$2\sqrt{2}F_c < F_{eff}$	Helical buckling

In other engineering disciplines, buckling is considered as failure. In well design, buckling is limited by contact, either with casing or formation, thus some degree of buckling can be tolerated (Bellarby, 2009). The buckling severity depends on the pitch of the buckles pipe and the radial clearance. For helical buckling the helix angle is assumed to be constant. However, for sinusoidal buckling, the helix angle will not be constant throughout the S-shape. A maximum helix angle is needed and it can be approximated by (Bellarby, 2009).

Sinusoidal buckling:

$$\lambda_{max} = \frac{1.1227}{\sqrt{2EI}} {F_{eff}}^{0.04} \left(F_{eff} - F_c\right)^{0.46} \tag{50}$$

Helical buckling:

$$\lambda_{max} = \sqrt{\frac{F_{eff}}{2EI}} \tag{51}$$

where λ_{max} is the maximum helix angle.

The resulting buckling induced dogleg severity is calculated as:

$$\alpha_b = 68.755 r_c \lambda^2 \tag{52}$$

where the buckling induced dogleg severity, α_b, is given in ^{o}/100 ft, and replaces α in equation (46) to give the bending stresses due to buckling (Bellarby, 2009).

Appendix C Probability Distributions

C.1 Probability Distributions from DEA-130

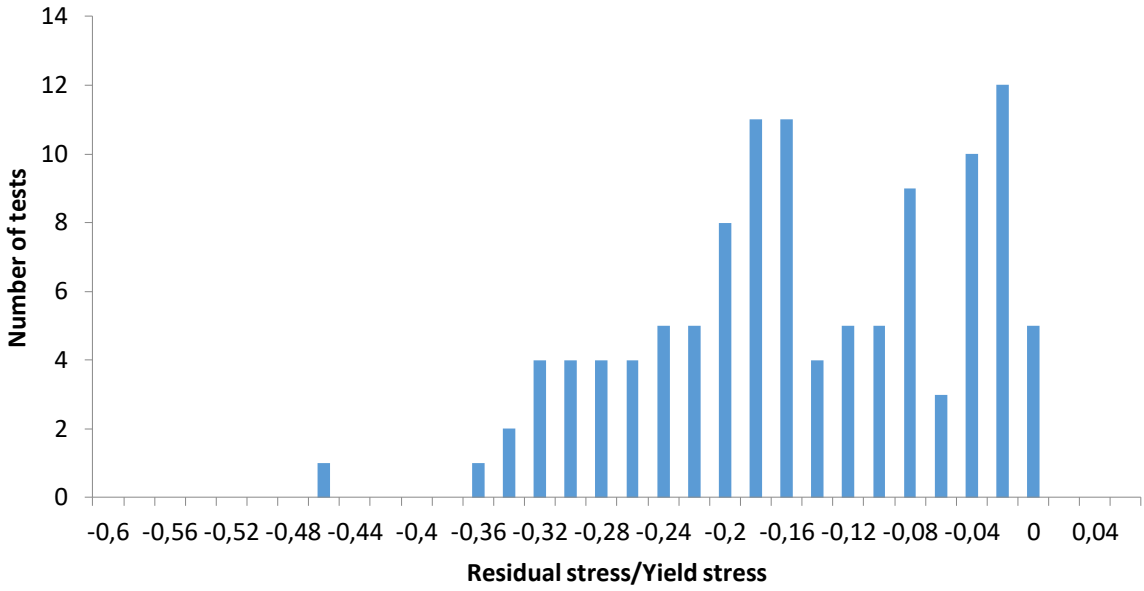

Figure 39: Probability distribution of rs/ys using 113 tests from DEA130

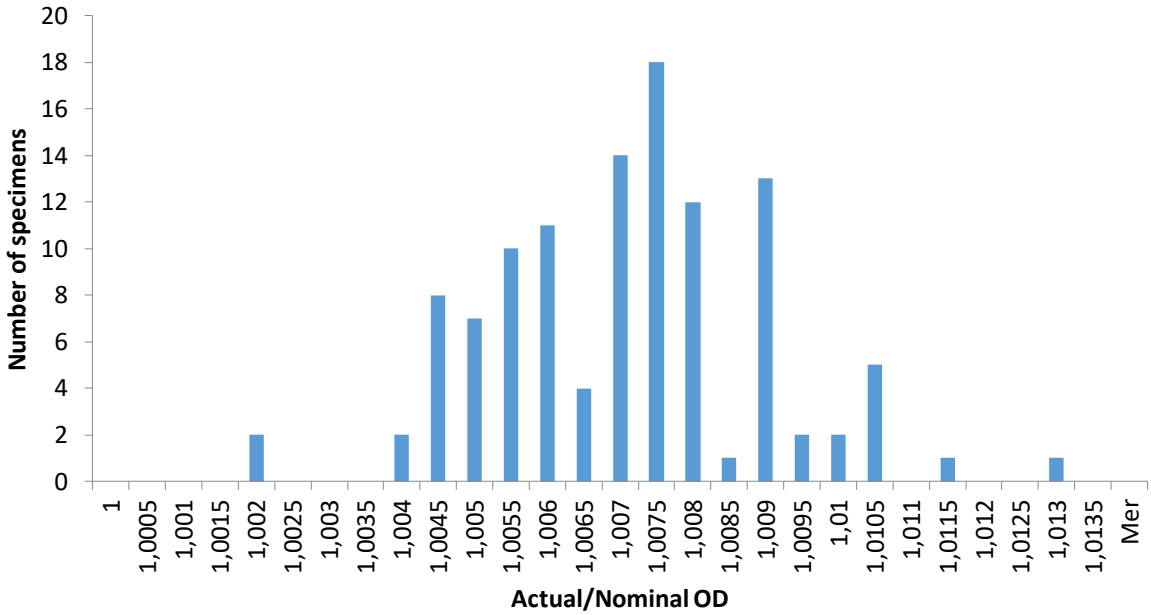

Figure 40: Probability distribution of outer diameter using 113 tests from DEA130

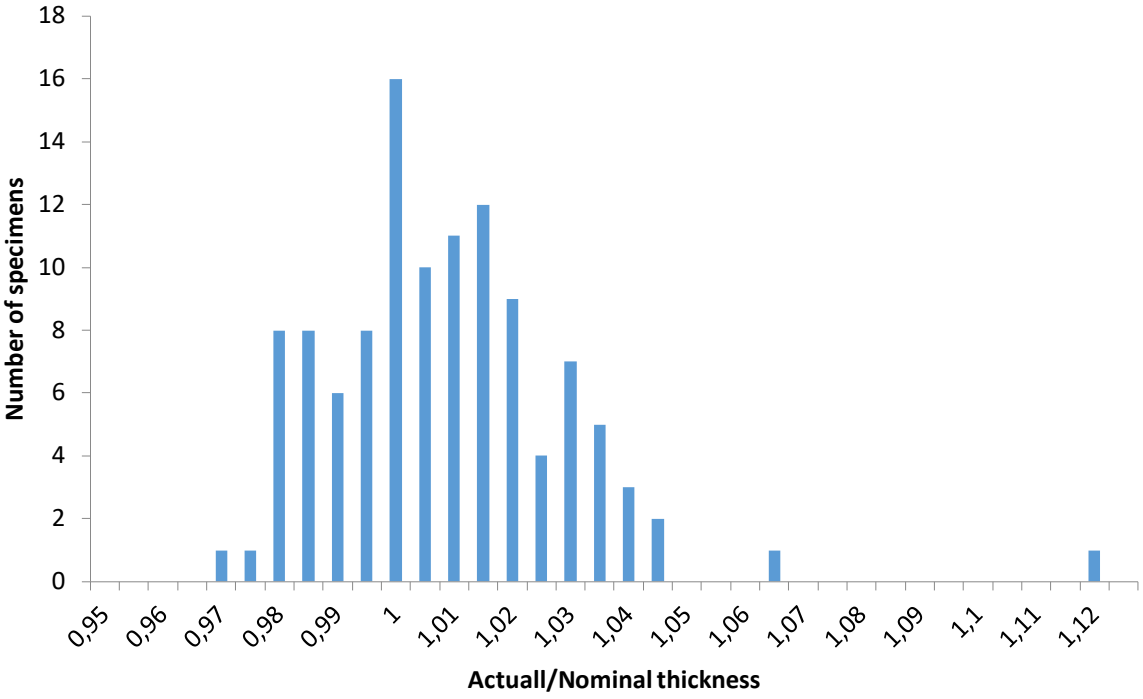

Figure 41: Probability distribution of wall thickness using 113 tests from DEA130

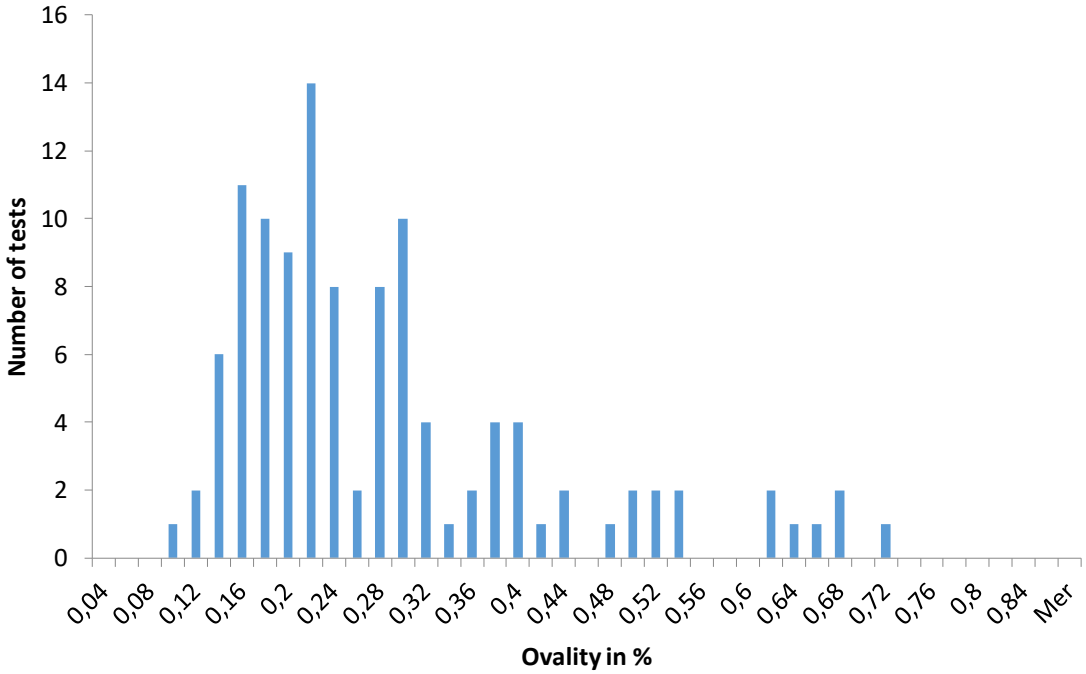

Figure 42: Probability distribution of ovality using 113 tests from DEA-130

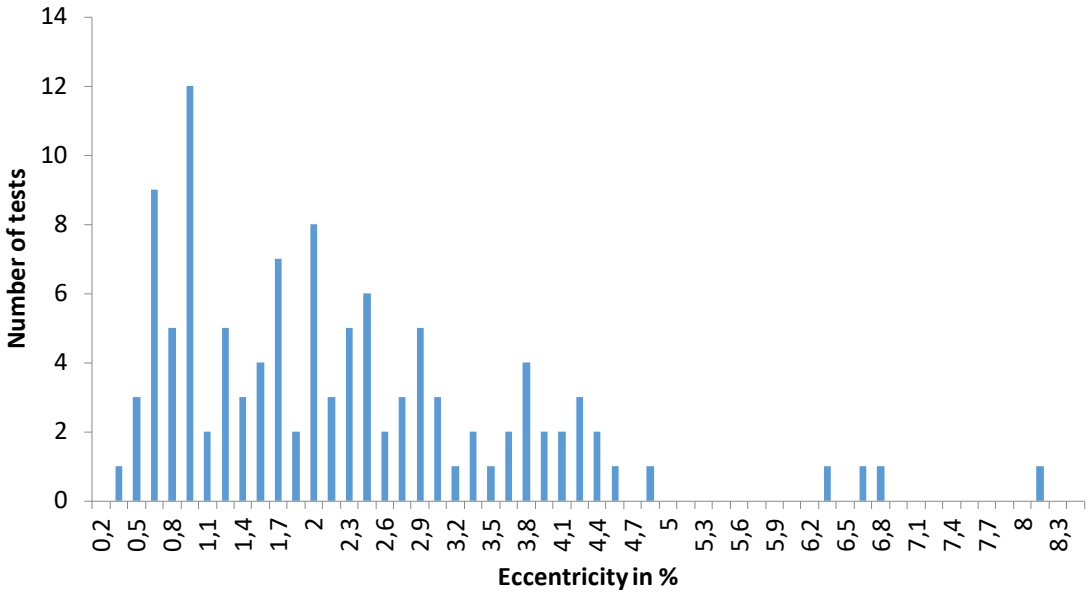

Figure 43: Probability distribution of eccentricity using 113 tests from DEA130

C.2 Probability Density Functions from DEA-130

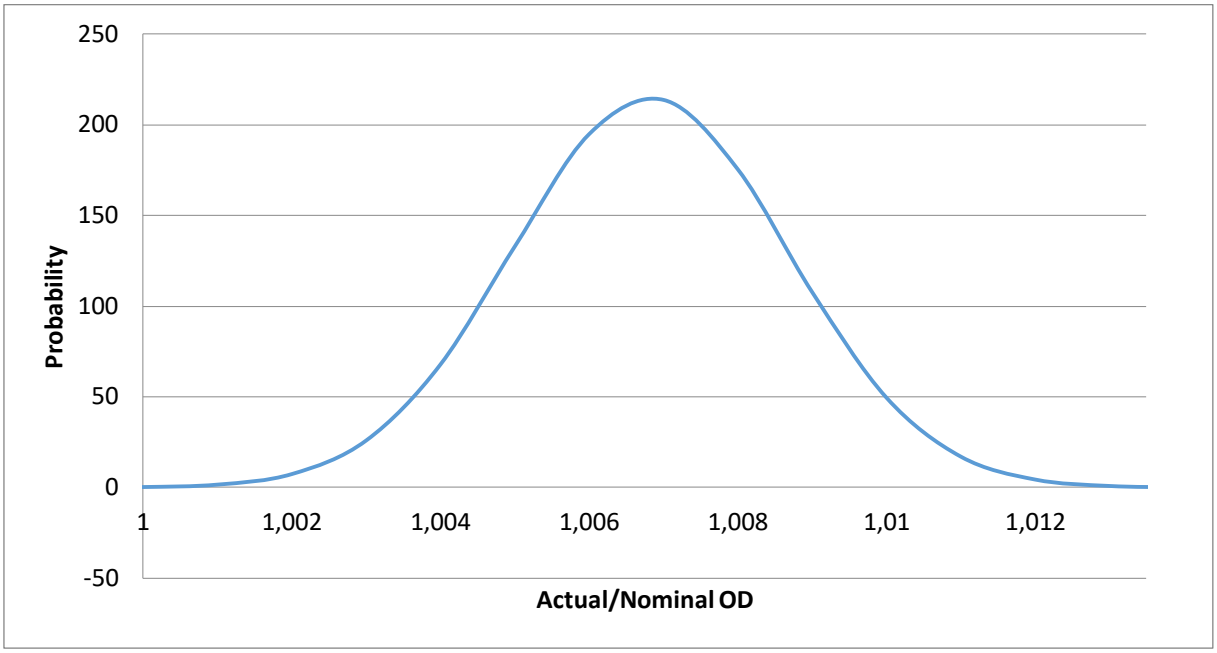

Figure 44:Probability density function (Gaussian) of OD using 113 tests from DEA-130

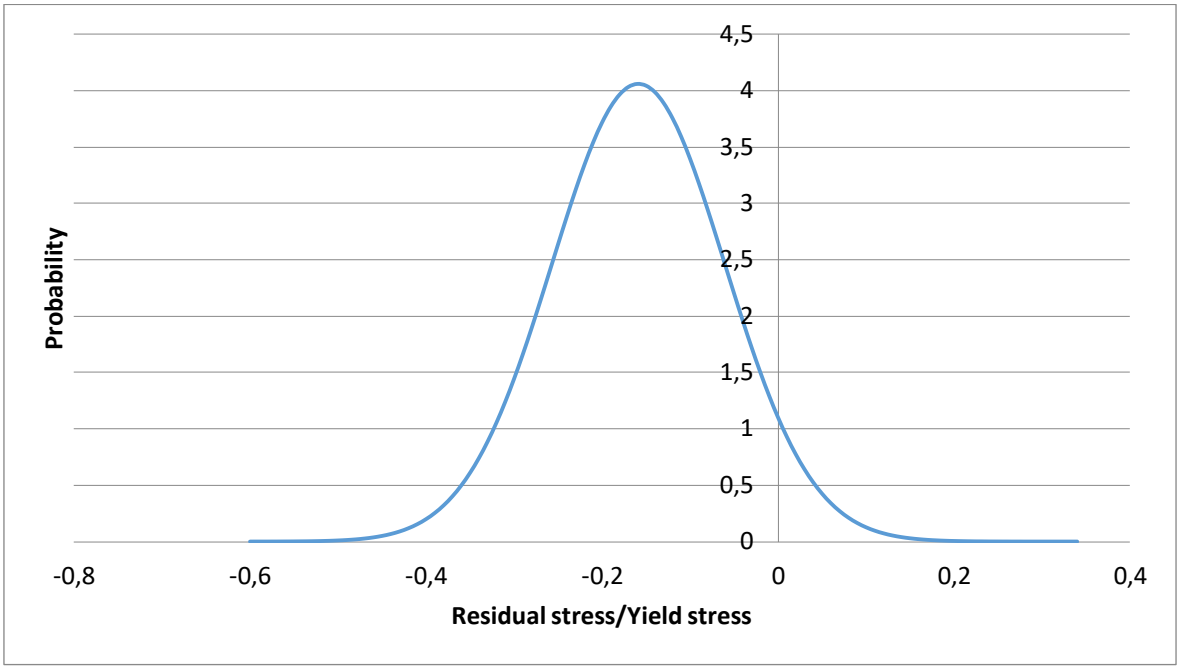

Figure 45: Probability density function (Gaussian) for residual stress using 113 tests from DEA-130. Note: Includes both HRS and CRS

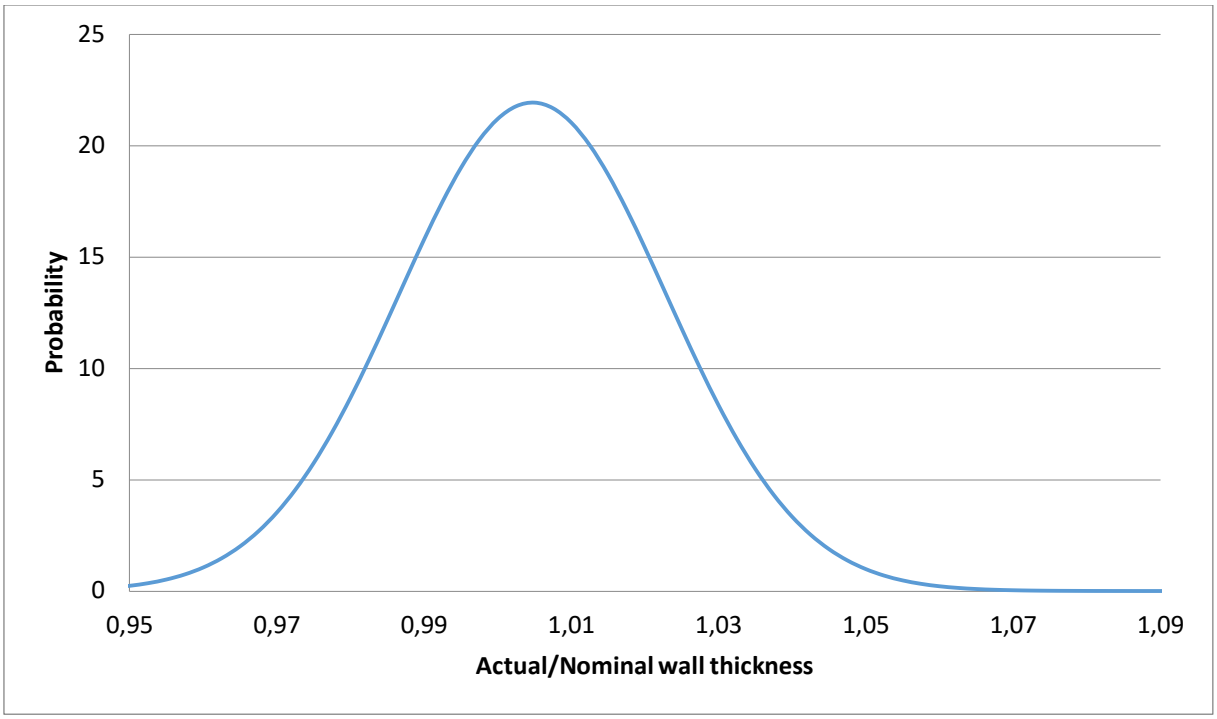

Figure 46: Probability density function (Gaussian) of wall thickness using 113 tests from DEA-130

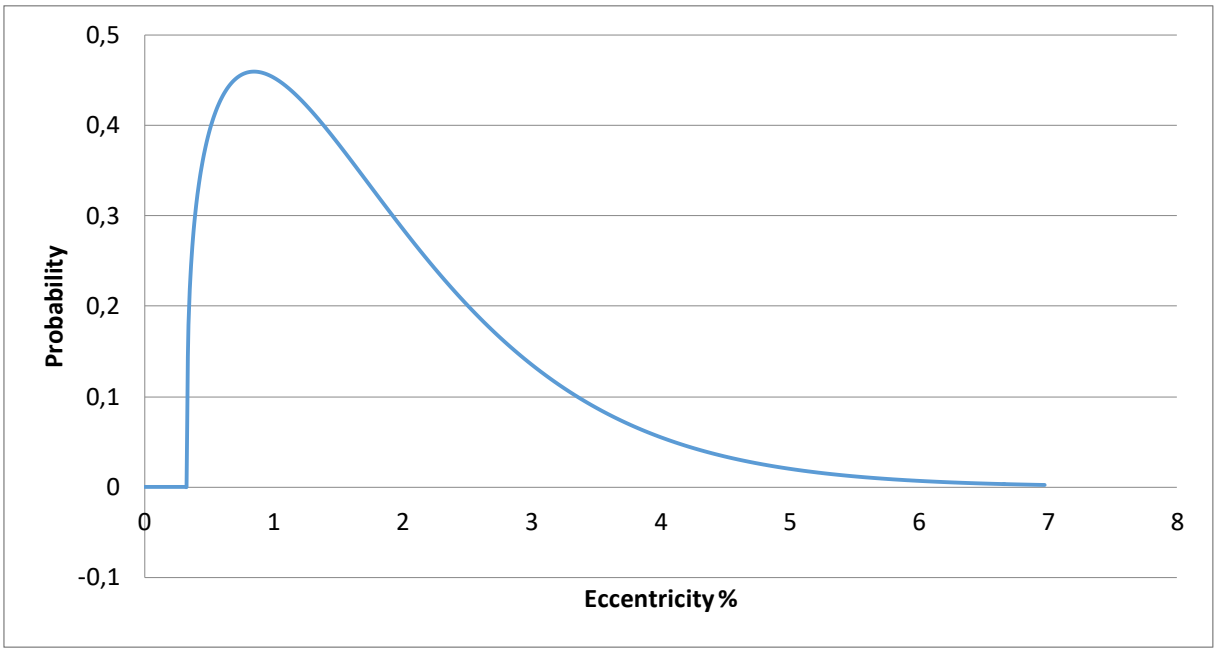

Figure 47: Probability density function (2-parameter Weibull) for eccentricity using 113 tests from DEA-130

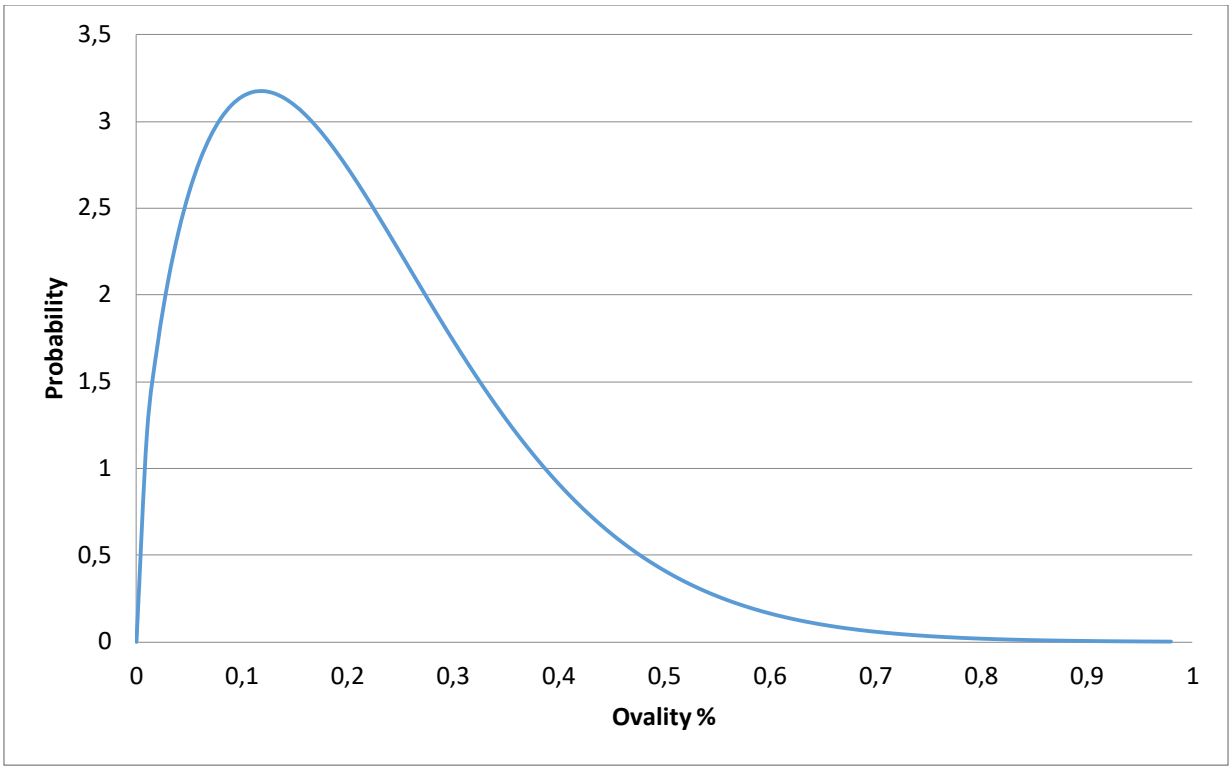

Figure 48: Probability density function (2-parameter Weibull) of ovality using 113 tests from DEA-130

C.3 Probability Density Functions from ensemble data

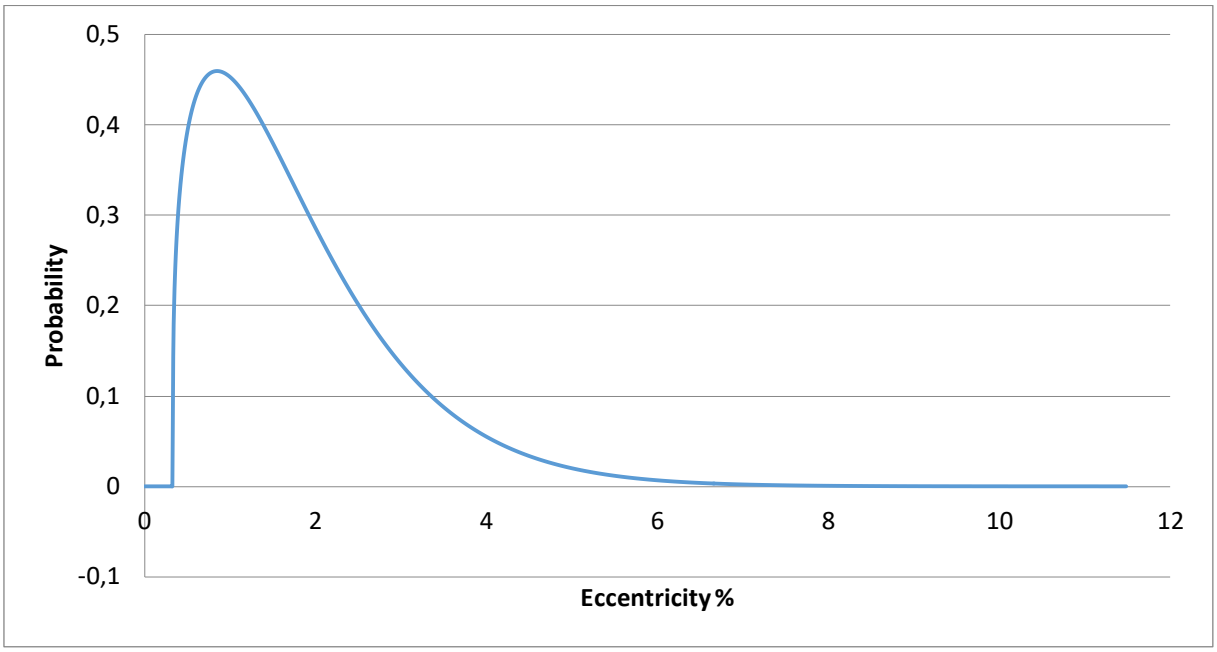

Figure 49: Probability density function (2-parameter Weibull) of eccentricity using ensemble data

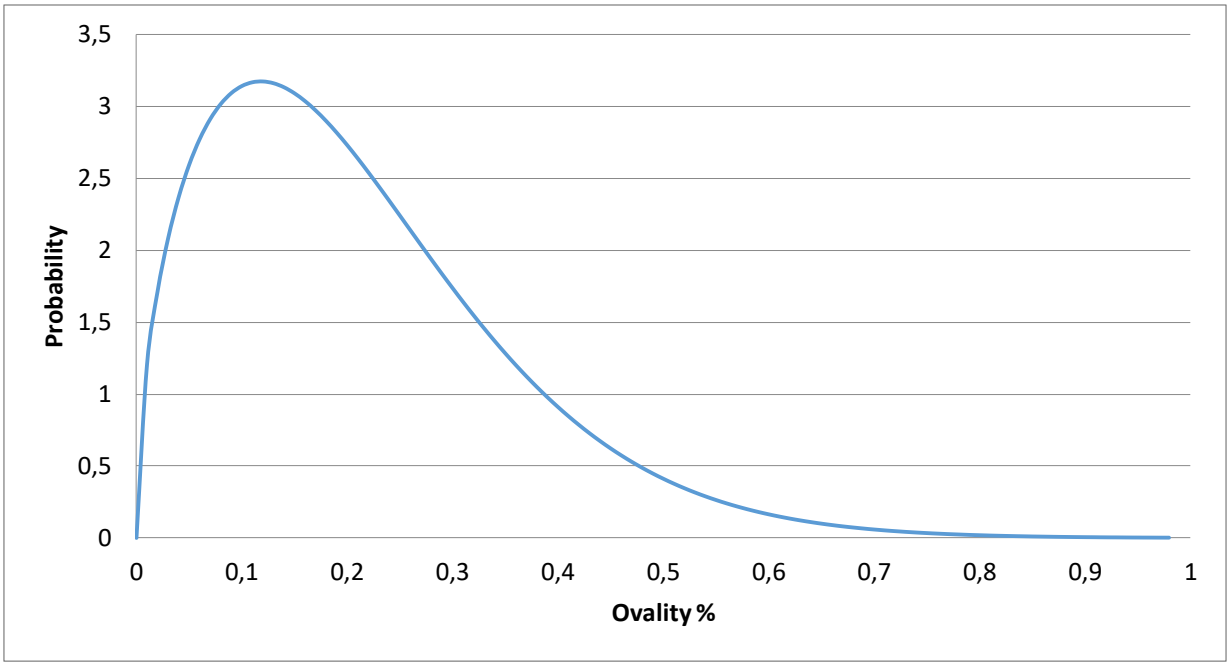

Figure 50: Probability density function (2-parameter Weibull) of ovality using ensemble data

C.4 P-110 Yield Strength

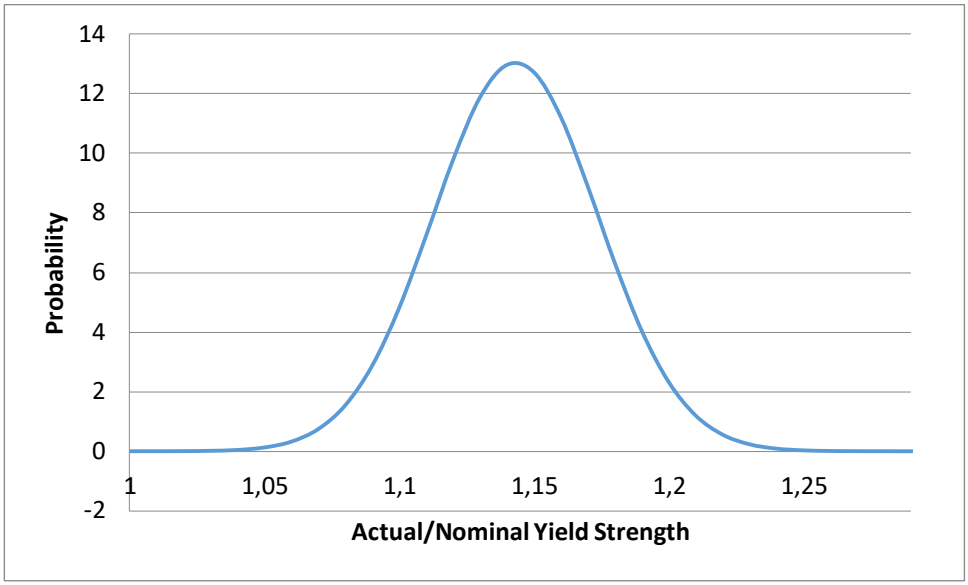

Figure 51: PDF using data from 15 P-110 samples of DEA-130

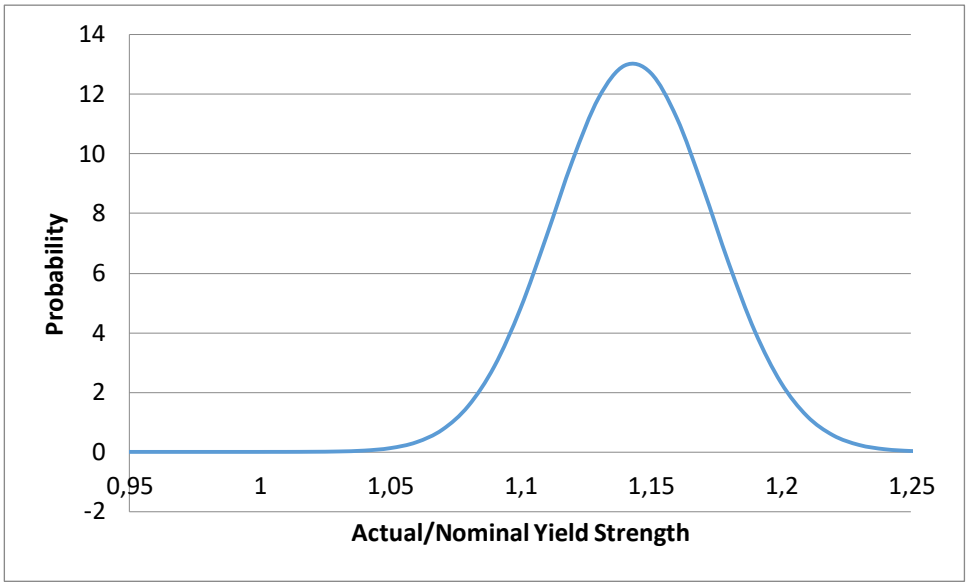

Figure 52: PDF using ensemble data

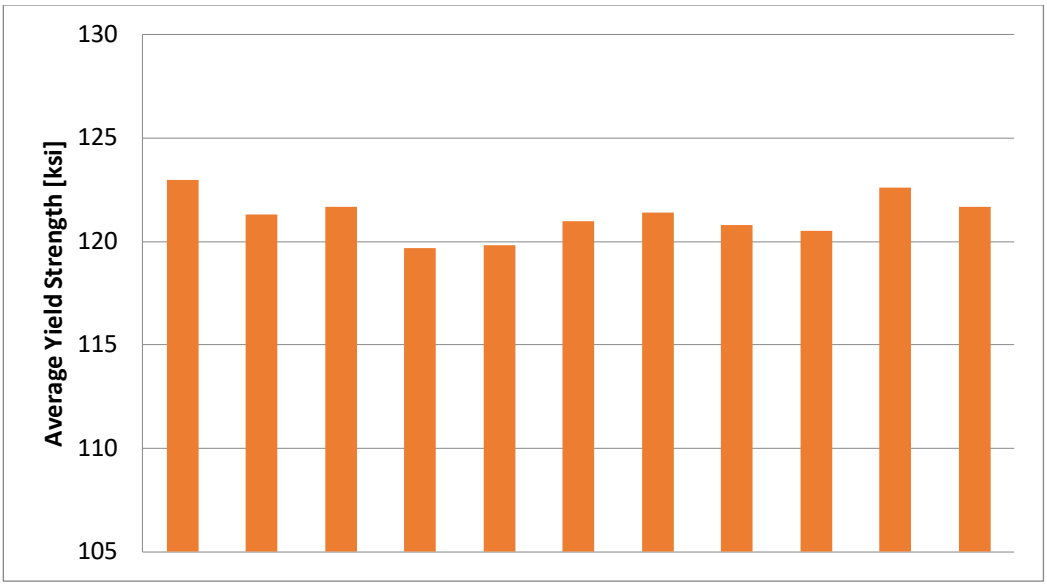

Figure 53: Average yield strength of 11 tested specimens from pipe certificates

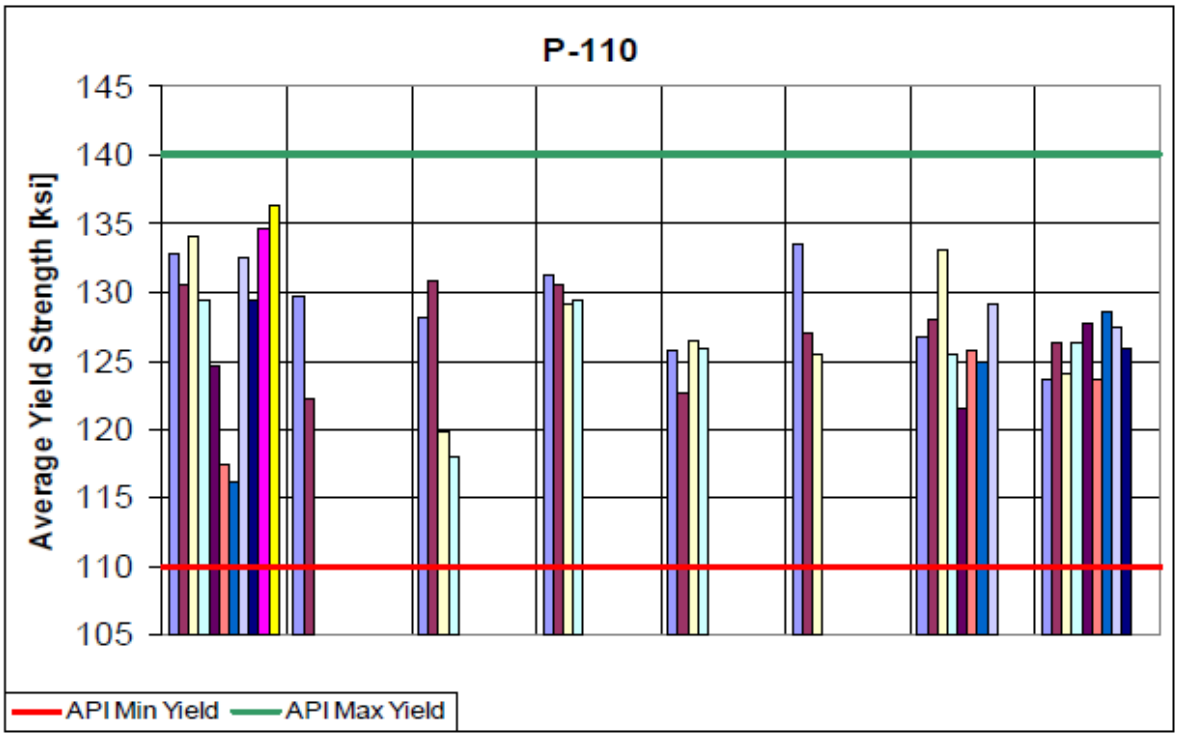

Figure 54: Average actual yield strength of P-110 casings. Extracted from DEA-130 (2002)

Appendix D Results from Monte Carlo Simulations

D.1 DEA-130

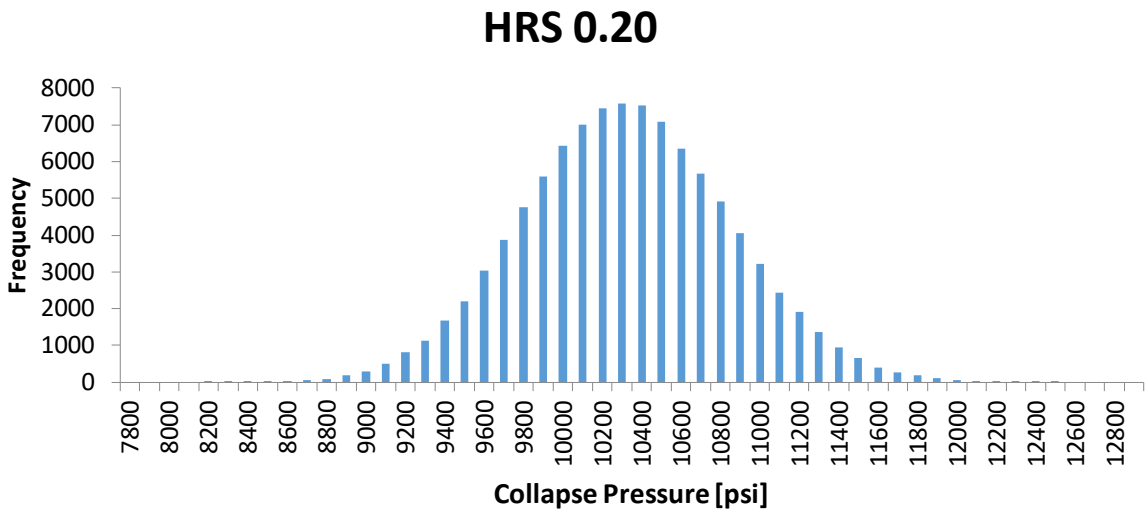

Figure 55: Collapse strength of HRS casing using DEA-130 production quality statistics and governing decrement function

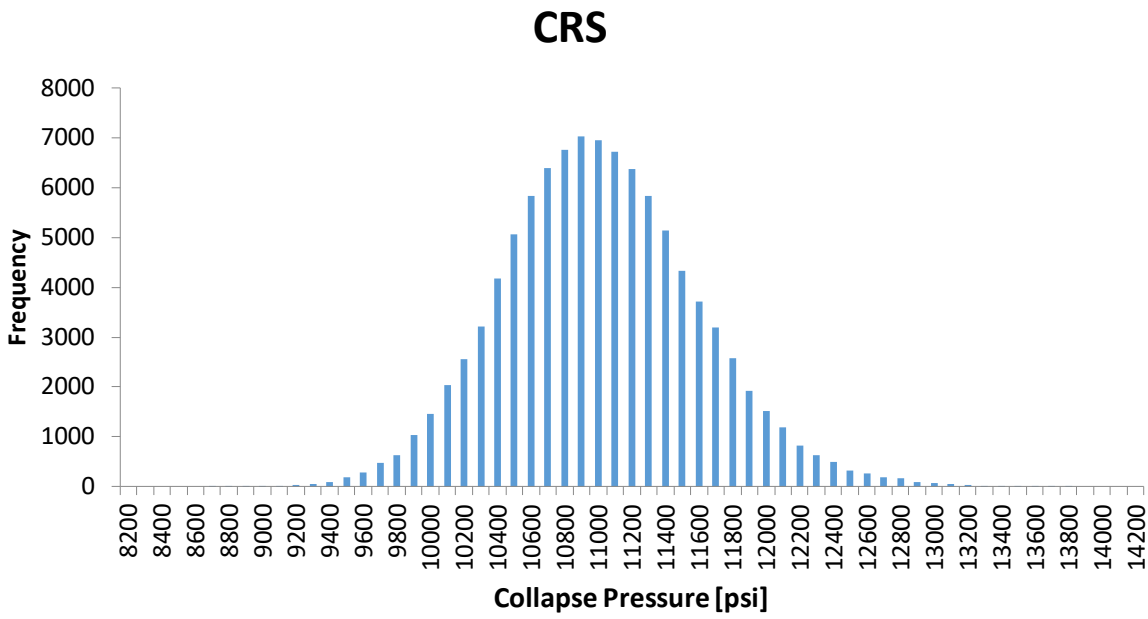

Figure 56: Collapse strength of CRS casing using DEA-130 production quality statistics

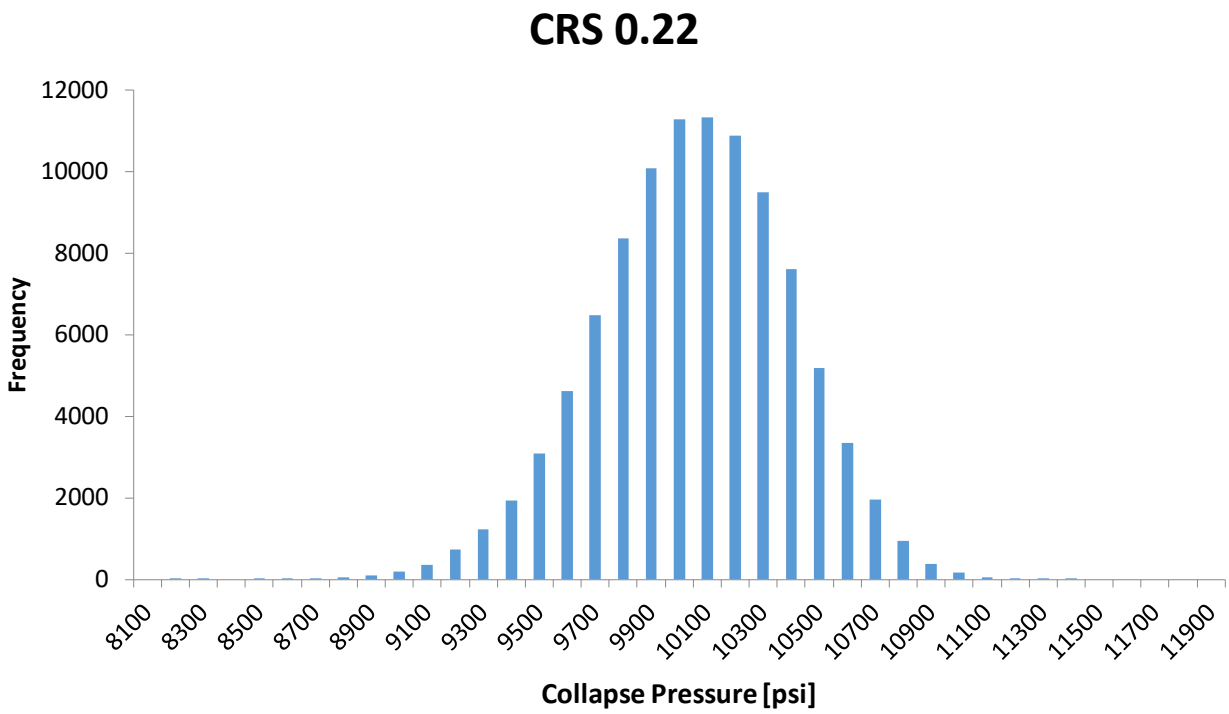

Figure 57: Collapse strength of CRS casing using DEA-130 production quality statistics and governing decrement function

D.2 Ensemble Data

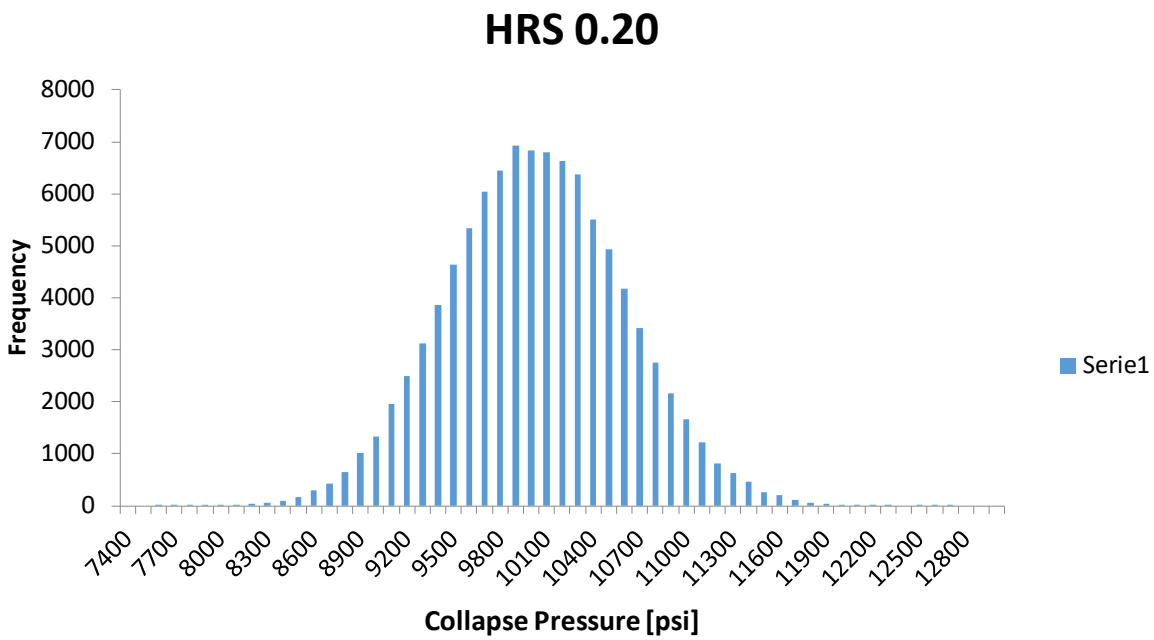

Figure 58: Collapse strength of HRS casing using ensemble production quality statistics and governing decrement function

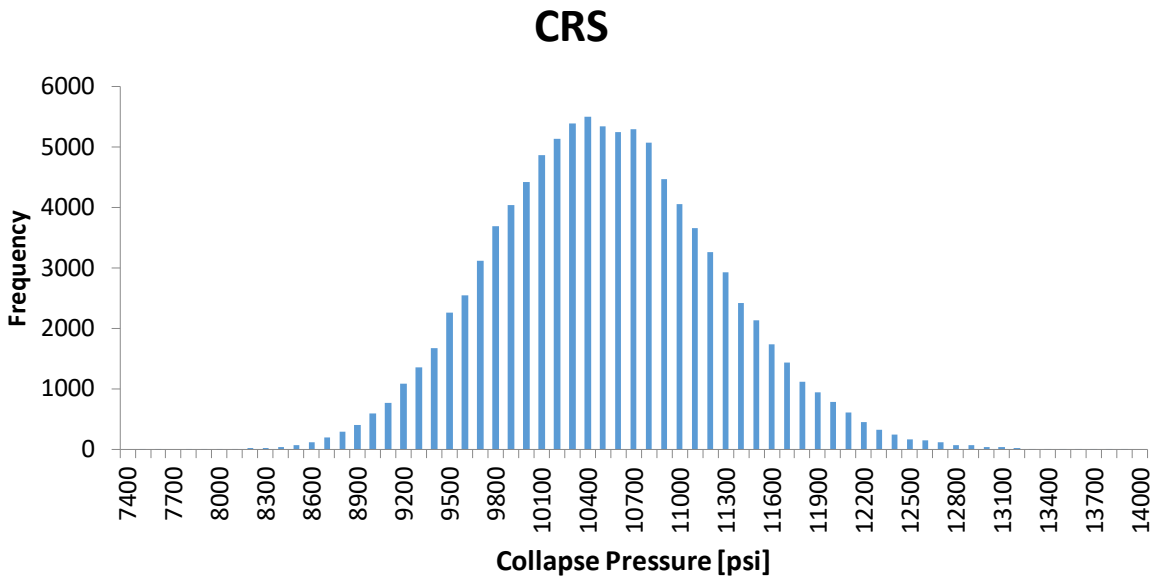

Figure 59: Collapse strength of CRS casing using ensemble production quality statistics

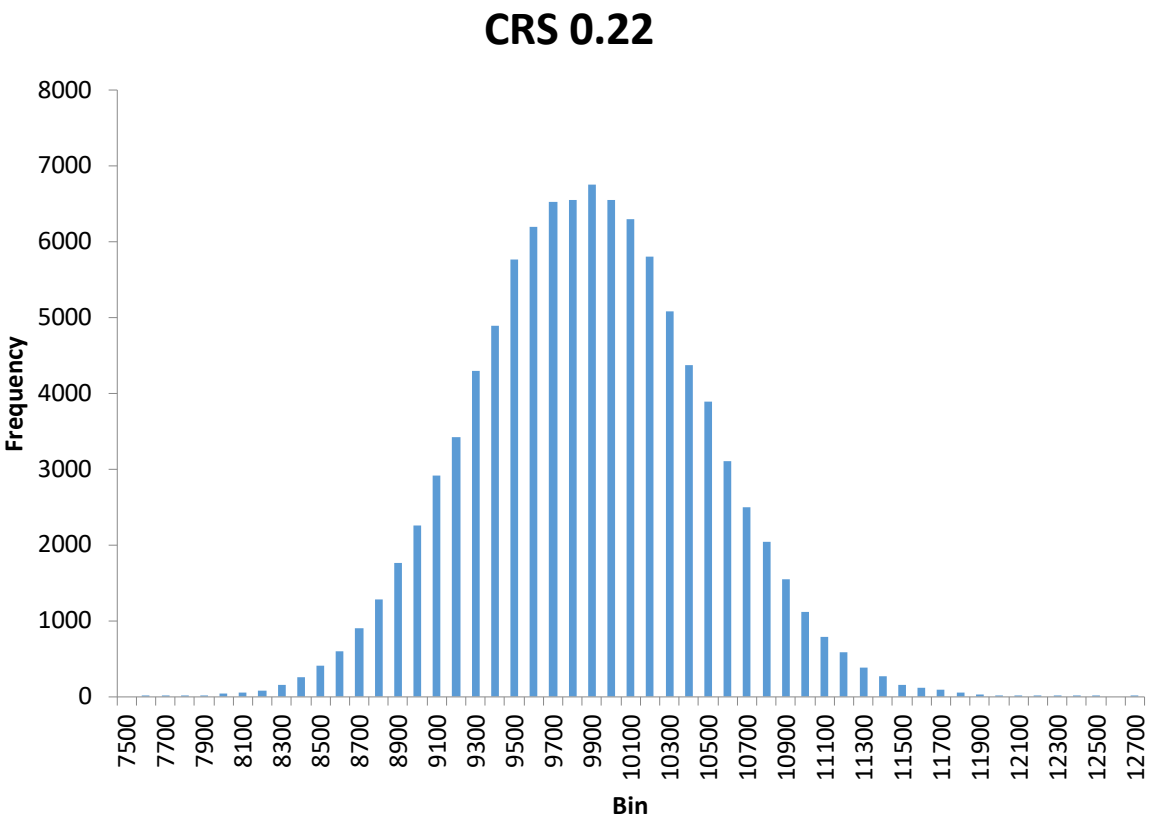

Figure 60: Collapse strength of CRS casing using ensemble production quality statistics and governing decrement function

Appendix E Literature Review

E.1 Bending

Bending of casings in highly deviated wells will reduce collapse strength. The mechanism of bending causes additional axial loads, i.e. compression on the inside of the bend and tension on the opposite side. Induced stress varies through the cross section but is assumed to be constant for practical calculations. The ILS includes the induced axial loads in a pessimistic fashion where additional tension is only added to casings already subjected to tension loads. Compression induced by bending should increase strength but is disregarded. The ILS outputs the effective axial force which is used in the ULS model.

According to Kuriyama et al. (1992) another consequence of bending is flattening of the casing. The casings tend to be more ovalised in bend sections which will reduce collapse strength. Only manufacturing ovality is included in relevant casing collapse models. Imposed ovality is discussed in section 4.3. Kuriyama et al. (1992) suggest an equation for ovality caused by bending based on bending radius but fail to specify units for the input parameters. Using consistent SI or field units do not reproduce meaningful or plausible results.

According to theoretical studies, reduction of collapse strength under bending is mainly caused by bending stress and is only slightly affected by flattening (Kuriyama et al., 1992). Theoretical studies can easily compare a bent pipe with and without flattening. However, isolating the effect of flattening is impractical for experimental purposes.

Table 39: Experimental setup and results (Kuriyama et al., 1992)

Grade [-]	YS [psi]	OD ["]	t ["]	rs/fy [-]	Bending [deg/100ft]	Collapse Pressure [psi]
S-45C	56840	5,5	0,315	-0,16760	0	5902
S-45C	56840	5,5	0,315	-0,16760	0	6047
S-45C	56840	5,5	0,315	-0,16760	24	5713

Table 39 summarized collapse tests for a 5 ½" S-45C 17.00 ppf casing. Only a single data point is available for collapse of a bent casing. The dog leg severity is 24 degrees per 100 feet, greater than in any well reviewed in this report. The reduction of collapse strength corresponds to the trends discussed in the separate chapter regarding axial loading (section 4.2).

Obtaining the ovality of an entire casing string requires calliper logs or similar. For a completed well this requires pulling of the production tubing. If calliper logs are already performed and available it will be difficult to analyse and determine the ovality caused by bending. Manufacturing ovality may be recorded upon construction but ovality may also be imposed by geotectonic forces, field handling, storing of casings, as well as casing wear. Ovality is simply defined as $(D_{max}-D_{min})/D_{avg}$. Caliper logs or ultrasonic imaging provide those values, albeit not discretely for which process it was induced from. Since the effect of flattening is minor, accounting for such ovality will be neglected, and the bending effect is exclusively reflected through additional tensional loads.

E.2 Cement Support by Jammer et al. (2015)

Table 40: Measurements performed by Jammer et al. (2015)

Sample	Nom. OD	Grade	σ_y	OD	t	Ov	Ec	Rs
[-]	["]	[-]	[psi]	["]	["]	[%]	[%]	[-]
83	11,75	P-110	135429	11,861	0,540	0,462	4,476	0,155
144	11,75	P-110	130198	11,858	0,540	0,388	8,815	0,198
171	11,75	P-110	130658	11,860	0,536	0,280	5,617	0,141
175	11,75	P-110	132042	11,854	0,533	0,344	6,285	0,236
242	11,75	P-110	130191	11,856	0,536	0,297	5,158	0,231
256	11,75	P-110	129905	11,860	0,528	0,301	5,782	0,257
532	11,75	P-110	131401	11,858	0,548	0,379	4,777	0,113
533	11,75	P-110	133553	11,853	0,529	0,360	8,06	0,183
539	11,75	P-110	132630	11,860	0,528	0,348	5,27	0,120
16	13,625	Q-125	131977	13,720	0,628	0,328	7,274	0,205
24	13,625	Q-125	131913	13,724	0,625	0,290	8,07	0,170
200	13,625	Q-125	125755	13,719	0,631	0,335	6,76	0,164
91	13,625	Q-125	135730	13,728	0,627	0,222	7,132	0,207
92	13,625	Q-125	134490	13,737	0,636	0,220	5,858	0,162
135	13,625	Q-125	132376	13,722	0,637	0,288	4,229	0,120
177	13,625	Q-125	133350	13,732	0,625	0,255	6,879	0,179
199	13,625	Q-125	133352	13,727	0,630	0,306	6,031	0,183
359	13,625	Q-125	127200	13,734	0,628	0,258	7,725	0,196

Appendix F Results from ILS

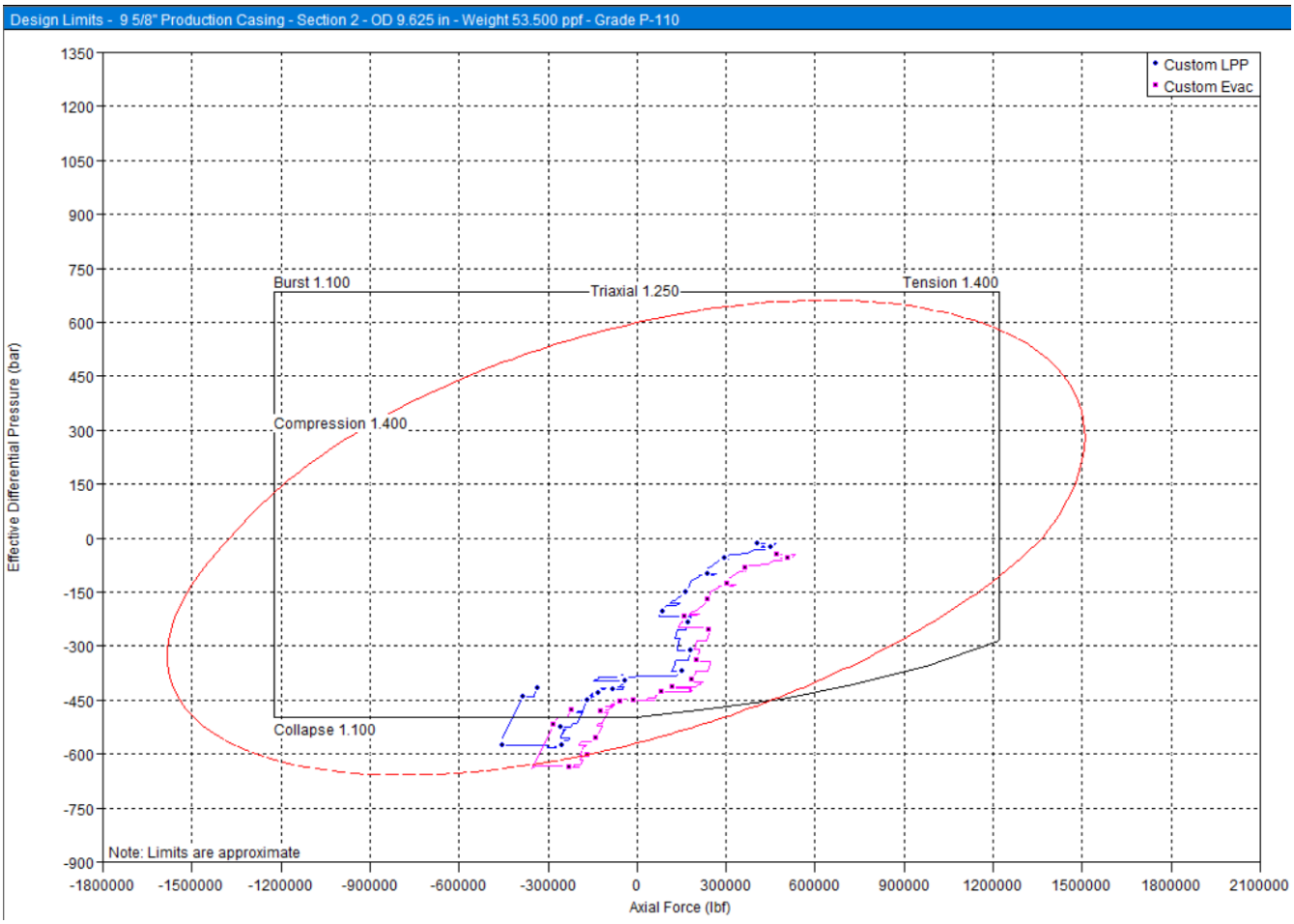

Figure 61: Design Limits Plot